Taurine Depletion and Schwann Cell Dysfunction in Diabetic Neuropathy

By Trevor Askwith

A thesis submitted to
The University of Birmingham
for the degree of
DOCTOR OF PHILOSOPHY

Department of Clinical and Experimental Medicine

University of Birmingham Medical School

The University of Birmingham

June 2010

Abstract

It is estimated that 2.6 million people in the UK suffer from diabetes, 50% of whom suffer from diabetic neuropathy. Patients with diabetes have low levels of platelet and plasma taurine and in animal models taurine supplementation ameliorates neuropathic symptoms. The mechanisms behind taurine depletion and taurine supplementation are not well understood. Schwann cells are highly vulnerable to hyperglycaemia-induced stress which plays a key role in the pathogenesis of diabetic neuropathy, however, the mechanisms behind these effects are not well understood. In these studies I have elucidated the effect of hyperglycaemia on taurine transport in isolated human Schwann cells and the mechanisms behind the beneficial effects of taurine supplementation.

I demonstrated that high glucose reduces TauT expression in a dose-dependent manner and that high glucose inhibited the pro-oxidant increase in TauT expression and taurine uptake. This high glucose response was ablated by inhibition of aldose reductase, nitric oxide synthase as well as antioxidant treatment. Taurine supplementation reduced glucose-induced increases in oxidative stress, lipid peroxidation nitrosative stress and poly(ADP-ribosyl)ation and these effects were not accompanied by changes in antioxidant defence. Taurine also restored glucose-induced increases in iNOS and nNOS expression along with phospho-p38 MAPK abundance.

Acknowledgements

Firstly I would like to express my sincere thanks to Martin Stevens for his guidance and support during my PhD studies; it has been an honour to be his first UK PhD student and his clinical expertise and guidance has been much appreciated.

Many thanks to Margaret Eggo for her much appreciated help, support and technical guidance through-out the duration of my time in the laboratory and also her ongoing support during the write up process.

A big thank you to everyone within the laboratory. Special thanks to Wei Zeng and Sharon Hughes for their practical and technical support at the lab bench, and to Kiran Dubb and Elena Gillespie for their clinical guidance.

Sincere thanks to the University of Birmingham for providing the funding for this project.

I would also like to thank all my family and in-law family for their help, encouragement, and patience during my studies.Thank you to my friends for their support, in person and via email and supportive phonecalls.

Special thanks to my wife Louise for her love, care and continual support during the good times and bad. Thank you for your, faith, courage, and sense of humour, helping to keep us smiling and laughing, even during the challenging days.

Contents

List of Illustrations

List of Tables

List of Abbreviations

Aldose reductase (AR)

Aldose reductase inhibitor (ARI)

Advanced glycation end products (AGE)

Advanced glycation end products receptor (RAGE)

Endothelial nitric oxide synthase (eNOS)

Inducible nitric oxide synthase (iNOS)

Mitogen activated protein kinases (MAPK)

Michaelis-Menton constant (Km)

Na^{+}Cl--dependent taurine transporter (TauT)

Neuronal nitric oxide synthase (nNOS)

Nitric oxide synthase (NOS)

Nitric oxide (NO)

Nitrotyrosine (3NT)

Poly(ADP-ribose) polymerase (PARP)

Poly(ADP-ribosyl)ated proteins (PAR)

Protein kinase C (PKC)

Reactive nitrogen species (RNS)

Reactive oxygen species (ROS)

Retinal pigment endothelial cells (RPE)

Reduced glutathione (GSH)

Streptozotocin-diabetic (STZ-D)

Superoxide dismutase (SOD)

Chapter 1 Introduction

Diabetes mellitus is an endocrine disease characterised by elevated blood glucose. The name is derived from two words; the Greek ‘diabetes’ which means ‘to siphon or pass’, (reflecting polyuria suffered by patients) and the Latin word, ‘mellitus’, which means ‘sweet as honey’. Hence, the term diabetes mellitus literally means passing excessive and sweet urine.

In healthy individuals, insulin is secreted from β-islet cells of the pancreas in response to elevations of glucose. Peripheral cells, especially those in muscle and fat, respond by increasing cellular glucose uptake mediated by the transporter, glut 4, increasing glycogen synthesis as well as by reducing gluconeogenesis. In individuals with diabetes, this mechanism does not work, either due to decreased insulin secretion, or peripheral insulin resistance. The ‘gold standard’ used for diagnosis is an oral glucose tolerance test (OGTT) where 75g glucose is consumed by the patient within 5mins, and the blood glucose concentration measured two hours later. Normal glucose concentration at 2h is <7.8 mM. A glucose concentration 7.8-11.1 mM indicates ‘impaired glucose tolerance’ and >11.1 mM confirms the patient has diabetes. To reduce the need for an OGTT, in 1997 the American Diabetes Association (ADA) suggested lowering threshold for fasting glucose from 7 mM to 6 mM and with this classification, fasting glucose measurements are now the diagnosis of choice (see table 1 for full WHO (World Heath Organisation) classification).

Using this criterion approximately 2-6% of the UK (United Kingdom) population have diabetes, but only half to two thirds have been diagnosed (9). There are two major types of diabetes; Type 1, previously known as insulin-dependent diabetes mellitus (IDDM) and Type 2, previously known as non-insulin dependent diabetes mellitus, (NIDDM). Other types of diabetes exist but are much less common, such as maturity onset diabetes mellitus of the

young (MODY), which accounts for approximately 3% of sufferers of diabetes (9). The clinical manifestation of the diabetes depends upon the type of diabetes suffered.

		Venous Plasma Glucose (mM)
Normal	Fasting *and* 2hr OGTT	<6.0 <7.8
Diabetes	Fasting *or* 2hr OGTT	>7.0 >11.1
Impaired glucose tolerance	Fasting *and* 2hr OGTT	<7.0 7.8-11.1
Impaired fasting glucose	Fasting	6.0-6.9

Table 1-1 - WHO Classification for Diagnostic Criteria of Diabetes (9)

1.1 Type 1 Diabetes-Insulin Dependent Diabetes Mellitus

Type 1 diabetes usually occurs in young people below the age of 35 and accounts for between 5-25% of cases (9). Clinical manifestations are weight loss, polydipsia and polyuria. Diabetic comas are a common problem for Type 1 patients. Hyperglycaemic comas can be non-ketotic where dehydration results in a coma, or ketotic which is due to extreme insulin deficiency, where the body metabolises fatty acids, producing ketone bodies (10). Accumulation of ketone bodies results in metabolic acidosis, which is fatal in 6-10% of patients (11). Hypoglycaemic comas occur due to extremely low blood glucose.

The precise causes of Type 1 diabetes are not completely clear although the aetiology suggests an autoimmune condition resulting in T-cell destruction of pancreatic β cells (10). Many genetic traits are implicated in Type 1 diabetes, most linked to the histocompatibility complex (MHC) antigens/human leukocyte antigens (HLA). Over 90% of patients with Type

1 diabetes in the UK have either HLA-DR3, DR4 or both. Environmental factors implicate viral infections such as coxsackie, especially B4, rubella, cytomegalovirus, Epstein-Barr virus, mumps, retroviruses and rotavirus (9).

1.2 Type 2 Diabetes

Type 2 diabetes accounts for the vast majority of cases of diabetes (75-95%) (9). Type 2 diabetes is due either to a defect in insulin secretion, to peripheral insulin resistance or both (10). Type 2 diabetes is often asymptomatic, diagnosed later in life and it is rarer that patients will fall into either a hypoglycaemic or hyperglycaemic coma (10). Clinically, patients often present with other symptoms, such as recurrent urinary tract infections, or diabetic complications (see below) whereupon diagnosis is made.

Type 2 diabetes is less strongly linked to autoimmunity than type 1 diabetes, but is more commonly part of the metabolic syndrome (also known as insulin-resistance syndrome, or Syndrome X) which consists of impaired insulin-stimulated glucose uptake, hyperinsulinaemia, truncal obesity, dyslipidaemia, hypertension, hypercoagulable state, polycystic ovary syndrome and microalbuminuria (10). As with Type 1, there are many genetic components associated with Type 2 diabetes, however, the genetics appear to be polygenic affecting many factors such as insulin signalling as well as fat metabolism.

1.3 Epidemiology of Diabetes

The prevalence of diabetes is increasing rapidly. In the UK there were 1.7 million cases in 2000 AD, and this is expected to rise to 2.7 million by 2030 AD. World-wide there were 171 million cases in 2000 AD which is expected to increase to 366 million by 2030 AD. (WHO http://www.who.int/diabetes/facts/world_figures/en/). The disease prevalence varies greatly

world-wide (figure 1-1) and the same distribution is found within multiethnic countries, such as in the United States of America (USA) and UK demonstrating genetic predisposition. In the UK relatively higher Type 2 diabetes prevalence is oberserved in ethnic groups, such as Caribbean, West African as well as those from the Indian subcontinent compared with white Caucasians (12). The same has been reported in the USA with higher disease prevalence among the Hispanic and African-American populations compared with white Caucasian groups (13). The higher prevalence within these populations highlights life-style factors affecting disease prevalence, however genetic polymorphisms in minority groups have also been found to associate with susceptibility to Type 2 diabetes. Large-scale studies such as the United Kingdom Asian Diabetes Study are being conducted to identify additional polymorphisms.

1.4 Complications of Diabetes

The acute complications of diabetes, i.e. hypoglycaemic and hyperglycaemic comas are serious medical emergencies but chronic microvascular and macrovascular complications affect many patients and these are associated with considerable morbidity and mortality. The macrovascular complications, such as coronary artery disease, are complications linked to the metabolic syndrome. However a series of microvascular complications, such as retinopathy, nephropathy, and neuropathy occur, where hyperglycaemia *per se* is the key contributing factor (10). During the 1990s, two large-scale clinical trials evaluating the effect of tight glycaemic control on the microvascular complications were conducted i.e. the Diabetes Control and Complications Trial (DCCT) in subjects with Type 1 diabetes (14) and the UK Prospective Diabetes Study (UKPDS) in patients with Type 2 diabetes (15). Both studies

demonstrated that tight glycaemic control was beneficial in reducing the microvascular complications of diabetes.

Improvements in the management of diabetes have resulted in improved patient morbidiy and mortality. However the development of long-term complications is related to the duration of diabetes and the quality of antecedent glycaemic control. In addition, many patiens with Type 2 diabetes are unaware of their condition and therefore present late with complications already developed.

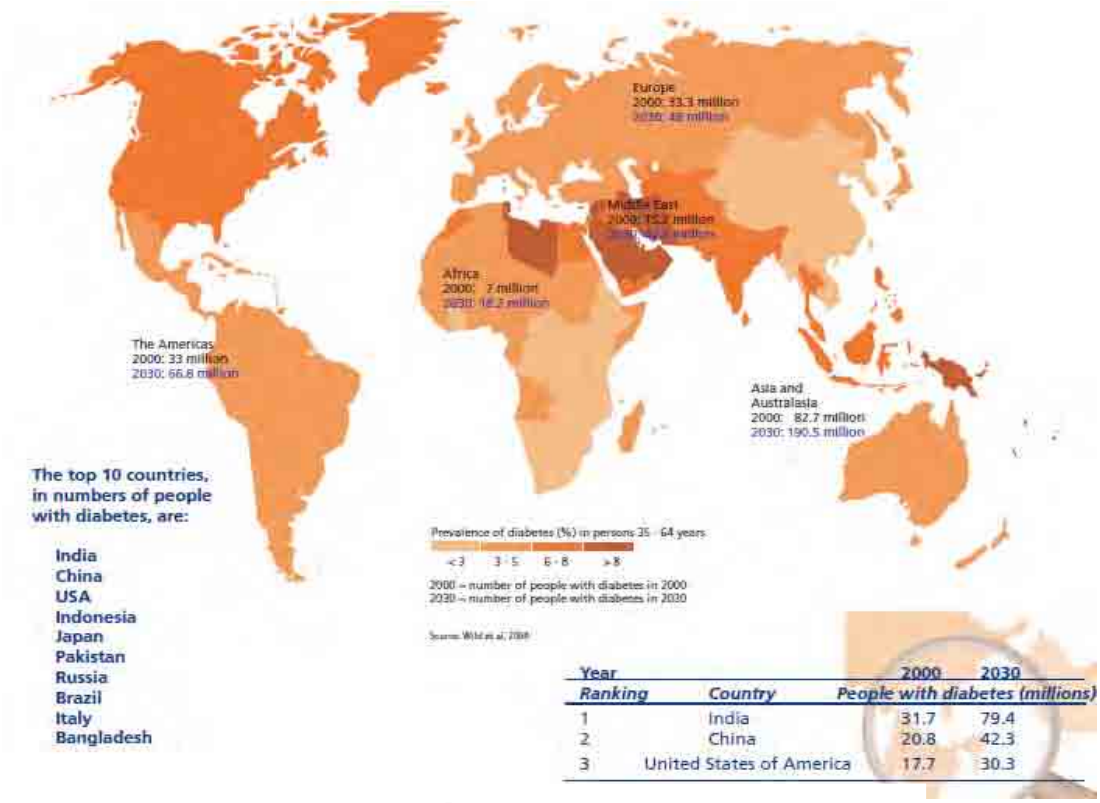

Figure 1-1 - Prevalence Map Demonstrating World-Wide Diabetes Incidence

Top 10 countries are indicated on the left, showing high prevalence in Asia. (Source:WHO)

1.4.1 Microvascular Complications of Diabetes

1.4.1.1 Retinopathy

Approximately 10% of patients suffering from either Type 1 or 2 diabetes for 15 years or more will develop severe visual impairment and approximately 2% will become blind. During early stages in the condition the capillary basement membrane thickens and is associated with a loss of pericytes embedded within. In these early stages of the disease the patient may suffer capillary microaneurysms, where small retinal haemorrhages can be seen clinically as red 'dots'(16; 17). There may also be large areas of retinal capillaries with reduced blood flow. This induces the formation of new blood vessels either along the disc, or elsewhere (17; 18). These changes are asymptomatic, but may progress to haemorrhage, scar tissue formation and finally retinal detachment, which will result in loss of vision (16).

1.4.1.2 Nephropathy

After 15 years of diabetes, 35% of patients will have nephropathy and between 10-20% of the patients will die from kidney failure. Nephropathy is associated with increased kidney size, afferent and efferent arterial fibrosis, thickening of the glomerular basement membrane and expansion of the mesangium (19). The electrical charge of the basement membrane is altered increasing the passage of albumin. Hence, the initial sign of nephropathy is microalbuminuria which usually occurs 5-15 years after onset of diabetes (20). This can progress into proteinuria and albuminuria, signifying the beginning of nephropathy. From this point there is on average a reduction of 10ml/min/1.73m^2 in glomerular filtration rate, ultimately leading to end-stage renal failure (19).

1.4.1.3 Neuropathy

There are three classical syndromes of diabetic neuropathy, (i) distal symmetrical sensorimotor polyneuropathy, (ii) diabetic autonomic neuropathy (DAN) and (iii) focal neuropathy. The prevalence of DAN depends upon the criteria used for study, but estimates range between 20-40% of patients with diabetes (21). The most studied and clinically important form of DAN is cardiovascular autonomic neuropathy (CAN), which results from damage to autonomic nerves that innervate the heart. This can produce tachycardia, exercise intolerance, postural hypotension and there is a five fold increase in five year mortality rate in individuals with CAN than those without cardiovascular autonomic involvement (21; 22). As well as CAN, DAN also results in other autonomic dysfunctions, such as constipation, diarrhoea and incontinence (21; 23).

Diabetic focal neuropathies are normally seen in patients over 50 years of age (24). These can occur suddenly and are caused by microvascular infarcts. Depending upon the nerve(s) affected this can result in cranial, truncal, proximal or multifocal diabetic neuropathy (25). Electrophysiological studies demonstrate a reduction in both nerve conduction as well as amplitude due to both demyelination and axonal degeneration (26). The prognsosis for focal neuropathy is generally good and the condition will frequently resolve itself (24; 26).

Estimates vary for the prevalence of diabetic peripheral neuropathy, however, it is thought that up to 50% of diabetic patients may have the condition, half of which maybe asymptomatic (26). Due to the subtle nature of both Type 2 diabetes as well as neuropathy at the point of diagnosis of diabetes, 10% of patients already have diabetic peripheral neuropathy (27).

In general, the pathology of diabetic peripheral neuropathy in Type 1 and Type 2 diabetes is considered to be similar (although some authorities dispute this). Diabetic peripheral

neuropathy is associated with progressive nerve fibre degeneration (26). Initially the condition affects the small nerve fibres. Early on there is a loss of intra-epidermal nerve fibres as shown in figure 1-2, which can be measured by immunohistochemical staining (1; 28). Pain also occurs early in diabetic neuropathy. Nerve fibre loss is also associated with noiceceptive pain, however, neuropathic pain can also result from DRG hyperexcitibility (29; 30) and sensitisation which occurs in brainstem nuclei (31).

The condition can progress with loss of vibration, pressure and proprioception perceptions. Finally motor deficits and muscle wasting may develop affecting up to 5% of diabetic patients. Diabetic peripheral neuropathy and the consequent lack of sensation is the second largest cause for amputations, following accidental trauma (32) with the lifetime risk of foot amputations for neuropathic patients being 15% (27).

Parallelling the clinical symptoms is the histopathology. Microangiopathy which is common to all microvascular complications appears as a thickening of the basement membrane and swollen endothelial cells and occurs in early stage diabetic neuropathy (28). The microangiopathy also correlates with a reduction in nerve fibre density (33). Nerve fibre degeneration occurs due to severe demyelination. Onion bulb formation is also visible, which occurs due to successive demyelination and remyelination (34). In the absence of this regeneration, the nerve fibre will be lost.

Both DCCT and UKPDS demonstrated that progression of diabetic peripheral neuropathy was dependent on glycaemic control (35; 36). The DCCT also demonstrated a causal relationship between glycaemic control and disease incidence, a finding that was inconclusive in UKPDS (37; 38). This is primarily due to the vascular component of diabetic peripheral neuropathy and the metabolic syndrome being similar; as are many of the risk factors such as cigarette

smoking, alcohol consumption, hypercholesterolemia, low HDL, elevated triglycerides and hypertension (27; 39-42). It is also of note that men develop neuropathy earlier than women (27; 43).

Studies in the USA have found no differences between the rates of neuropathy between blacks and Hispanics (44), on the other hand, in France rates of neuropathy are higher in Algerians (45). In a recent study Asians with type 2 diabetes were found to have less large and small fibre neuropathy compared to Europeans. In this study it was concluded this occurance was due to improved skin microvascularisation (46).

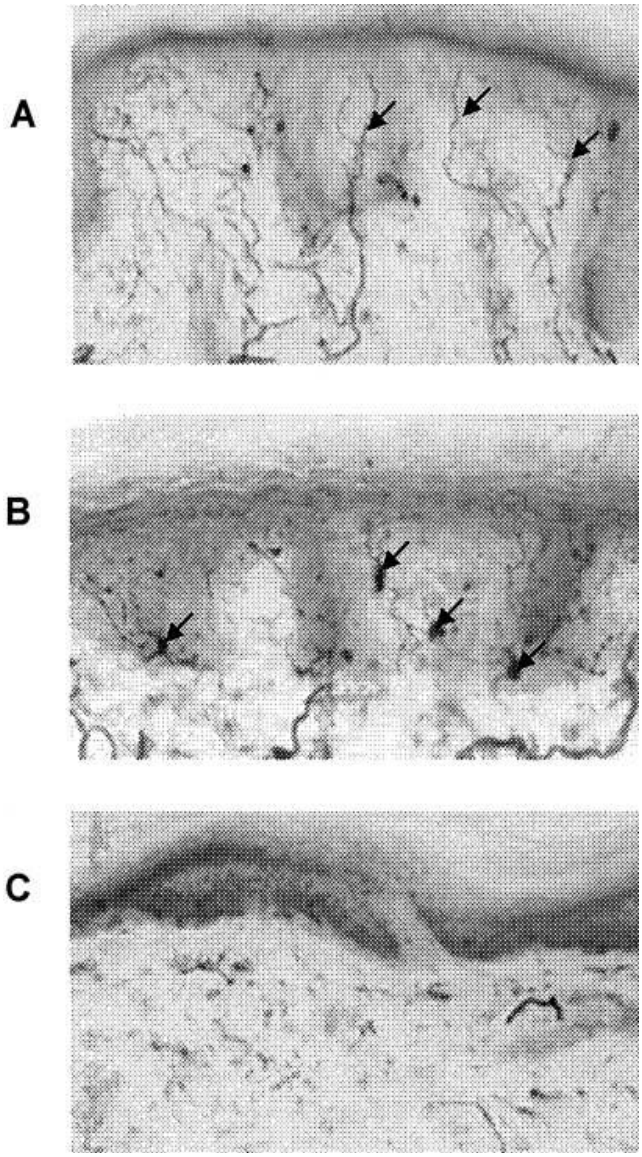

Figure 1-2 - Progressive Loss of Epidermal Nerve Fibres in Diabetic Patients

(1)

A Healthy patient, with normal density of epidermal nerve fibres

B Slightly reduced nerve fibre density

C Complete clearance of nerve fibres

1.4.1.4 Diabetic Foot Ulceration

Patients with diabetes can have dry, atrophic skin due to reduced collagen production and an increased abundance of active matrix metalloproteinases (47). This reduced skin integrity means patients can more easily be wounded, especially on their feet, where foot deformities, ill-fitting shoes or the presence of foreign bodies can easily damage the skin, forming ulceration (48). Exacerbating this effect is peripheral neuropathy (see above) whereby decreased sweating contributes to skin cracking and fissure formation. Reduced sensation predisposes to wound formation and approximately 80% of patients with foot ulceration also have neuropathy (48). Peripheral vascular disease and reduced peripheral blood flow can result in local ischaemia and together with hyperglycaemia can impair skin repair and reduce immune defence (49). The combination of neuropathy and ischaemia has been termed “the neuroischaemic foot” and predisposes to infections, and finally necrosis and gangrene (48).

1.4.1.5 Vascular Deficits in Diabetic Neuropathy

The presence of endoneurial microangiopathy, thickening of the basement membrane of the vasa nervorum, and endothelial cell swelling may contribute to the development of diabetic peripheral neuropathy. These defects are induced by hyperglycaemia as well as vascular risk factors associated with neuropathy such as increased blood pressure, cholesterol, triglycerides as well as smoking (42). The above facts, combined with increased platelet aggregation, result in reduced nerve blood flow, lumen occlusion and ischaemia (50). A vascular component to diabetic peripheral neuropathy is supported by the salutary effects of vasodilators such as angiotensin-converting enzyme inhibitors, which improve nerve blood flow and subsequently nerve conduction velocity and Na^{+}/K^{+}- ATPase activity in experimental diabetic peripheral neuropathy (51).

It was initially thought the vascular and metabolic aspects of diabetic peripheral neuropathy were separate; it is now clear they are linked (52). Increased glucose flux results in augmented oxidative stress, and decreased NADPH. Oxidative stress contributes to endothelial damage reducing endoneurial blood flow and increasing tissue ischaemia. These result in a vicious cycle with local ischaemia directly increasing oxidative stress and reduced blood flow reducing oxidant buffering from the blood (53). NADPH is an essential cofactor for nitric oxide (NO) generation by endothelial nitric oxide synthase (eNOS) as illustrated in figure 1-3 (51). NO generation from eNOS is essential for vasodilation; therefore NADPH depletion impairs vasodilation, further aggravating the vascular deficits (53; 54).

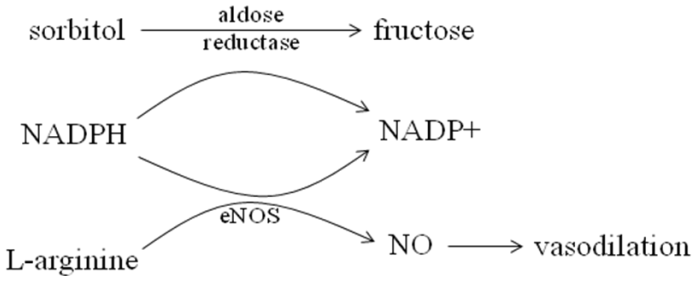

Figure 1-3 – Adose Reductase Flux and Vasodilation

Increased flux through aldose reductase depletes intracellular NADPH, which is a cofactor for the generation of NO by eNOS required for vasodilation. Increased aldose reductase flux inhibits NO generation by eNOS, therefore reducing vasodilation.

1.4.1.6 Schwann Cells in Diabetic Neuropathy

Schwann cells are the support cell of the peripheral nervous system (PNS), the most obvious function being to wrap around neuronal axons acting as an insulating barrier impenetrable to ion movement. In myelinating Schwann cells, this barrier is created by proteins and lipids that form concentric layers of myelin surrounding the axon, with the bulk of the Schwann cell cytoplasm and nucleus residing close to the external plasma membrane, an area known as the neurilemma (55; 56) (figure 1-4A). In non-myelinated cells, the barrier is the plasma membrane of the Schwann cell. The Schwann cell barrier is discontinuous and at most each Schwann cell covers 1-2mm of the axon (57). The unmyelinated areas of the discontinuous barrier are known as nodes of Ranvier where ions can cross the axonal membrane (figure 1-4B). This enables currents to jump between nodes, resulting in fast, energy- efficient transmission known as 'saltatory conduction'.

Schwann cells play large role in the response of the PNS to injury. When Schwann cells lose axonal contact they de-differentiate, and along with invading macrophages are able to phagocytose debris such as myelin and axons produced by injury. Schwann cells distal to the lesion however, remain differentiated and secrete growth factors such as neurotrophic factor (NT) 4, glial derived neurotrophic factor (GDNF) and nerve growth factor (NGF) to promote axonal survival and re-growth (7; 58).

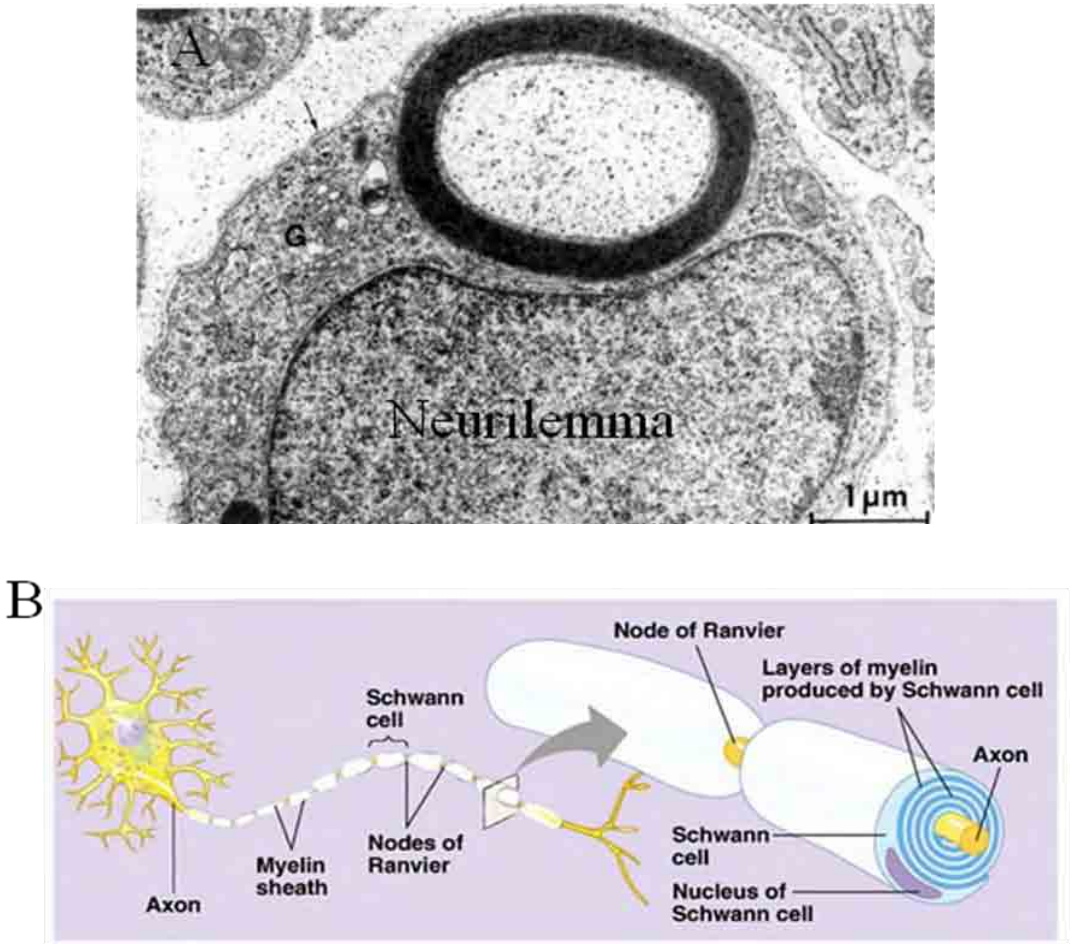

Figure 1-4 – Schwann Cell Structure

A. Micrograph of myelinating Schwann cell. The myelin sheath surrounds the peripheral axon forming barrier to ion transport. The bulk of the Schwann cell cytoplasm is in the neurilemma close to the external plasma membrane. Taken from http://dekmaihiso.web44.net/Neurons_I.html

B. Image of the myelinating Schwann cell surrounding the axon creating nodes of Ranvier down the axon enabling fast, energy efficient salutatory conduction. Taken from http://cc.oulu.fi/~aheape/Myelin3.gif

The role of Schwann cells in neuropathy is demonstrated by demyelination and onion-bulb formation, caused by repeated episodes of demyelination and remyelination as well as reduced nerve re-generation and reduced neurotrophism observed in models of neuropathy (28; 34). Glucose uptake into Schwann cells is insulin-independent (59). They highly express the enzyme aldose reductase (60), which has been implicated in glucose toxicity (61; 62) (see section 1.4.2.1). Together these make Schwann cells vulnerable to hyperglycaemic toxicity; hence Schwann cells have been identified as the critical focus of oxidative/nitrosative stress in diabetic models (28). Despite neuropathy progressing independently in Schwann cells and nerve most studies on neuropathy have been performed on whole nerves and the effects on Schwann cell signalling are not well understood (63).

Studies examining the effects of diabetes and hyperglycaemia on Schwann cells are limited; however, those conducted demonstrate clear Schwann cell dysfunction. Oxidative/nitrosative stress, poly(ADP-ribosyl)ation and inducible nitric oxide synthase (iNOS) protein expression are increased (64). Additionally there is altered arachidonic acid biosynthesis (65) and reduced neurotrophic factor-induced nerve growth factor secretion (66), the latter of which is restored with aldose reductase inhibition (67). Glial derived neurotrophic factor expression is increased in Schwann cells in models of diabetic as well as non-diabetic peripheral neuropathies, an effect correlated to axonopathic diseases (68). Nerve regeneration is also impaired in neuropathy and Schwann cells demonstrate altered neurotrophism in neuropathic models in response to injury. Nerve growth factor and insulin-like growth factor-1 expression are altered; these effects are reversed with aldose reductase inhibition (63). Lastly Myelin proteins P0 as well as myelin basic protein are both glycated in neuropathy, and animals with heterozygous knockout of peripheral myelin protein 22 suffer neuropathic-like symptoms (63).

1.4.2 Metabolic Deficits of Diabetic Neuropathy

The DCCT and UKPDS demonstrated the beneficial effect of tight glycaemic control on microvascular complications and identified hyperglycaemia as the initiating cause of tissue damage instigating microvascular complications. Most cells are able to regulate the intracellular glucose concentration and will maintain a constant intracellular glucose concentration independent of plasma glucose. However, those cells damaged by hyperglycaemia e.g. retinal pigment endothelial cells (RPE), mesangial cells as well as Schwann cells and neurones, are unable to effectively do this (2). Increased intracellular glucose results in the pathogenic complications through four main mechanisms, i) increased polyol pathway flux, ii) increased advanced glycated end product generation, iii) protein kinase C (PKC) activation and iv) increased hexosamine pathway flux.

1.4.2.1 Polyol Pathway

Aldose reductase is the first enzyme in the polyol pathway. Aldose reductase catalyses the reduction of toxic aldehydes produced by reactive oxygen species (ROS) into inactive alcohols. This process uses the cofactor NADPH which is oxidised to NADP+ (figure 1-5). Aldose reductase has low affinity (high Km) for glucose and in normal glucose concentrations metabolism of glucose through aldose reductase is very small (4). In the hyperglycaemic environment however, high intracellular glucose increases polyol pathway flux. The result is a large proportion of glucose being converted into the polyalcohol and osmolyte, sorbitol. Sorbitol is further oxidised into fructose by sorbitol dehydrogenase (SDH) using the cofactor NAD^+ which is reduced to NADH (figure 1-5). Increased polyol pathway flux augments intracellular sorbitol and fructose content, which has been seen in the lens (69) nerve (52; 70) and retina (71) of diabetic animal models.

There are a number of mechanisms by which this pathway contributes to the microvascular complications. The increase in intracellular sorbitol results in osmotic disturbances and compensatory efflux of other organic osmolytes such as myoinositol and the antioxidant taurine (72; 73). Depletion of these factors have been identified as key components in the complications of diabetes (74-76). Conversion of glucose into sorbitol by aldose reductase requires the cofactor NADPH, which is also required for the generation of the antioxidant reduced glutathione (GSH) as shown in figure 1-5. Aldose reductase-mediated depletion of NADPH results in the reduction of intracellular GSH observed in many different studies of diabetes (3; 4; 77), with aldose reductase inhibition restoring GSH content (78). The end-product of the polyol pathway is fructose. Although fructose feeds into glycolysis by conversion into fructose-1-phosphate by fructokinase, it is a much better substrate for non-enzymatic glycation than glucose. Hence, increased polyol pathway flux also results in an increase in non-enzymatic glycation. Finally increased aldose reductase flux also increases diacylglycerol (DAG) formation increasing PKC activation (3). Therefore increased polyol pathway flux increases intracellular sorbitol and fructose, whilst depleting NADPH and NAD+.

The importance of aldose reductase flux in the development of diabetic complications remains controversial, although it has been demonstrated that aldose reductase inhibition has many beneficial effects in animal models (52; 67; 79-83). Genetic studies have demonstrated patients with high aldose reductase expression are predisposed to complications such as neuropathy, whereas patients with a low aldose reductase expression have a lower susceptibility to such complications (58; 84). Diabetic mice that over-express aldose reductase in Schwann cells developed nerve GSH depletion and exacerbated nerve conduction

velocity deficits (85), whereas aldose reductase knockout mice are protected from GSH depletion and experimental neuropathy (86).

Although aldose reductase inhibitors, such as sorbinil showed promising results in animal models, clinical trials with these agents struggled to demonstrate efficacy and high levels of side-effects were reported (3). Since then, different versions of the drug have been trialed with some success. Fidarestat demonstrated good efficacy both at restoring sorbitol content and improving nerve conduction velocity, however, due to side-effects, phase three trials were halted in early 2000 (54). Data from more recent aldose reductase inhibitors such as Zenarestat and Ranirestat have proven to be more positive, both in reducing sorbitol content and improving nerve conduction velocity (54; 87). However, side-effects remain a complicating factor for Zenarestat where high creatinine levels were recorded, demonstrating kidney toxicity (3).

Currently the only aldose reductase inhibitor licensed for use is Epalrestat, which is licensed in Japan. Although well tolerated, the clinical benefits are limited and only high doses display benefits with slightly delayed onset of neuropathy (54). Even though aldose reductase inhibitors have been trialled for 30 years they still remain a promising therapeutic target and with each generation the efficacy improves while side effects decrease.

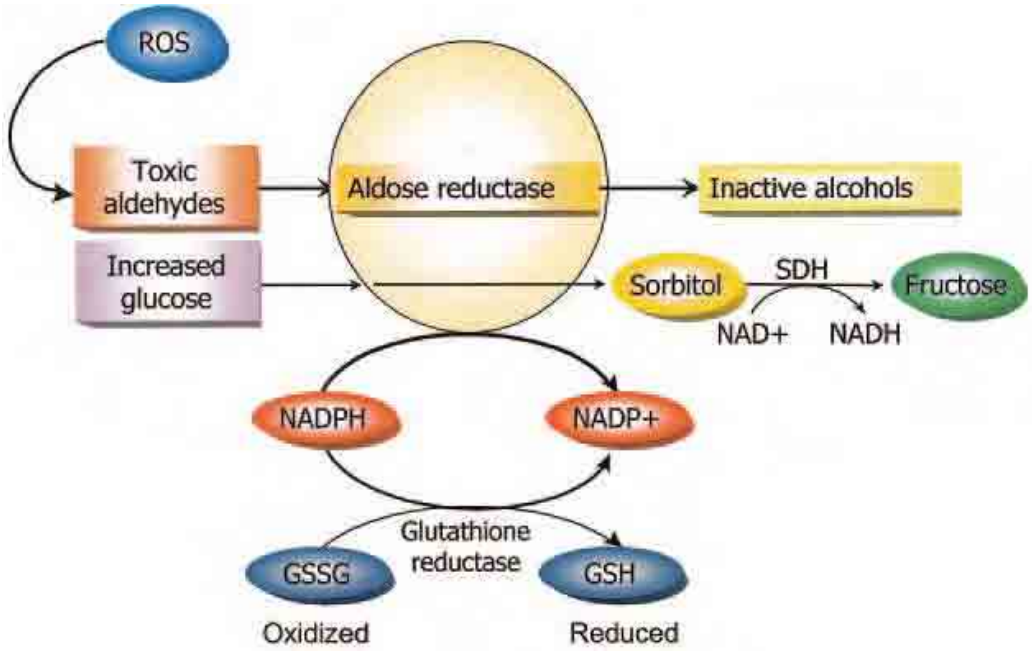

Figure 1-5 - The Polyol Pathway

Aldose reductase reduces toxic aldehydes produced by ROS into inactive alcohols and glucose into sorbitol using the cofactor NADPH, which is oxidised to NADP+. Sorbitol dehydrogenase (SDH) oxidises sorbitol into fructose using NAD+ as a cofactor. In hyperglycaemia, increased polyol pathway flux increases intracellular accumulation of sorbitol as well as fructose, whilst depleting NAD+ and NADPH, the latter of which is required for the regeneration of GSH. (2)

1.4.2.2 Advanced Glycated End Products

Protein glycation is the result of non-enzymatic addition of saccharides to proteins, lipids and nucleic acids. There are four major sources of advanced glycated end products (AGEs) in *vivo* which all originate from reactive carbonyl intermediates (88). These comprise i) intracellular oxidation of glucose to form glyoxal, ii) degradation of Amadori products, iii) aberrant metabolism of glyceraldehyde-3-phosphate and iv) dihydroxyacetone phosphate to form

methylglyoxal. These precursors react with amino groups of intracellular and extracellular proteins, lipids and nucleotides to form advanced glycated end products (AGE) (89; 90).

Glycation has been seen in transcription factors (91; 92), along with tubulin, neurofilament, axons in nerve fibres and myelin proteins in Schwann cells (88; 93). Glycated proteins have altered functions (2) and in models of diabetes, glycation of superoxide dismutase (SOD) reduces activity (94; 95).

AGE precursors can diffuse out of the cell and modify extracellular matrix components and plasma proteins. AGE modification alters the functional properties of several extracellular matrix proteins. For example AGE modification of type I collagen causes cross-linking and reduced elasticity in large vessels (4; 96). AGE modification of extracellular matrix proteins also interferes with the interaction between the matrix and the cell. For example AGE modification of laminin molecules reduces neurite outgrowth (4).

AGE modified plasma proteins can bind to the AGE receptor (RAGE) activating the receptor and triggering production of inflammatory cytokines. Activation of RAGE on macrophages and mesangial cells results in increased production of interleukin-1 (IL-1), insulin-like growth factor-1 (IGF-I), tumour necrosis factor-α (TNF-α), transforming growth factor-β (TGF-β), nuclear factor kappa beta (NFκB), macrophage colony-stimulating factor, granulocyte-macrophage colony stimulating factor and platelet derived growth factor (PDGF), resulting in increased iNOS expression and generating oxidative/nitrosative stress (2-4; 32). Diabetic RAGE knockout mice show significant improvement in diabetic peripheral neuropathy and display decreased expression of NFκB and PKC compared to wild-type diabetic models.

Although this decrease in NFκB and PKC was present in peripheral nerves and DRGs, the most pronounced effect was witnessed in Schwann cells (97).

Clinically, compounds capable of cleaving AGE have low efficacy and produce relatively high proportions of adverse events. For example aminoguanidine reduced Hb-AGE in patients, but no benefit was seen in neuropathic end-points and one trial had to be ended due to flu-like side effects and gastrointestinal disturbances (3; 98).

1.4.2.3 Hexosamine Pathway

The majority of intracellular glucose is metabolised through glycolysis, initially being converted into glucose-6 phosphate and then to fructose-6 phosphate before progressing through the rest of the glycolytic pathway. However, some fructose-6 phosphate is diverted from glycolysis through a glycolytic signalling pathway, the hexosamine pathway, as shown in figure 1-6. Here fructose-6 phosphate is converted into uridine diphosphate-N-acetyl glucosamine (UDP-GlcNAc), which donates GlcNAc to serine and threonine residues on transcription factors such as Sp1, often at phosphorylation sites.

In aortic endothelial cells, hyperglycaemia induces a 2.4-fold increase in the hexosamine pathway flux (4). This results in a 1.7 fold increase in Sp1 glycosylation by GlcNAc and a 70-80% decrease in serine/threonine phosphorylation, increasing Sp1 activity (99). This increased Sp1 activation is responsible for increased expression of genes including TGF-β and platelet plasminogen activator inhibitor PAI-1 (100), the expression of both is increased in hyperglycaemia (3).

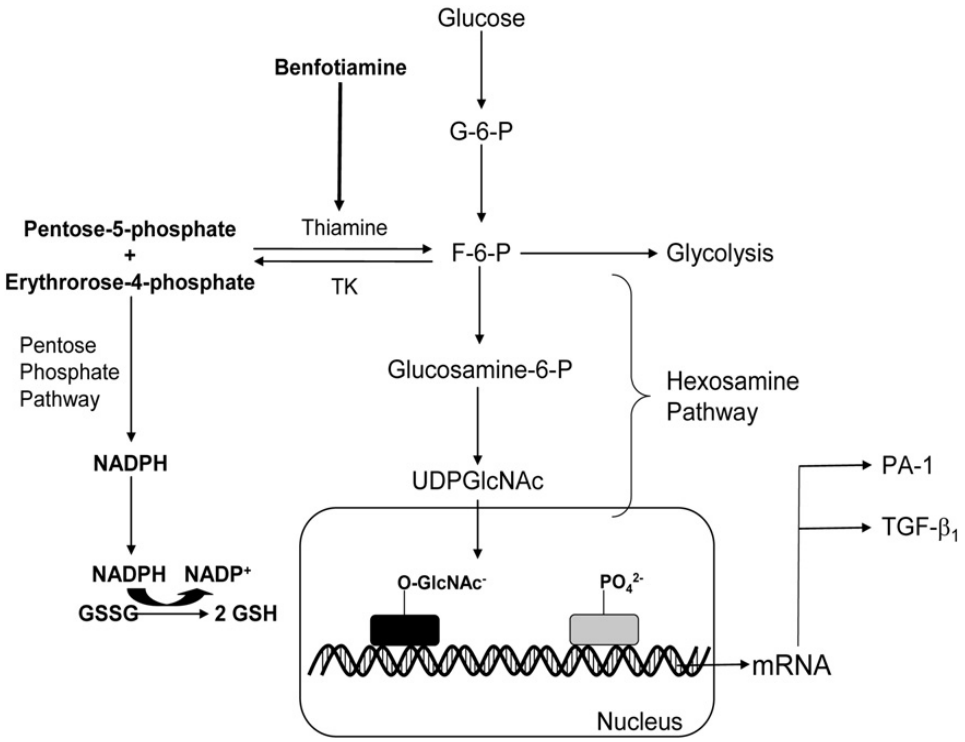

Figure 1-6 - The Hexosamine Pathway

Fructose-6 phosphate (F-6-P) is diverted from glycolysis into the glycolytic signalling pathway, the hexosamine pathway. Glucosamine:fructose-6 phosphate amidotransferase converts fructose-6 phosphate into glucosamine-6 phosphate which is then converted into diphosphate-N-acetyl glucosamine (UDP-GlcNAc). Glycosylation by the addition of GlcNAc is catalysed by O-GlcNAc transferase (OGT) which donates GlcNAc to serine and threonine residues on transcription factors such as Sp1. Glycosylation of Sp1 in this way increases production of PAI-1 and TGF-β1.

Benfotiamine is an analogue of transketolase (TK) which diverts fructose-6 phosphate away from glycolysis into the pentose phosphate pathway (3).

Benfotiamine is a lipophilic analogue of thiamine/vitamin B1 that diverts fructose-6 phosphate from the hexosamine pathway into the pentose pathway by activating transketolase, which converts fructose-6 phosphate into pentose-5 phosphate. This reduces both hexosamine

pathway flux as well as AGE whilst generating NADPH by increasing pentose-pathway flux. Clinical studies have demonstrated benfotiamine improves neuropathic pain as well as nerve conduction velocity and is currently available in the USA as a dietary supplement (3).

1.4.2.4 PKC Activation

PKC is a ubiquitous second messenger, the activation of which (primarily β and δ) is increased in various tissues in diabetic animal models, such as the retina (101), heart, aorta (102) and renal glomerulus (103-105). This is due to increased levels of *de novo* synthesis of diacylglycerol (DAG) which activates PKC. PKC activation has a plethora of effects, but one example is that increased activation of PKC-β which has been implicated in the over-expression of vascular endothelial growth factor (VEGF), PAI-1, NFκB and TGF-β, all associated with microvascular complications (3). PKC-β activation has also been implicated with vascular deficits, being associated with decreased NO production, reducing eNOS expression in cultured endothelial cells (106) and inhibition ameliorates vascular dysfunction in diabetic rats (105).

This same pattern does not follow in the nerve, where PKC activity is unchanged (104; 107; 108). Despite this, in STZ-D rats, selective PKC-β inhibition improved motor nerve conduction velocity, sciatic nerve blood flow and reduced nerve sorbitol content without affecting PKC-β activity within the nerve itself (108). This suggests the inhibitor may not have been acting directly upon the neurone and the beneficial effects observed were due to improvements in vascular deficits rather than metabolic components. This also potentially explains why ruboxistaurin, a competitive PKC-β inhibitor, that in clinical trials demonstrated effective management of retinopathy, nephropathy and endothelial vasodilation, does not have the same beneficial effect for neuropathy (3). This drug is in development for the US market

for treatment of retinopathy, but the Federal Drug Administration requires additional efficacy data before approval for patient use.

1.4.3 Oxidative stress

1.4.3.1 The Biochemistry of Oxidative Stress

A radical is a molecule with an unpaired electron (e^-) in the outer orbit which can initiate reactions by removal of an e^- from other molecules to complete its own orbital. The electronic structure of O_2 favours reduction by the addition of one electron at a time, generating oxygen radicals. Reactive oxygen species (ROS) such as superoxide (O_2^-) and hydrogen peroxide (H_2O_2) are generated naturally through biochemical processes such as oxidative phosphorylation and inflammation. These radicals are themselves highly reactive, however, they can also form even more reactive species such as the hydroxyl radical ($OH^\cdot$) and singlet oxygen (O_2^{2-}) (figure 1-7). Due to the highly reactive nature, the production of ROS is under tight control, however, when the cellular antioxidant capacity is overwhelmed by ROS production, oxidative stress occurs causing cellular damage (7; 109).

Oxidative stress will cause damage to all major macromolecules within cells, i.e. proteins, lipids as well as nucleotides. ROS are also able to attach to iron sulphur centres of enzymes, releasing the iron atoms and inhibiting enzyme function (7). Additionally $OH^\cdot$ reacts with proline, histidine, arginine, cysteine and methionine residues on proteins resulting in cross-linking, fragmentation and aggregation (109).

Phospholipids present in membranes are subject to lipid peroxidation. This is initiated by $OH^\cdot$ removing hydrogen from polyunsaturated fatty acids. The resulting lipid radical reacts with O_2 forming lipid peroxy radicals, lipid peroxide, 4-hydroxynoneal adducts (4HNE) and monoaldehyde (MDA), the latter two being commonly used to detect levels of lipid

peroxidation (110). One common product of lipid peroxidation is ‘age spots’ observed on the hands of the elderly. Lipid peroxidation products and the pigment lipofuscin cross-link causing brown spots to form. Lipid peroxidation also increases membrane permeability leading to increased Ca^{2+} influx. Ca^{2+} influx also occurs in organelles and increased mitochondrial Ca^{2+} may lead to apoptosis (109).

The most important consequence of ROS is damage to both mitochondrial and nuclear DNA. Since the majority of ROS arise from the electron transport chain (ETC), mitochondrial DNA (mtDNA) is more vulnerable to damage from ROS compaired with nuclear DNA. Damage to mtDNA will result in mutations affecting energy production. This would be most important in neurones with high energy demand. Nuclear DNA is protected to some degree from oxidant damage by the protective coat of histones; however, $OH^{\cdot}$ radicals can attack, especially where Fe^{2+} ions non-specifically bind to DNA, and result in single-strand DNA breaks (2; 7; 109).

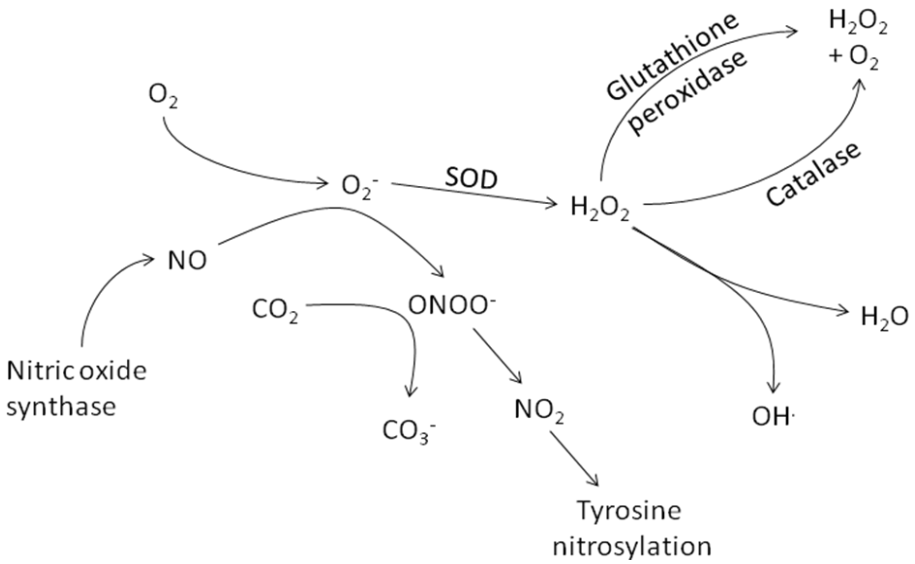

Figure 1-7 - The Formation and Decomposition of Reactive Oxygen Species

Superoxide (O_2^-) is formed from processes such as electron transport in the mitochondria and inflammation. O_2^- is converted into hydrogen peroxide (H_2O_2) by superoxide dismutase (SOD). H_2O_2 is converted into H_2O and O_2 by either glutathione peroxidase or catalase. In the presence of a metal, ion H_2O_2 will form the highly reactive hydroxyl radical ($OH^·$). Nitric oxide produced by NO synthase, can react with O_2^- forming the highly reactive peroxynitrite ($ONOO^-$). Peroxynitrite reacts with CO_2, forming CO_3 and NO_2 and the latter reacts with the aromatic ring of the amino acid tyrosine, forming covalent tyrosine nitrosylation.

1.4.3.2 Oxidative Stress in Diabetes

Increased oxidative/nitrosative stress has been implicated as a key pathogenetic pathway in the complications of diabetes (4; 7; 111; 112). Increased oxidative stress has been identified in the nerve (113-115), eye (71), vasculature, kidney (116; 117) and heart (118) in diabetic rodent models, and in diabetic patients (119-122). Each of the four pathways outlined in sections 1.4.2.1-4 as well as vascular dysfunction contribute unique stresses in diabetes, however they do have one end result in common; they all increase oxidative stress. The

unifying hypothesis states that oxidative stress is the main factor contributing to the metabolic and vascular components of microvascular complications of diabetes (2; 123).

Furthermore, excess glucose metabolism leads directly to the generation of oxidative stress. Glucose metabolism through the Krebs cycle generates electron donors NADH and $FADH_2$. In the ETC NADH donates electrons (e^-) to complex 1; $FADH_2$ donates e^- to complex 2. Both these complexes pass e^- to coenzyme Q (CoQ) from where the e^- are passed to complex III, cytochrome C, complex IV and finally to molecular oxygen from where they are reduced to form water. As e^- move through the complexes I, III and IV energy stored within the e^- is used to pump protons across the inner mitochondrial membrane into the intermembrane space, creating a potential difference across the inner mitochondrial membrane. This potential difference provides the energy for ATP synthase to add a phosphate to ADP, generating ATP (figure 1-8) (2; 4; 109).

Hyperglycaemia increases flux through glycolysis and the Krebs cycle, causing overproduction of both NADH and $FADH_2$, increasing the potential difference across the inner mitochondrial membrane (124). This occurs up to a point, at which electron transfer inside complex III is blocked causing e^- to back up at CoQ, which donates e^- to molecular oxygen, generating superoxide. This results in increased superoxide production (2; 4).

1.4.3.3 Antioxidant Treatment and Neuropathy

Considering the association between oxidative stress and diabetes, treatment with antioxidants has been an attractive prospect to reduce diabetic complications. The most thoroughly examined is α-lipoic acid (ALA) (also known as thioctic acid). ALA is a naturally occurring antioxidant found ubiquitously in animal products as well as plants such as spinach and

broccoli. ALA is a potent scavenger of ROS and RNS, and also reduces other antioxidants such as vitamin C and glutathione from their oxidised to reduced active state (125; 126).

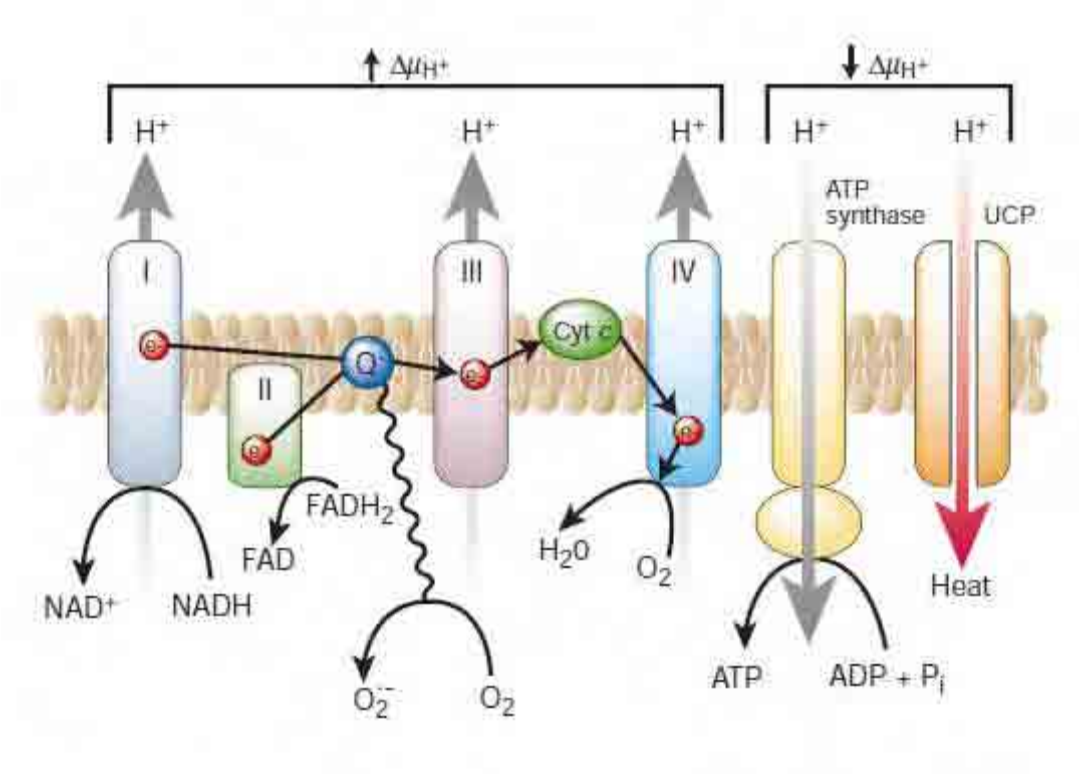

Figure 1-8 - The Electron Transport Chain

NADH and $FADH_2$ donate electrons to complex I and II. These pass electrons through complex Q and through complex III and IV. As complex I, III and IV the energy stored is utilised to pump protons across the inner mitochondrial membrane, into the inter-membrane space. The potential difference generated is used to drive ATP synthase which adds a phosphate (Pi) onto ADP to generate ATP. Alternatively, uncoupling proteins release the potential difference generating heat. This mechanism is utilised by hibernating animals, helping them to keep warm (4).

In animal models ALA corrects nerve growth factor deficits (127), sensory nerve conduction velocity, endoneurial blood flow, restores GSH and GSH/GSSG ratio and taurine content in the sciatic nerve of STZ-D diabetes (115). Clinical studies examining the effect of ALA

treatment on diabetes have shown significant improvements in some neuropathic symptoms and reduced nerve fibre degradation (128; 129). In a review of current clinical trials, Foster concluded ALA treatment improved neuropathic deficits and sensory symptoms, but not the pain associated with diabetes (130; 131). One difficulty with ALA treatment is achieving sufficient bioavailability. Although ALA is rapidly absorbed and plasma concentration is reached within 30 minutes to 1 hour, the drug also has a high clearance rate and the half-life is 30 minutes (131). Hence, clinical studies using parenteral administration have demonstrated more positive outcomes. Further large –scale trials with ALA are being conducted (3; 131).

1.4.3.4 Antioxidant Defence System

Oxidative stress is potentially damaging therefore ROS production, a consequence of many biochemical processes, is tightly controlled. There are enzymes e.g. superoxide dismutase (SOD) and catalase and small molecules (such as glutathione, taurine, vitamin C and E), that detoxify ROS and a balance exists between ROS production and the activity and abundance of these detoxifying molecules. In physiological situations increased ROS results in increased expression and activity of the antioxidant defence system, quenching ROS and reducing oxidative damage.

In diabetes, however, this does not always occur and although the response of the antioxidant defence system is tissue-specific, despite increased ROS production, the activity of one or more members is often reduced. This dysregulation exacerbates the effect of increased ROS production and tips the balance further towards oxidative damage, resulting in tissue damage. The action and response of each member is considered below.

1.4.3.4.1 Glutathione

Glutathione (GSH) is a major cellular antioxidant made up of a tripeptide consisting of glycine, cysteine and glutamic acid (γ-glutamylcysteinylglycine) (132). The sulphydryl group

(SH) of glutathione is able to reduce ROS, whereupon it becomes oxidised into oxidised glutathione (GSSG) (133). This protective action of GSH against ROS is facilitated by the interaction of GSH with enzymes such as glutathione peroxidase (GPx), where GSH acts as a cofactor. GPx is a selenium-containing antioxidant that catalyses the reduction of hydrogen peroxide as well as lipid peroxides (figure 1-7), using GSH as a cofactor, which is converted into GSSG. The reduction of GSSG back into GSH is performed by glutathione reductase, which uses NADPH as a cofactor and hydrogen donor (132; 134).

In diabetes, increased aldose reductase flux depletes the cellular pool of NADPH, required for the regeneration of GSH from GSSG by glutathione reductase. In concert the activity of glutathione reductase is reduced in experimental (77) as well as clinical diabetes (135). This in combination with increased ROS (hence GSH utilisation) results in GSH depletion in the nerve of diabetic rodents (75; 115) as well as immortalised mouse Schwann cells (65) and patients with diabetes (136).

1.4.3.4.2 Superoxide Dismutase

Superoxide dismutase catalyses the dismutation of superoxide into oxygen and hydrogen peroxide (figure 1-7), thereby reducing the chance of superoxide reacting with nitric oxide (NO) to form peroxynitrite. There are three different isoforms of SOD; SOD1 (Cu/Zn SOD) is cytosolic and contains a copper and zinc ions as metal cofactors (137). SOD2 (MnSOD) is contained in the mitochondria and contains a manganese metal cofactor and SOD3 (extracellular SOD) is secreted into the extracellular matrix where it forms glycosylated homotetramer with the extracellular matrix (138).

It is known that SOD 2 can be glycated on lysine residues reducing its activity (94) and this increased glycation and reduced activity have been observed in erythrocytes from diabetic

patients (95). Despite this, results from animal models as well as in cell culture have shown varied results with respect to SOD activity (65; 77; 139). In the nerve in STZ-D rats, SOD activity tended to decrease and in immortalised Schwann cells SOD activity was significantly decreased. Similarly, although clinical data have demonstrated reduced SOD activity in erythrocytes of diabetic patients with both type 1 and type 2 diabetes (140-142), the results have not been unanimous and many studies also observe increases in SOD activity (135; 143; 144).

1.4.3.4.3 Catalase

Catalase is a tetrameric enzyme consisting of four identically arranged subunits each containing a porphyrin haem centre (134). Catalase is located intracellularly in peroxisomes where, like glutathione, it decomposes H_2O_2 into H_2O and O_2 (see figure 1-7). As with SOD, variable results are observed in models of diabetes suggesting that responses maybe tissue-specific. Increases in catalase activity were observed in the heart, aorta and brain in animal models, but decreases in kidney, liver and erythrocytes (77). In nerve of STZ-D rats catalase tended to decrease, whereas in immortalised Schwann cells, there was no change in catalase activity (65). In clinical studies decreased catalase activity in erythrocytes isolated from diabetic patients (135; 142) was also discovered.

1.4.3.4.4 Antioxidant Treatment and Antioxidant Defence

The response of the antioxidant defence to antioxidant treatment appears to be both tissue- and drug-specific. For example, despite consistently reducing oxidative stress, ALA restores GSH, GSH/GSSG ratio, taurine content and reverses the trend to decrease in SOD and CAT activities in the nerve of STZ-D rats (115). In isolated immortalised mouse Schwann cells ALA, but not N-acetyl cysteine, restored GSH content; but ALA failed to restore SOD

activity (65). Although taurine reduced oxidative stress markers in nerve, it failed to restore GSH content only affecting the ascorbate/dehydroascorbate system (145). This suggests antioxidants affect different tissues to differing degrees and the response of the antioxidant defence system to hyperglycaemia may not represent oxidative stress present.

1.4.4 Nitric Oxide

Increased levels of nitrate and nitrite (NOx) have been observed in serum of patients with diabetes (142). Nitric oxide (NO) is a short-lived, second messenger generated by nitric oxide synthases (NOS), neuronal NOS (nNOS), inducible NOS (iNOS) and endothelial NOS (eNOS), also known as NOS I-III respectively. NOS catalyses the conversion of L-arginine into NO and L-citrulline, using the cofactor NADPH as an electron donor. Regulation of NO production from iNOS is thought to be primarily by *de novo* synthesis and mRNA stability (146). NO production from eNOS and nNOS is dependent upon phosphorylation by Akt, eNOS at Ser 1177 (147) and nNOS at Ser 1412 (148) and Ca^{2+} influx. NOS activation is dependent upon calmodulin. Calmodulin is constitutively bound to iNOS, however, the binding of calmodulin to eNOS and nNOS which results in their activation, is dependent upon Ca^{2+}. Therefore eNOS and nNOS activation is dependent upon elevations in Ca^{2+} concentration.

NO produced by each NOS has specific actions. The expression of iNOS is increased by cytokines and by NFκB which acts as a transcription factor. At high concentrations > 1μM NO produced from iNOS forms part of the inate immune system with direct cytotoxic actions on pathogens (149). At lower concentrations NO production by iNOS can modulate production of inflammatory cytokines indirectly after reacting with the superoxide anion (146; 150; 151) and iNOS inhibitors reduce inflammation (152). In diabetes, increased iNOS has

been seen in clinical as well as experimental models of diabetes e.g. in the retina (153; 154), heart (155), vascular endothelium (156), smooth muscle (157), human Schwann cells (64), retinal cells (158) and coronary artery endothelial cells (159). Increases in iNOS expression are thought to be linked to increases in inflammatory pathways mediated by NFκB and TGF-α (160-162). *In vitro a*ldose reductase inhibition as well as PARP-1 inhibition prevents increased iNOS expression (64; 163). In addition diabetic iNOS knockout mice have improved motor and sensory nerve conduction velocity compared to diabetic wild type mice (164).

In neurons nNOS is often localised close to NMDA (N-methyl-D-aspartic acid) receptors and is activated by glutamate binding. The subsequent Ca^{2+} influx (165), together with the NO generated, is able to mediate neurotransmission. Studies on nNOS expression in diabetes have produced varied results; nNOS expression is increased the retina (166; 167) and gastroduodenal tract (168) of STZ-D rats and in the kidney cortex of Otsuka Long Evans Tokushima Fatty rats (169), but is decreased in the kidney cortex of STZ-D rats (170) and in high glucose-treated, immortalized mouse Schwann cells (171). nNOS knockout STZ-D mice demonstrate improved motor and sensory nerve conductivity compared with diabetic wild type mice, suggesting an impact of increased nNOS expression (172).

NO production from eNOS activates signal transduction via cGMP initiating vasodilation. In diabetic neuropathy, vascular deficits are an important component of the condition. It would therefore be anticipated that eNOS expression and NO production would be reduced. However in models of diabetes eNOS expression is variable, for example eNOS expression increased (173) and decreaed in human aortic endothelial cells (174). eNOS knockout mice demonstrate accelerated nephropathy (175), but this may simply suggestthe local effects of

eNOS on the vasculature may be different from NO produced from either iNOS or nNOS (53).

Clinically, increases in nitrate and nitrite are observed in serum of patients with both Type 1 (176) and Type 2 diabetes (142; 144), demonstrating overall increased NO production. NO signalling is locally acting, therefore it is likely that dysregulation of each NOS contributes individual components in diabetic complications. For example, it is possible that increased iNOS expression is a consequence and contributing factor to increased inflammation in diabetes, nNOS affects neurological components and eNOS vascular deficits.

1.4.4.1 Reactive Nitrogen Species

As well as a signalling molecule, NO is a reactive radical which reacts with O_2^- forming highly reactive nitrogen species (RNS) such as peroxynitrite ($ONOO^-$) or nitrite (NO_2) (figure 1-7). These can further react with CO_2, or H^+ to form other RNS such as nitrosoperoxycarbonate ($ONOOCO_2^-$) and nitrogen dioxide (NO_2) (177). RNS are known to react with all classes of biomolecules such as transition-metal ions in metalloproteins, amino acid residues (thiols, amines and tyrosines) unsaturated lipids and DNA bases (178). The reactions between peroxynitrite and DNA can cause single strand breaks and nitration of guanine, which can activate PARP (179). Physiologically RNS protein modification, such as 3-nitrotyrosine and S-nitrosylation is used in cell signalling, however, excess protein modification may have pathological consequences. In diabetes, treatment of STZ-D mice with a peroxynitrite decomposition catalyst (FP15) corrected both motor and sensory nerve conduction velocities (180).

1.4.4.2 3-Nitrotyrosine

Protein tyrosine nitration is a covalent protein modification in which an NO_2 group is substituted onto *ortho* carbons of the aromatic ring of tyrosine. Peroxynitrite reacts with CO_2

generating CO_3^- and NO_2. NO_2 reacts with carbons in the aromatic ring of the amino acid tyrosine, forming covalent tyrosine nitration (181).

Tyrosine nitration can result in loss, gain or no change of function, however these modified proteins are also more susceptible to proteolytic degradation (182). There is speculation that nitrotyrosine is used in physiological cell-signalling, however definitive evidence is lacking. However, abundant evidence exists to suggest that pathological tyrosine nitration is increased in the lung in respiratory diseases such as asthma (183), cardiovascular diseases (184) and in the serum of diabetes patients (182; 185). In neuropathy increased nitrotyrosine levels have been observed in the peripheral nerve, spinal cord and dorsal root ganglion in animal models of both Type 1 and Type 2 diabetes and in cultured human Schwann cells exposed to high glucose (32).

Phosphorylation by the addition of a phosphate group from ATP onto a target residue is an essential mechanism for signal transduction. *In vitro*, protein tyrosine nitration has been seen to impair intracellular processes dependent upon tyrosine phosphorylation, e.g.tyrosine nitration has been seen to prevent phosphorylation of p34 cdc2 (cyclin-dependent kinase) (186), platelet cell adhesion molecule 1 (187) and a focal adhesion kinase (188; 189). Since many signalling pathways are dependent on tyrosine phosphorylation, widespread tyrosine nitration could inhibit many signalling pathway, for example, since, the insulin receptor is a tyrosine kinase, tyrosine nitration could patially inhibit tyrosine phosphorylation and affect insulin signalling, resulting in insulin resistance (190). In human umbilical vein endothelial cells in vitro both peroxynitrite and high glucose were shown to inhibit Akt activation at Ser473 and thus inhibit insulin signalling (191). Although this finding requires confirmation in other systems, it demonstrates a potential mechanism behind peripheral insulin resistance induced by hyperglycaemia.

1.4.4.3 S-nitrosylation

NO is also able to nitrosylate reduced sulphur (thiol) protein residues by formation of a nitrosylating intermediate N_20_3 (192). Nitrosylation occurs in a wide variety of proteins, most commonly on cysteine residues. S-nitrosylation will alter protein conformation, most commonly resulting in rapid degradation, but can also increase protein stablility (193), either way, the conformational change can alter protein function (194). Like nitration, nitrosylation can regulate protein function in physiology, however, hyper S-nitrosylation has been observed in many different disease pathologies such as Alzheimer's, asthma, pulmonary hypertension and both Type 1 and Type 2 diabetes (192).

In diabetes increased S-nitrosylation is attributed to increased iNOS expression and, like increased nitrotyrosine, is linked to insulin resistance. S-nitrosylation of Akt, the insulin receptor substrate 1 (IRS-1) and the insulin receptor β subunit are all increased in diabetic mouse models (195; 196). S-nitrosylation of Akt inhibits insulin mediated activation (195), whereas S-nitrosylation of the IRS-1 appears to target it for ubiquitination (197).

1.4.5 Poly(ADP-ribose) polymerase

There are a wide range of protein modifications which regulate protein function e.g. glycation, phosphorylation and ubiquitination. Poly(ADP-ribosyl)ation is the process by which ADP-ribose polymers (PAR) are attached via an ester bond to glutamic acid, aspartic acid or lysine residues, mediated by the enzyme poly(ADP-ribose) polymerase (PARP) (198). There are currently 18 known members of the PARP family, two of which, PARP1 and 2 are known to play a role in DNA repair (198). PARP1 binds as a homodimer to single-strand

DNA breaks, or nicks, where it is activated and catalyses the cleavage of nicotinamide adenine dinucleotide (NAD+) forming nicotinamide and ADP-ribose, the polymers of which are added to nuclear proteins (199; 200).

Increased oxidative/nitrosative stress seen in diabetes results in DNA damage and PARP1 activation (3; 7; 201). In both isolated culture as well as animal models of diabetes, both increased activation of PARP1 as well as increased PAR have been observed. Although PARP1 plays a beneficial role in DNA repair, it is possible that hyperactivation in diabetes leads to detrimental effects (3; 200). Excess cleavage of NAD+ by PARP, would exacerbate the effect of increased flux through sorbitol dehydrogenase further depleting NAD+, leading to energy dysfunction (3). In addition NAD+ is required as a cofactor for the conversion of glyceraldehyde dehydrogenase (GAPDH). GAPDH is modified with ADP-ribose polymers in response to diabetes- induced superoxide, reducing GAPDH activity (99; 202). Reduced flux through GAPDH will increase the abundance of the glycolytic intermediates such as glucose and fructose-6 phosphate, which will increase flux through the polyol and hexosamine pathways respectively as well as increasing AGE formation (2) (figure 1-9).

In models of diabetes increased PAR and PARP-1 activation are corrected by both aldose reductase inhibitors as well as a peroxynitrite decomposition catalyst, FP15 (203). In addition PARP inhibition reduces oxidative/nitrosative stress as well as iNOS expression in high glucose-treated human Schwann cells (64) as well as improving thermal hypoalgesia, mechanical hyperalgesia, nerve conductivity and restoring intraepidermal nerve fibre loss in animal models (203-205).

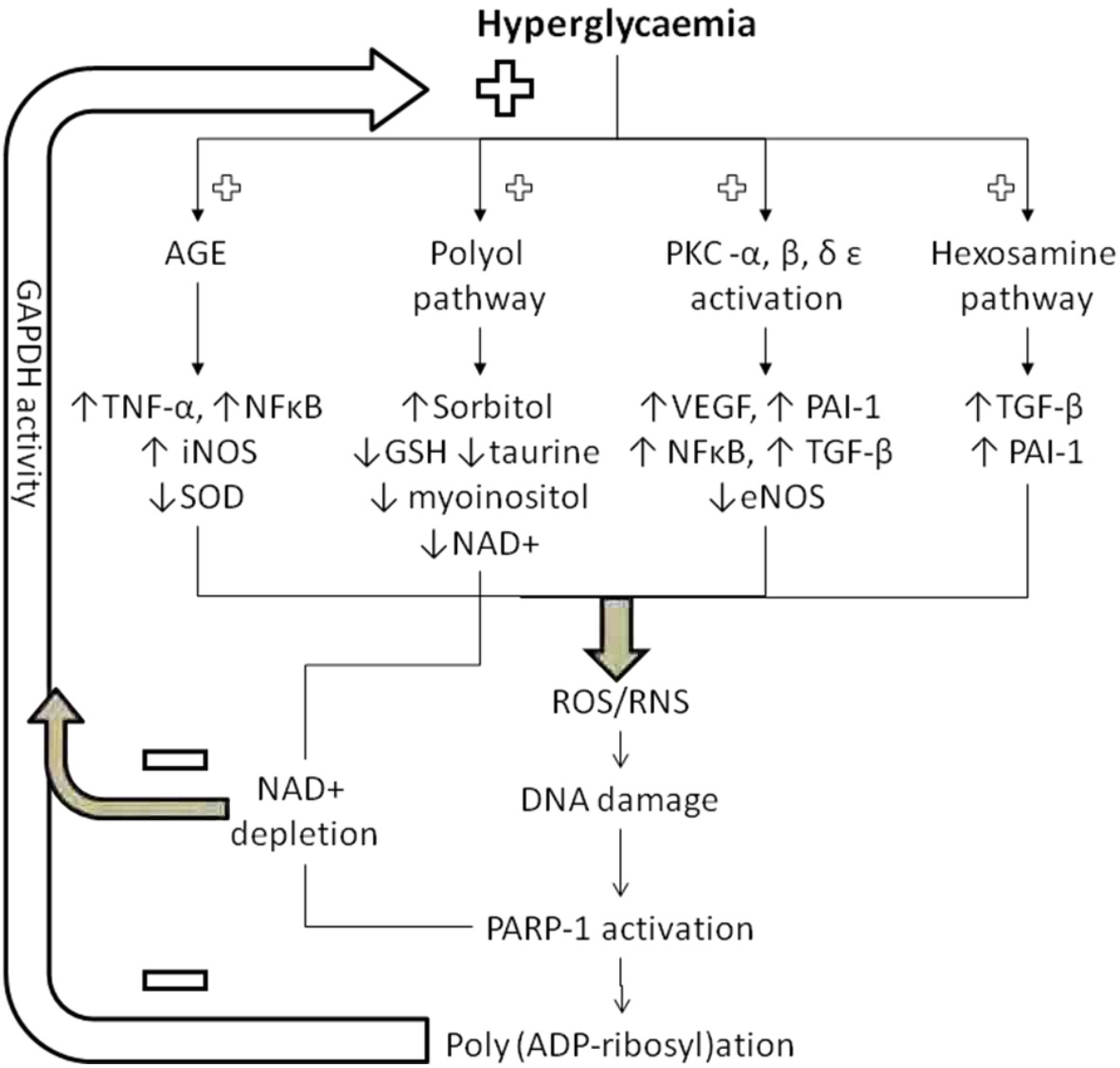

Figure 1-9 - Feed-Forward Cycle of Microvascular Complications

The four major pathways of microvascular complications (increased AGE, increased polyol flux, increased PKC activity and increased hexosamine pathway flux) all increase oxidative/nitrosative stress. This induces DNA damage and PARP-1 activation. PARP-1 activity depletes NAD+ , which exacerbates the effect of increased flux through sorbitol dehydrogenase also decreasing NAD+. PARP-1 adds poly(ADP-ribose) residues onto nuclear proteins, including GAPDH. Combined the reduction in NAD+ along with poly(ADP-ribosyl)ation of GAPDH reduces GADPH activity, resulting in back-up of glycolytic intermediates such as glucose and fructose-6 phosphate. This acts as a feed-forward cycle further increasing AGE, PKC activity and flux through polyol and hexosamine pathways, exacerbating the effect of hyperglycaemia.

1.4.6 Mitogen Activated Protein Kinase

Mitogen activated protein kinases (MAPK) are a group of serine/threonine kinases that are activated by phosphorylation at conserved tyrosine and threonine residues, in response to extracellular stimuli. There are three main groups of MAPKs i.e. p38 MAPK, extracellular signal-regulated kinases (ERK, also known as p42/44 MAPK) and c-Jun N-terminal kinase/ stress activated protein kinase (JNK/SAPK, also known as p46/54 MAPK) each of which consist of several isoforms (206). Each MAPK has a specific signalling cascade leading to activation (figure 1-10). The first member of the cascade is a MAPK kinase kinase (MAPKKK), which is activated by small GTP-binding proteins that phosphorylate and activate MAPK kinase (MAPKK) (207). These phosphorylate and activate the MAPKs themselves, which subsequently phosphorylate their nuclear and cytoplasmic targets. Each signalling cascade is specific for the MAPK. Each MAPKK has specificity to the MAPK subgroup and each MAPK has a unique set of targets upon which it acts, causing a variety of effects (206). For example in Schwann cells p42/44 MAPK activation is required for survival and proliferation as well as synthesis of growth factors such as BDNF, NGF or GDNF (6). P38 MAPK and JNK/SAPK mediate cellular stress with activation of both, increased in response to oxidative, nitrosative stress and osmotic stress (59; 190). Aditionally MAPK signalling cascades are also facilitated by scaffold proteins. Although these have no enzymatic activity, they organise the specific MAPK pathways enabling simultaneous interaction, increasing efficiency.

As with many signalling cascades, MAPK activity depends upon the balance between phosphorylation and dephosphorylation. Mostly activation of MAPK is transient with phosphorylation/dephosphorylation occurring rapidly and MAPK are only phosphorylated for

a matter of minutes (207). Dephosphorylation of MAPK is mediated by MAPK phosphatases (MKP) (6). MKPs are divided into three groups, depending upon their preference for (i) dephosphorylating tyrosine, (i) serine/threonine or both (iii) tyrosine and threonine (6; 207).

In diabetes, MAPKs have been seen as the transducers between hyperglycaemia and the biochemical stress in diabetic complications. Increases in p38 MAPK and JNK/SAPK phosphorylation have been observed in DRGs (208) and sciatic nerve (209) of STZ-D rats as well as in hyperglycaemia-treated immortalized Schwann cells (210) and sural nerves from patients with end-stage neuropathy undergoing lower-limb amputations (208). There also is evidence demonstrating an association between activation of p38 MAPK and JNK/SAPK in relationship to chronic pain in diabetic neuropathy (211).

P38 MAPK is a mediator of osmotic stress and is thought to be involved in aldose reductase regulation (212; 213). Aldose reductase inhibition reduces p38 activation and specific inhibition of p38 MAPK also prevents the diabetes-induced reduction in motor and sensory nerve conduction velocity (209). The downstream consequences of increased JNK/SAPK are less clear. JNK/SAPK activation can have a neuroprotective role in sensory neurons. In antioxidant treated STZ-D rats the normalisation of nerve conduction velocity was associated with further increases in JNK/SAPK activation (214). However, in aldose reductase knockout mice there was no increase in JNK/SAPK activity in response to diabetes (86), and treatment of STZ-D rats with an aldose reductase inhibitor reduced JNK/SAPK activation (215). The discrepancy between the data may demonstrate cell and model specificity as well as the use of regenerating/non-regenerating models with JNK/SAPK not active in non-regenerating models (6).

The response of p42/44 MAPK is more varied than either p38 MAPK or JNK/SAPK. Many studies have demonstrated increases in p42/44 in DRGs from STZ-D rats (208) sciatic nerves from STZ-D rats (216) as well as in high glucose- exposed human RPE cells, where the increase was linked to increases in iNOS. However, no change was seen in p42/44 MAPK in sural nerves from STZ-D rats (217) and no consistent results seen in immortalised Schwann cells treated in 25 mM glucose (210). Inhibition of p42/44 MAPK reduced hyperalgesia in STZ-D rats (218), iNOS expression, but neither ROS nor cell viability in RPE cells (219).

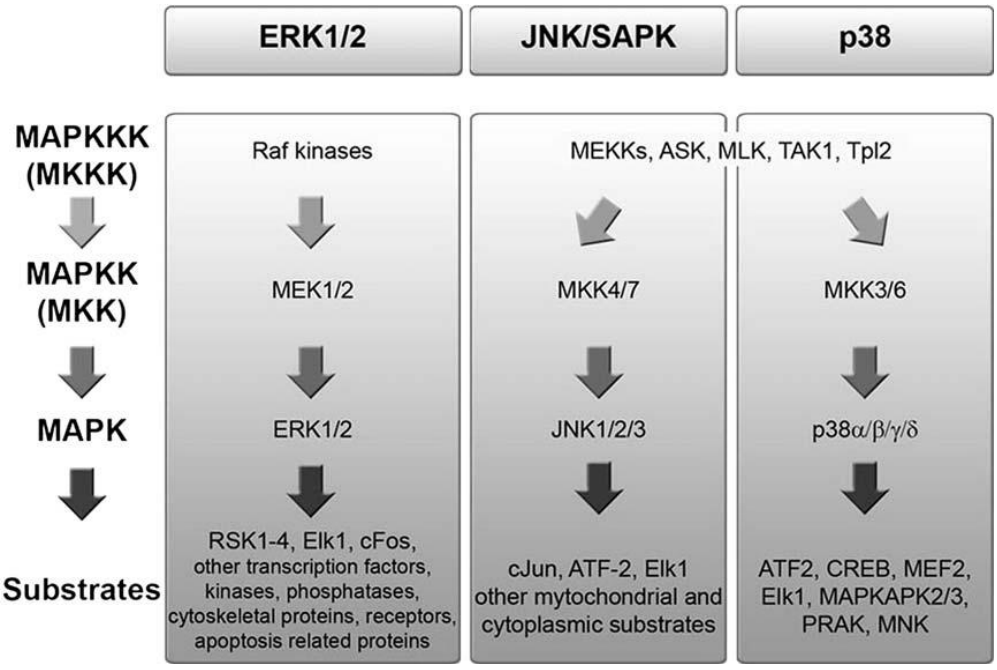

Figure 1-10 - MAPK Signalling Pathways

Each MAPK subgroup is part of a three kinase cascade with unique MAPKK and effectors (6).

1.4.6 Akt/ Protein Kinase B

Akt/ Protein kinase B (PKB) is a serine/threonine kinase with a pleckstrin homology domain (PH) in its NH2 terminal region and a catalytic domain that is closely related to protein kinase C (PKC) and protein kinase A (PKA) (8; 190). Akt is activated by receptor tyrosine kinases (RTK) by a variety of stimuli such as growth factors, cytokines or insulin. Upon insulin binding, the RTK dimerises, resulting in autophosphorylation and downstream phosphorylation of insulin receptor substrate (IRS) 1 and 2. Phosphorylation of IRS provides binding sites for phosphatidylinositol 3-kinase (PI3K), which binds at the SH2 domain, of IRS producing phosphatidylinositol 3-phosphate (PI3P) (8). Akt has an affinity for PI3P via the plecstrin homology domain (PH) and binding of Akt to PI3P triggers translocation of Akt to the plasma membrane (220; 221). The increase in phosphoinositides also activates phosphoinositol- dependent kinases (PDK1 and PDK2), which activate Akt upon its membrane translocation by phosphorylation at threonine 208 and serine 473 (figure 1-11) (222). Dephosphorylation of Akt is performed by protein phosphatases such as protein phosphatase 2A, protein tyrosine phosphatase or agonists of Akt such as ceramides.

The downstream targets of Akt are many and varied, such as modulating growth and cell survival, increasing nitric oxide production by phosphorylation of eNOS at serine 1177/1179 (147), influencing glucose metabolism via glucose transporter 4 (Glut4), or glycogen-synthase kinase-3 (GSK-3) (figure 1-11) (8). Upon activation by the insulin receptor, Akt associates with vesicles containing Glut4 inducing translocation of the vesicles to the plasma membrane, whereby Glut4 mediates glucose uptake (220). Akt also promotes glycogen synthesis by phosphorylating and inactivating GSK-3(222); when active GSK-3 inhibits glycogen synthesis by phosphorylating glycogen synthase, shown in figure 1-11.

Considering the involvement of Akt on insulin signalling and glucose uptake it is not surprising that Akt has been investigated in models of insulin resistance, or that Akt phosphorylation is reduced in models of both Type 1 and Type 2 diabetes. What is unclear, however, is whether the reduction in Akt phosphorylation is secondary to insulin resistance/impaired insulin secretion, or due to prolonged hyperglycaemia. Consequences of prolonged hyperglycaemia such as ROS and RNS (190) as well as glucosamine, a product of the hexosamine pathway, reduce Akt activation (124; 223). The potential downstream effects of reduced Akt activation are unclear; however, it is possible this could contribute to secondary insulin resistance in type 1 patients. Reductions in Akt phosphorylation could also contribute to vascular dysfunction, by reducing NO production from eNOS. In addition considering the essential role Akt has in growth and cell-cycle progression, reduced Akt activation may reduce cell survival and lead to increased apoptosis.

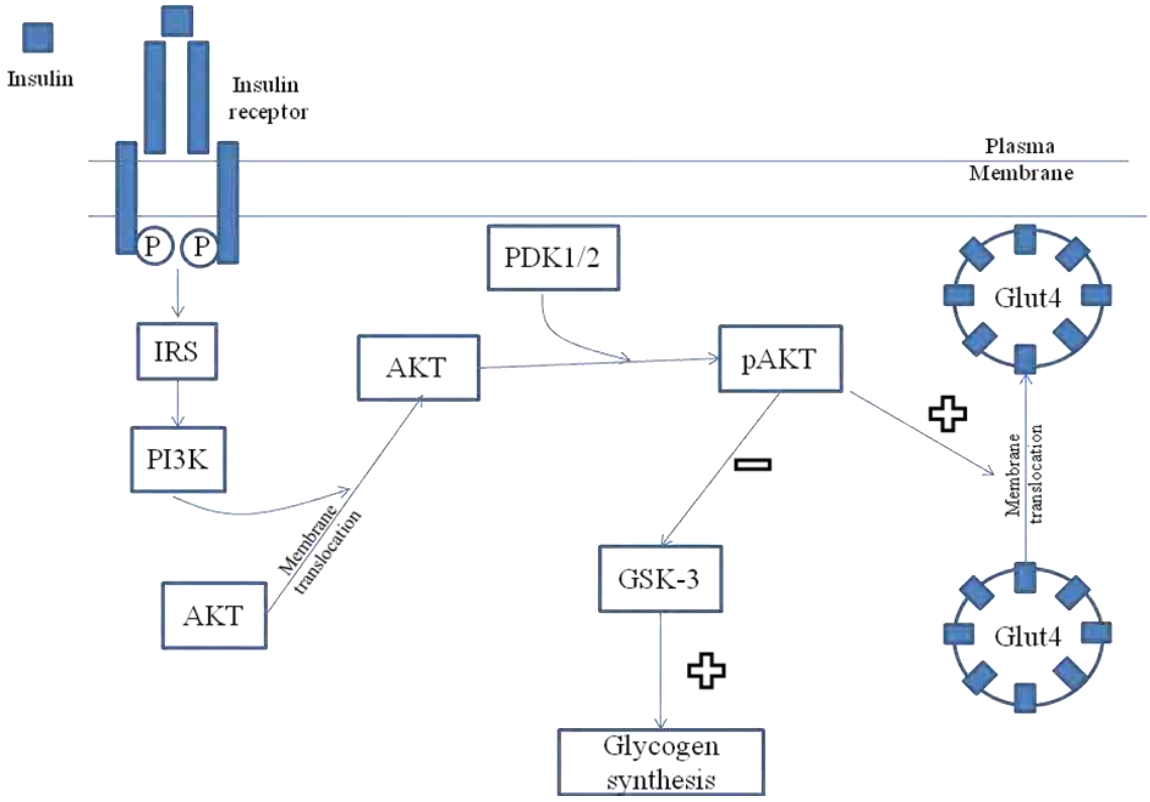

Figure 1-11 - Insulin Signalling via Akt

Insulin binding to the insulin receptor phosphorylates and activates the insulin receptor substrate (IRS), providing a binding for phosphatidylinositol 3-kinase (PI3K), which binds at the SH2 domain. This produces phosphatidylinositol 3-phosphate, which induces Akt translocation to the plasma membrane. PI3K also increases abundance of other phosphoinositides which activate phosphoinositol dependent kinases (PDK1/2), which in turn phosphorylate and activate Akt. Activated Akt is involved in translocation of Glut4 containing vesicles to the plasma membrane and also inactivates glycogen-synthase kinase-3 (GSK-3), increasing glycogen synthesis (8).

1.5 Taurine

Taurine (2-aminoethanesulphonic acid) (figure 1-12) is a free amino acid found as zwitterions in most body fluids. Taurine was first discovered in 1827 as a component of bile (224) where taurine plays an essential role in conjugation to bile acids thus enabling solubility at physiological pH (224). Taurine has since been found to act as an organic osmolyte, an antioxidant, a scavenger of carbonyl compounds, a modulator of cytosolic calcium, an analgesic, and to have neurotrophic properties (75; 76; 113; 145; 225; 226).

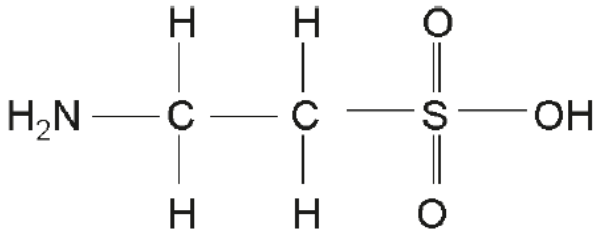

Figure 1-12 - Chemical Structure of Taurine (2-aminoethanesulphonic acid)

Humans have relatively low levels of taurine synthesis and are dependent upon dietary taurine intake. Taurine is therefore described as being conditionally essential. Taurine is found ubiquitously in animal products along with nuts, legumes and sulphur rich vegetables such as sprouts, cabbage, onions, garlic and turnips. Taurine deficiency is rare; however, it has been seen in both vegans (227) as well as patients with diabetes. The uncommon nature of taurine deficiency is, in part due to the ability to synthesise taurine from cysteine (see section 1.5.1) and partly due to the inverse regulation of taurine transport in the renal proximal tubules (228). TauT expression is down-regulated in the proximal tubule in response to high taurine

diet and increased following taurine deprivation, hence, regulating the taurine body pool. Newborn children however, have very low capacity to either synthesise, or preserve taurine stocks (74), hence since the 1970's taurine has been added into baby formula. Taurine is also required for normal skeletal muscle function (229).

1.5.1 Taurine Biosynthesis

Taurine is synthesised from cysteine by metabolism through the cysteine sulphate pathway (figure 1-13). Cysteine is oxidised to cysteine sulphinic acid by cysteine dioxygenase, which is then decarboxylated by cysteine sulphinate decarboxylase (CSD) to form hypotaurine. This latter step is rate-limiting, hence the capacity for taurine synthesis is thought to be dependent upon the level of CSD. All cells appear capable of different levels of taurine synthesis, with CSD activity higher in the liver and brain than in the sciatic nerve (230) and maybe absent from the axon altogether (5; 230; 231). CSD activity has not been measured in Schwann cells. All mammals are dependent upon dietary taurine intake (232), however, levels of taurine synthesis varies between mammals. Rodents such as rats and mice have high levels of taurine synthesis, compared to humans (5; 230; 233; 234). Cats do not express CSD and are entirely reliant upon dietary taurine intake; as such cats with taurine- restricted diets have been used as models of taurine deficiency.

1.5.2 Taurine Transporter

The plasma taurine concentration is approximately 50 μM (235) whereas the intracellular taurine concentrations range from 5-50 mM (74; 236; 237) varying due to the demand for taurine. For example leukocytes have high taurine concentrations 20-50 mM, due to the ability for taurine to scavenge HOCl generated during an inflammatory response (74). This high intracellular taurine concentration is achieved by active transport across the cell membrane, mediated by a high affinity low capacity transporter known as the taurine transporter (TauT). The active transport of taurine across the cell membrane is dependent upon the movement of $2Na^+$ ions and one Cl^- ions per taurine molecule. The energy required for taurine transport is derived from the movement of sodium down its electrochemical energy gradient generated by the Na^+K^+ ATPase and taurine uptake is by secondary active transport (228; 236).

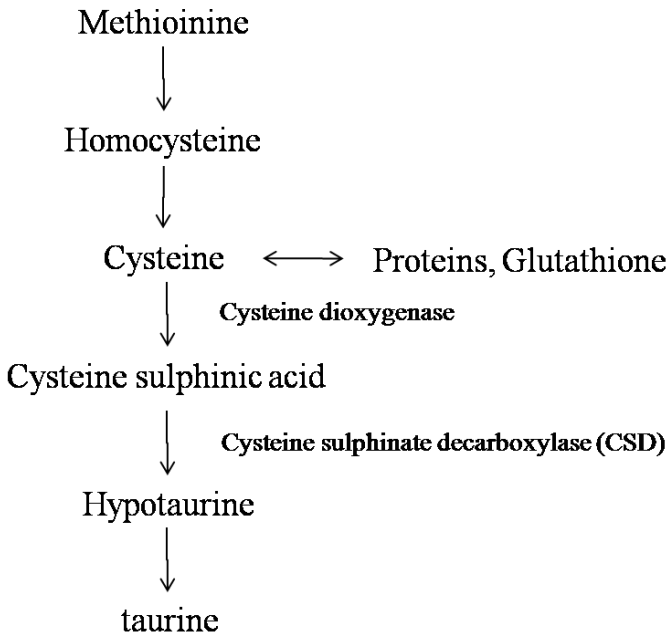

Figure 1-13 – Taurine Biosynthesis

Pathway of taurine biosynthesis from cysteine and methionine (5)

Intracellularly it is unclear whether taurine is evenly concentrated across the cytoplasm, whether there are intracellular stores of taurine, or even whether there are different concentrations in organelles such as the mitochondrial or nucleus. The case is the same for TauT. It is unclear whether TauT protein is expressed entirely on the cell membrane, if there are intracellular stores of TauT or even if TauT it is required for the movement of taurine into the mitochondria. Since there is an unsaturable Na^+-independent taurine uptake it is possible that TauT is only required for the intracellular concentration of taurine and the transporter is not required for taurine movement between organelles.

1.5.3 Taurine Deficient Animal Models

Cats have very low levels of CSD expression and are reliant upon dietary taurine intake; hence cats were used as a model for taurine deficiency. Cats deficient in taurine suffer taurine deficiency syndrome, characterised by CNS dysfunction, growth retardation and immune deficiency (5) and interestingly blindness caused by retinal degradation (238).

As well as cats being used as a taurine deficient animal model, the TauT knockout mouse has also been developed (239). Although the levels of CSD are higher in all mice compared to humans, taurine concentrations were decreased by about 98% in skeletal and heart muscle, by 80 to 90% in the brain, kidney, plasma, and retina and by 70% in the liver. The intracellular taurine content has not been recorded (240), however, this does demonstrate an important model illustrating the importance of TauT for sufficient taurine content. In a similar manner to taurine-deficient cats, the most prominent morphological feature of TauT knockout mice is retinal degeneration with a rapid loss of the photoreceptor cells due to apoptosis (239).

Although there is no recorded reduction in lifespan TauT knockout mice do suffer age-related disorders such as visual, auditory and olfactory dysfunctions along with liver fibrosis (239).

Unfortunately despite the studies which have been performed on taurine-deficient animal models, none has explored the similarities between taurine-deficient animal models and diabetic animals. Neither have they explored the effects on Schwann cell function or nerve conductivity, the effects of which maybe subtle and therefore require specific measurement. The TauT knockout model does however demonstrate the importance of TauT expression for maintaining sufficient circulating and tissue taurine content.

Studies have been conducted in both cell culture and animal models using guanidinoethane sulfonate (GES) as a competitive inhibitor for taurine uptake. These studies are commonly used to investigate the effects of taurine as a neurotransmitter, for example demonstrating taurine activation of glycine receptors in subplate neurons in the rat cerebral cortex (241) or enhancing corticostriatal neurotransmission in the rat forebrain via gamma-aminobutyric acid and glycine receptors (242) . Corresponding to animal models, no studies have been conducted specifically exploring the effects of GES in diabetes.

1.5.4 Molecular Identity of the Taurine Transporter

TauT has been cloned from various tissues and animal species such as mouse (243) and rat brain (244), dog renal MDCK (Madin-Derby canine Kidney) cell line (245), human thyroid (246) placenta (247), retinal pigment epithelial cell line (248), mouse retina (249) and bovine endothelial cells (250). These have demonstrated that TauT shares up to 90% sequence

similarity between mammals, illustrating the importance of TauT in mammals. These studies also showed that TauT belongs to the super-family of Na^+ and Cl^- dependent transporters, such as those for serotonin, dopamine, noradrenalin, γ-aminobutyric acid (GABA) and creatinine (237). The TauT gene is located on human chromosome 3p21-25, encoding a protein between 590 and 655 amino acids in length with a molecular weight of approximately 65-70kDa. Hydropathy plots indicate there are 12 transmembrane regions with the protein having intracellular C and N terminals (237).

1.5.4.1 Gating of Transport

Several potential phosphorylation sites have been identified on TauT that affect taurine transport. Han et al., 1999 identified Ser 322 on S4 loop as a location for PKC phosphorylation leading to reduced taurine affinity (251). Furthermore by substituting charged residues in the S4 loop, other amino acid residues on S4 were found to play an important role in the gating of taurine transport by altering the Km of the transporter, demonstrating direct interaction between this loop and taurine binding (236). In addition elevations in cAMP and subsequent PKA activation increased taurine uptake, an effect blocked by PKA inhibition (228). As for PKC-mediated phosphorylations, these effects were shown to alter TauT affinity for taurine rather than its expression, (252; 253). In these studies however, the site of PKA phosphorylation was not ascertained.

1.5.4.2 Regulation of Expression

The compatible osmolyte hypothesis suggests organic osmolytes are co-ordinately regulated; hence accumulation of one leads to depletion of another. Accumulation of sorbitol leads to depletion of other organic osmolytes such as myoinositol and taurine, which occurs through TauT downregulation. In common with the function of taurine as an osmolyte, the promoter region of TauT contains a tonicity response element (TonE) and TauT expression is increased

in hypertonic conditions. The other major function of taurine is as an antioxidant and the TauT promoter also contains an antioxidant response element (ARE) and expression is increased in pro-oxidant conditions. In addition TauT expression is also upregulated by NO donors and down regulated by glucose, calmodulin as well as taurine. The promoter region of TauT has been identified in both rat (254) and human leukocytes (73). These studies also demonstrated TauT promoter region contains binding sites for proto-oncogenes such as p53, WT1, ERG the activator protein 1 (AP-1) as well as two oestrogen receptor half sites and the transcription factor Sp1 (236), the activity of which is increased by increasing hexosamine pathway flux.

1.5.5 Taurine Efflux Pathway

Taurine efflux pathway has been measured pharmacologically and is mediated by the volume sensitive organic-anion channel (VSOAC) which is an unselective mediator of efflux of organic osmolytes such as myoinositol, glutamate, betaine, sorbitol and taurine (255). Regulation of VSOAC is by osmolarity with hypotonicity inducing taurine efflux. Unlike taurine uptake, efflux is independent of Na^+, Cl^- (256) as well as extracellular taurine (236). It is unsaturable and taurine flow is linear down the concentration gradient, all characteristics typical of an ion channel (256). However, the molecular identity of VSOAC has not yet been identified, nor whether the changes observed in diabetes, (i.e. sorbitol accumulation), affect function.

1.5.6 Taurine and Diabetes

No studies exist comparing the effects of taurine deficiency and diabetes in either cats or TauT knockout mice. The clearest similarity is the retinal degradation suffered by both. Patients with poorly controlled diabetes have high urinary taurine excretion (5) and in patients with either Type 1 or Type 2 diabetes, platelet and plasma taurine concentration is reduced (74; 235; 257). In addition an inverse correlation between HbA1c and log plasma taurine content has been observed (257). This reduction in taurine is due to a reduction in renal taurine reabsorption (258) and hyperglycaemia causes taurine depletion in major sites of diabetic complications such as the nerve, lens (259), RPE cells (73) and mesangial cells (260).

1.5.6.1 TauT Regulation in Diabetes

The down regulation of TauT by high glucose was first demonstrated by Stevens et al. 1999 (261) in retinal pigment epithelial cells (RPE) where glucose decreased taurine transport and TauT expression. This observation has since been repeated in erythrocytes isolated from patients with Type 2 diabetes, where taurine uptake via TauT was reduced compared to non-diabetic controls (235). TauT downregulation in the vascular endothelium, Schwann cells, axons and neurovasculature would result in taurine depletion in key sites implicated in diabetic neuropathy.

The proposed mechanisms mediating this down-regulation are shown in figure 1-14. One mechanism centres on the increased aldose reductase flux and accumulation of the organic osmolyte, sorbitol, seen in hyperglycaemia. The increase in intracellular sorbitol causes a compensatory decrease in intracellular osmolytes such as myoinositol and taurine. This occurs in concert with the compatible osmolytes hypothesis studying that organic intracellular

osmolytes respond co-ordinately to changes in external osmolarity. Confirming this hypothesis, Nakashima et al., 2005 (73) demonstrated that RPE cells which express high levels of aldose reductase have lower TauT expression and taurine content than low aldose reductase- expressing RPE cells.

As well as increased aldose reductase flux, protein kinase C (PKC) isoforms are upregulated in diabetes and by hyperglycaemia (see section 1.4.2.4). PKC activation is able to reduce taurine uptake both by reducing TauT expression (5) as well as function (236). In RPE cells exposed to high glucose, inhibition of PKC with bisindolylmaleimide (BIM) overcomes the glucose-induced reduction in taurine uptake (261), demonstrating the effect of PKC activity on taurine transport. The Na^+ gradient required for taurine uptake is generated by the Na^+K^+ ATPase. The activity of Na^+K^+ ATPase reduced in the diabetic nerve, acts to reduce the Na^+ gradient and therefore taurine uptake.

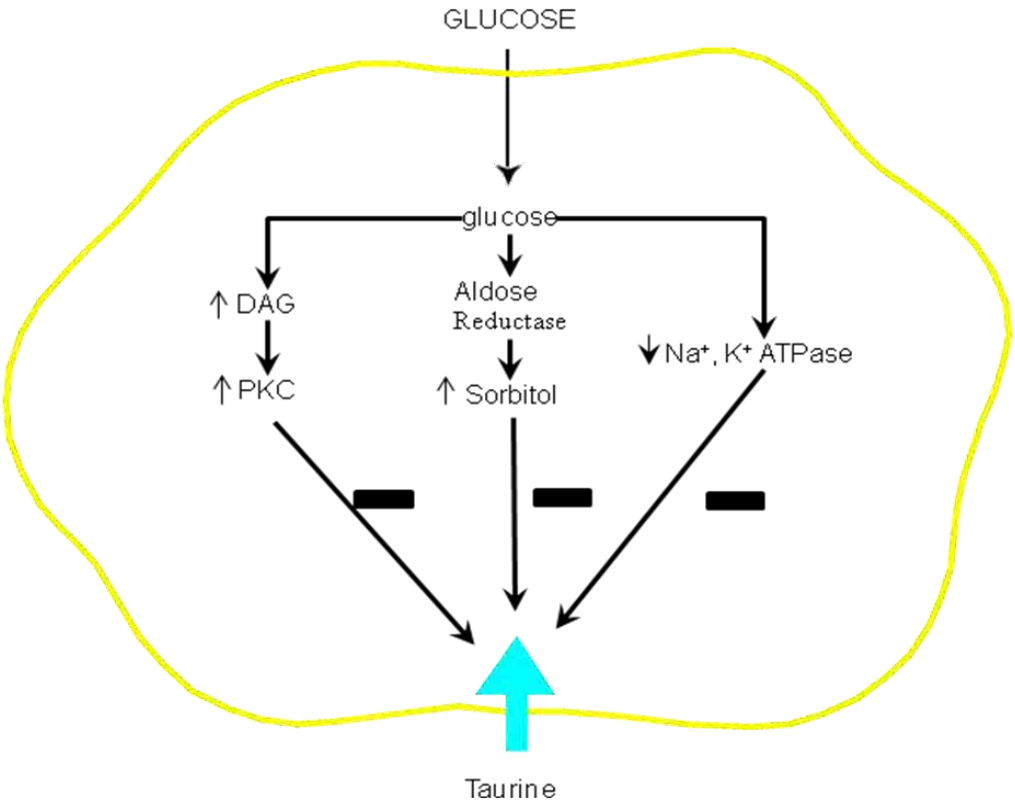

Figure 1-14 - Potential Mechanisms of Taurine Depletion

Hyperglycaemia increases DAG and PKC activity, which can phosphorylate TauT at Ser 322 and reduce taurine uptake.

Glucose increase aldose reductase flux, increasing intracellular content of the osmolyte sorbitol, which results in a compensatory decrease in other organic osmolytes such as taurine.

Taurine uptake is dependent upon Na^+ gradient. The activity of Na^+K^+ ATPase is decreased in diabetes, reducing the Na^+ gradient and therefore taurine uptake

1.5.6.2 Taurine Supplementation in Diabetes

The reduction in circulating and intracellular taurine can be replenished by taurine supplementation. This has been demonstrated in the nerve of STZ-D rats (145) as well as in plasma and platelet taurine concentration in diabetic patients (257). The latter study was after a short, 90 day supplementation with 1.5g/day taurine. This study was useful in demonstrating that dietary taurine intake can reverse taurine deficiency and platelet aggregation. The beneficial effects of taurine supplementation have been demonstrated in diabetic animal models, especially for models of peripheral neuropathy. Taurine prevents nerve blood flow and nerve conduction velocity reduction in Zucker diabetic fatty rats (262), along with hyperalgesia (225) nerve growth factor deficits (145) and calcium signalling in STZ-D rats. The potential mechanisms for the beneficial effects are discussed below.

1.5.6.2.1 Antioxidant Actions of Taurine

One of the major actions of taurine is as an antioxidant and *in* vitro TauT expression and taurine uptake are increased in response to pro-oxidants (73), suggesting increased taurine uptake as a defensive response. In isolated culture and animal models of diabetes, taurine supplementation reduces markers of oxidative stress in different tissues i.e. lipid peroxidation in plasma (263), heart, muscle, liver, kidney (264) and sciatic nerve (145) and decreased superoxide formation in β-islet cells from rats infused with high glucose (265). There is no human data measuring changes in oxidative stress following taurine supplementation.

The mechanism(s) by which taurine acts as an antioxidant however, are unclear. The taurine precursor hypotaurine is able to neutralize classic ROS, but, Aruoma et al., (1988) (266)

established that taurine is incapable of directly scavenging classic ROS, O_2^-, $OH^\cdot$ and H_2O_2. Many studies attribute the antioxidant effect of taurine to an indirect mechanism, by upregulating the cellular antioxidant defence system. In most of these studies, however the effects seem to be a reversal of toxic effects rather than directly increasing antioxidant defence enzymes (76).

One example of this is the prevention of glutamate-induced neurotoxicity and subsequent ROS increase. Prolonged activation of the N-methyl D-aspartate (NMDA) receptor by glutamate results in overload of intracellular and mitochondrial Ca^{2+}, causing mitochondrial damage and ROS production (267). Taurine reduces ROS production in glutamate-induced neurotoxicity, but neither by a direct antioxidant mechanism, nor by increasing the antioxidant defence system. Instead taurine has a direct effect on Ca^{2+} uptake via the Na^+/Ca^{2+} exchanger, reducing Ca^{2+} influx and thereby reducing cellular toxicity and ROS (268; 269). Hence, it is possible the effects of taurine on glucose-induced oxidative stress are due to an indirect effect on other mechanisms increasing oxidative stress such as a carbonyl scavenging, rather than directly on ROS, or antioxidant defence (76).

1.5.6.2.2 Anti-inflammatory Actions

Hypochlorous acid (HOCl) is a major bactericidal agent generated by polymorphonuclear leukocytes and eosinophils. Although taurine is unable to scavenge classic ROS, it does react with HOCl in a 1:1 ratio neutralizing HOCl and forming the less toxic oxidant taurine chloramines (74). Hence, taurine acts as an anti-inflammatory agent by neutralising HOCl. It has been demonstrated that taurine chloramines act as an inflammatory mediator to reduce iNOS, TNF-α, IL6 and IL8 in polymorphonuclear cells (270-273). These pro-inflammatory

mediators are seen to be increased in diabetic patients (162) and due to hyperglycaemia (161; 274).

1.5.6.2.3 Carbonyl Scavenging

Taurine is a free amino acid and therefore it has a free amino group which reacts with carbonyl groups forming a Schiff base with the sugar carbonyl, sparing the proteins from glycation (5; 275). Taurine supplementation reduces AGE and protein glycation in many diabetic models; isolated human erythrocytes (276; 277), fructose-fed rats, (278) and fructose-treated bovine lens (279). Taurine is able to scavenge both toxic aldehydes and other carbonyl compounds (74; 76).

1.5.6.3.4 Glucose Uptake and Insulin Sensitivity

As early as the 1930s, studies reported the hypoglycaemic effects of taurine (5). Subsequent work also showed that taurine supplementation improves insulin sensitivity and reduces circulating glucose concentration in diabetic models. Relatively recently taurine has been seen to increase insulin secretion from fresh mice islets (280). However, this observation is still controversial and in many diabetic animal models (69; 145; 225; 262) no change in blood glucose following taurine supplementation was shown. It is interesting to note that the earlier studies generally demonstrated the hypoglycaemic effects, which are not demonstrated in the more modern studies. It is unfortunate that Franconi *et al*., 1995 (257) did not measure either HbA1C or glucose concentration after taurine supplementation in the human study as this would have helped solve the discrepancy between the studies.

1.5.6.3.5 Calcium Signalling

Abnormal [Ca^{2+}] in diabetes is thought to contribute to the development of diabetic neuropathy and the associated pain (281). Resting [Ca^{2+}] is increased in sensory neurons and DRGs in both STZ-D rats and mice (282) and the amplitude of multiple voltage-gated

calcium channels is also increased in diabetic models (282). Ca^{2+} overload is reported in diabetic mitochondria, which is important as mitochondrial dysfunction is repeatedly cited as a result of the metabolic dysfunction observed in diabetes (282).

Taurine is known to modulate Ca^{2+} homeostasis (74). It is able to counter glutamate-induced Ca^{2+} elevations (see above, taurine as an antioxidant) (283), inhibit excessive Ca^{2+} accumulation in cardiomyocytes (284) and attenuate abnormal Ca^{2+} signalling in sensory neurons of STZ-D rats (225). How taurine does this is unclear and may differ in different situations. For instance in glutamate- induced neurotoxicity, taurine is able to lower [Ca^{2+}] by directly affecting the Na^{+}/Ca^{2+} exchanger (268; 269). However, other studies have demonstrated interactions between taurine and either phospholipids, or phosphoinositol, by inhibiting phosphoinositide turnover (283) or by altering Ca^{2+} binding to membrane phospholipids (225).

1.5.6.2.6 $Na^{+}K^{+}$ATPase

$Na^{+}K^{+}$ ATPase is a ubiquitously expressed membrane pump that utilises ATP to export three Na^{+} ions and import 2 K^{+} ions (285). Many cellular functions are coupled to the movement of sodium ions, for example in the nerve, the Na^{+} gradient is required for nerve impulses to travel, however it is also required for the transport of molecules such as myoinositol and taurine. $Na^{+}K^{+}$ ATPase activity is reduced by oxidative and nitrosative stress and in diabetes $Na^{+}K^{+}$ ATPase activity is disrupted (51). In the sciatic nerve, lens, heart and erythrocytes this disruption resulted in a decrease in activity. Considering the role of the $Na^{+}K^{+}$ ATPase in the nerve, decreased activity impairs nerve impulses and there is a close correlation between decreased $Na^{+}K^{+}$ ATPase activity and diabetic neuropathy (285). Taurine supplementation restores $Na^{+}K^{+}$ ATPase activity in the nerve of STZ-D rats (75), as well as the retina of STZ-

D rats (286) and in peroxynitrite-treated liver samples (287). Although the mechanism of this action is unclear, since the Na^+K^+ ATPase is down-regulated by oxidative and nitrosative stress, it is likely to be an antioxidant effect.

1.5.6.2.7 Blood Flow and Platelet Aggregation

As discussed above (section 1.4.1.5) there is considerable debate about the role of metabolic vs. vascular disturbances in the progression of diabetic neuropathy. In diabetic animal models taurine partially restored nerve blood flow in both STZ-D mice (75) and Zucker diabetic fatty rats (262). The mechanism of these effects is not clear, however, the results are similar to that of antioxidants observed in STZ-D rats (115; 277) demonstrating they could be due to reducing ROS and restoring function in vascular smooth muscle cells (74), or restoring NO signalling. Despite this, taurine has a wide-range of beneficial effects on blood flow.

Taurine is able to increase cholesterol solubility increasing its excretion and several studies have demonstrated that taurine administration is able to reduce serum cholesterol in both diabetic animals (288) and human subjects. In particular Zhang et al., 2004 (289) demonstrated taurine supplementation reduced circulating triglycerides and reduced BMI in obese young non-diabetic adults.

Platelet hyper-aggregation is a contributing factor for complications and there is a close relationship between platelet aggregation in diabetic patients and diabetic complications (5). Taurine is found in high concentration in platelets (10-50 mM (5)) and clinical studies have demonstrated this concentration is reduced in diabetic patients. Oral taurine supplementation however, can reverse this depletion and normalise platelet hyper-aggregation (74) in diabetic patients. Interestingly this effect was not found in obese, non-diabetic men (290). In this

study baseline plasma taurine levels were normal and although this was increased by taurine supplementation, platelet taurine content was not measured. It therefore appears taurine depletion, possibly induced by hyperglycaemia, would be required for taurine to be effective at normalising platelet aggregation.

Taurine is regularly seen to have anti-hypertensive effects both in non-diabetic animal models, as well as humans (291; 292). The anti-hypertensive effects of taurine could be due to antioxidant or anti-inflammatory effects; however, taurine also attenuates the actions of angiotensin II on Ca^{2+} signalling and protein synthesis demonstrating other possible mechanisms for the anti-hypertensive action of taurine (74). Many of the actions of taurine on hypertension are by suppression of the sympathetic nervous system which may also have effects on nerve blood flow, thereby reducing hypertension (292).

1.6 Rationale

As outlined in the introduction, the hyperglycaemia that accompanies diabetes causes cell dysfunction by a combination of pathways. These pathways are unified by increasing oxidative stress, nitrosative stress and poly(ADP-ribosyl)ation. In diabetic patients and in models of diabetes, circulating and intracellular taurine levels are depleted and TauT expression reduced. In diabetic animal models taurine supplementation reduces lipid peroxidation, attenuates functional deficits and ameliorates thermal and mechanical hyperalgesia (225; 262). The mechanisms behind the reduction in TauT expression and how taurine is able to achieve these beneficial effects are not clear. The research outlined in this thesis addresses these pathways in human Schwann cells.

The rationale for using Schwann cells is that they play an important role in maintaining peripheral nerve function with actions including neurotrophic support as well as the synthesis and maintenance of nerve myelin (34; 55; 63). In diabetes, nerve demyelination and the resultant impairment of nerve conduction velocity, are thought to reflect Schwann cell dysfunction (293). The enzyme aldose reductase is highly expressed in Schwann cells (60) and has been implicated in the development of oxidative/nitrosative stress and glucose-toxicity (61; 62). As glucose uptake into Schwann cells is insulin-independent (59) they are vulnerable to hyperglycaemic toxicity as well as oxidative/nitrosative stress. In early models, data obtained from whole nerves were thought to mirror that of Schwann cells. However, it is now clear that disease progression in neurones and Schwann cells are independent. As such, the impact of glucose insult on Schwann cells and the role it plays in the development of neuropathy is unclear. Another aim of the thesis is to clarify this role.

Although rodent models of diabetes have been used to study diabetic complications, they may not accurately reflect the human condition, especially since taurine synthesis is higher in rodents than humans. To perform these studies I utilised a cell strain derived from human Schwann cells isolated from spinal cord of a healthy male (ScienCell). *In vitro* work allows the environment to be defined giving reliable results which are less subject to uncontrollable and unknown influences. The cell strain is well characterised and has been used in other studies (64; 294). Cell identity has been confirmed by immunohistochemical staining with Schwann cell markers S-100, GFAP (glial fibrillary acid protein) and CD90. Cells grow for 15 passages with no reported changes in phenotype, after which growth slows. Passages 6-9 were used in all experiments.

Complications of diabetes arise due to chronic exposure to high glucose. For this reason cells were incubated for 7 days with pathophysiologically relevant high glucose concentrations (up to 30 mM). This glucose concentration is thought to model the effect of chronic hyperglycaemia in man. To determine the effect of moderate hyperglycaemia, cells were incubated in 10 mM glucose. To assess glucose-induced cellular dysfunction, 2 methods were used: i) Oxidative stress was measured directly using a fluorogenic dye and indirectly by ii) Western blots for a lipid peroxidation product, 4HNE adducts. The fluorogenic dye enables direct semi-quantitative assessment of ROS generation. Western blotting against 4HNE adducts was used to gain quantitative assessment of changes induced by oxidative stress and also enabled measurement of lipid peroxidation. Together these techniques enabled quantitative assessment of changes in oxidative stress. Tyrosine nitration and poly(ADP-ribosyl)ation were measured by Western blots using antisera against these protein modifications.

To explore the effects of glucose on TauT expression, I examined transcriptional changes in mRNA by qRT-PCR and I also examined protein expression by Western blotting. These methods are both quantitative and reproducible. The posttranslational regulation of TauT function is not well understood and it is not known whether there are intracellular pools of TauT. Hence, the relationship between TauT expression and taurine transport is unclear. As such taurine uptake studies were performed enabling accurate measurement of taurine uptake and a functional analysis of TauT. Calculation of Michaelis-Menten kinetics established whether perturbations of taurine uptake were related to Vmax or the Km of the transporter, enabling determination of whether changes in taurine uptake are transcriptional, post-translational or due to modification of the transporter.

The effect of taurine supplementation on the effects of hyperglycaemia in Schwann cells was examined. Despite taurine inversely regulating TauT expression in physiological cell culture systems and re-uptake in the kidney, exogenous taurine supplementation consistently increases intracellular taurine content. In human patients, dietary taurine supplementation restored plasma and platelet taurine content (257) and in STZ-D rats dietary taurine supplementation restored nerve taurine content (75). *In vitro* exogenous taurine supplementation, 150-250 μM restores taurine content in erythrocytes exposed to high glucose (276). Therefore in these studies exogenous taurine supplementation of 250 μM was used. To establish whether effects of taurine were mediated by antioxidant mechanism the effects of taurine were compared to that of a standard antioxidant, D-L α-lipoic acid (ALA). ALA is a potent free radical scavenger which has been shown to have therapeutic benefits in both experimental and clinical diabetic neuropathy.

In these ways the effects of hyperglycaemia on oxidative/nitrosative stress along with antioxidant defence systems in Schwann cells were explored along with the mechanisms of action of taurine supplementation in ameliorating these damages.

Chapter 2 Materials and Methods

2.1 Cell Culture Model Verification

The human Schwann cell strain, isolated from spinal cord of a healthy male (ScienCell Carlsbad, California) (295-298) was used. Identity was confirmed by immunohistochemical staining with Schwann cell markers S-100, GFAP (glial fibrillary acid protein) and CD90. Cells grow for approximately 15 passages with no visible change of growth or morphology and passages 6-9 are used in these studies. Cells were cultured at 37^{o}C in a 5% CO_2:95% O_2, humidified atmosphere in Dulbecco's modified Eagles' media (DMEM) (Lonza) supplemented with 10% fetal bovine serum (FBS), 100 U/ml penicillin, 100 µg/ml streptomycin, 2 mM L-glutamine. Cell medium was changed every 2-3 days. Twenty four h prior to treatment medium was changed, and replaced with DMEM containing high (7.5, 10, 15, 22 and 30 mM) or normal (5 mM) glucose and supplemented with 5% newborn bovine calf serum (BCS), and other experimental conditions and passaged as required

2.2 Protein assay

For all measurements of protein concentrations the Bicinchoninic Acid (BCA) method was used. In alkaline solutions, proteins reduce Cu^{2+} to Cu^{+} in a concentration-dependent manner. BCA is a chromogenic reagent specific for Cu^{+} that forms a purple reagent with an absorbance maximum at 562nm.

2.3 Western Blotting

Western blotting was used to measure the relative abundance of specific proteins. The procedure is divided into three separate stages; protein separation by sodium dodecyl

sulphate-polyacrylamide gel electrophoresis (SDS-PAGE), transfer of proteins onto a membrane and detection with target-specific antibodies.

Human Schwann cells were grown for 7 days in experimental conditions. At 7 days cells were washed in Hank's balanced salt solution (HBSS) (3 times) and lysed in 2% SDS containing 1% protease inhibitor cocktail (Sigma). Protein concentration was measured using the BCA method.

For protein separation, the standard Laemmli method (299) was used. Protein samples (40 μg) were denatured by heating for 5mins at 100^{o}C in Novagen sample buffer (Merck) in a 4:1 ratio. The sample buffer contained SDS, the head of which binds hydrophobic regions of proteins with the negatively charged tail pointing outwards. This ensures the protein charge is masked by the negatively charged SDS so the proteins have the same overall negative charge and are separated based on size rather than isoelectric point or shape. The sample buffer also contained a reducing agent, dithiothreitol (DTT), which reduces the intra and inter-molecular protein covalent disulphide bonds, denaturing the secondary and tertiary protein structure.

Polyacrylamide concentrations from approximately 5-20% enable resolution of different protein sizes, low percentage gels being more effective at resolving higher molecular weight proteins. The resolving gel contained 10% acrylamide:bisacrylamide (29:1), 0.1% SDS, 375 mM Tris-HCl pH 8.8 0.05% ammonium persulphate (APS). Polymerisation was initiated by 0.05% N, N, N', N'-tetramethylethylenediamine liquid (TEMED) and added into 1.5mm casting plates. To ensure oxygen did not penetrate and to form a meniscus-free surface, water was poured on top. A stacking gel of 10% acrylamide:bisacrylamide (29:1), 0.1% SDS, 125

mM Tris-HCl and 0.05% APS and 0.1% TEMED, pH 6.8 and poured on top of the resolving gel and wells were formed.

Denatured samples, along with Bio-Rad pre-stained proteins were loaded onto the polyacrylamide gel and the protein separated at 150V for 2hrs on ice, in running buffer containing 25 mM Tris 192 mM glycine and 0.1% SDS pH 8.3. The negatively charged proteins migrate towards the anode and are size-separated.

After separation, proteins are transferred onto a Polyvinylidene difluoride (PVDF) membrane. Proteins were transferred at 100V for 1hr 15min at 4^{o}C, in transfer buffer (25 mM Tris 192 mM glycine, pH 8.3). The proteins migrated out of the gel and into the membrane. The efficiency of the transfer was assessed by treating the membrane with ponceau red and the gel. After transfer, the proteins are stably bound to the membrane from where it is possible to detect the specific target with antisera.

2.3.1 Detection

The membrane was blocked in 3% non-fat dry milk in phosphate buffered saline (PBS, 10 mM phosphate buffer, 2.7 mM potassium chloride and 137 mM sodium chloride, pH 7.4) for 1hr at room temperature. Membranes were incubated overnight at 4^{o}C with target specific antibody (table 2-1) diluted in antibody diluent (PBS containing 3% non-fat dried milk as carrier protein , a detergent, 0.05% Tween-20 to aid antibody penetration and 0.05% sodium azide, to prevent bacterial growth and allow antibody re-use). Membranes were incubated for 2hrs at room temperature with species-specific secondary antibody (table 1), diluted in

antibody diluent. The secondary antibody binds specifically to the primary antibody and is coupled to an enzyme, in this case Horseradish Peroxidase (HRP).

Target	Animal	Dilution	Catalogue number	Supplier
TauT	Rabbit	1:1500	AB5414P	Millipore
4HNE	Rabbit	1:1500	393207	Merck
3NT	Mouse	1:1500	05-233	Millipore
PAR	Mouse	1:1000	ALX-804-220-R100	Alexis Biochemicals
Actin	Rabbit	1:200	A5060	Sigma
p38	Rabbit	1:1500	9926	Cell Signaling
Phospho-p38	Rabbit	1:1500	9211S	Cell Signaling
SAPK/JNK	Rabbit	1:1500	9926	Cell Signaling
phospho-SAPK/JNK	Rabbit	1:1500	4671S	Cell Signaling
p42/44	Rabbit	1:2000	9926	Cell Signaling
Phospho-p42/44 (Thr202/Tyr204)	Rabbit	1:2000	4370S	Cell Signaling
AKT	Rabbit	1:1500	9272	Cell Signaling
phospho-AKT (Ser 473)	Rabbit	1:1500	9271S	Cell Signaling
Anti-rabbit	Goat	1:4000	NA934	GE healthcare
Anti-mouse	Goat	1:2000	A9917	Sigma

Table 2-1 – Antibodies for Western Blots

If an HRP tagged secondary antibody is used, the membrane is incubated with the enzyme substrate so the bound secondary antibodies will emit light, proportional to the abundance of the protein. This can be visualised by incubation with film, the light emitted appearing as dark bands on the light film, or captured using CCD (charge coupled device) camera. Use of fluorescent secondary antibodies rather than HRP-linked enables protein visualisation using a

CCD camera with appropriate emission filters. This detection requires a more expensive set-up; however, it does improve detection sensitivity, quantitation and also enables multiplexing of samples.

In these studies HRP linked secondary antibodies were used with enhanced chemiluminescence detection reagents (Roche). To confirm equal loading, membranes were stripped 10min with stripping buffer (Pierce) at room temperature and membranes were re-probed as described above, using β-actin antisera.

2.3.2 Calculating Molecular Weight

The molecular mass of the developed bands can be accurately calculated by the use of calibration standards run alongside the protein samples. By plotting log protein size vs migration distance of the protein (relative mobility [RF]) a standard curve can be drawn and the size of the bands of interest can be calculated.

2.3.3 Quantitation

The bands on the Western blot can be quantified either indirectly from a dark film, or directly from capture of fluorescence emitted using a CCD camera. In this study Western blots were quantified indirectly from the dark film using a Syngene Ingenious system and quantified using automatic band location on GeneTools software. For all experiments bands were normalised for protein loading with β-actin.

2.3.4 Method Development

Initially only non-specific bands independent of the antibody used were seen on western blots, other than β-actin where specific bands were always visualised. Removal of Tween-20 from the antibody diluent and changing the blocking solution from a commercial blocking solution (Roche) to 3% milk, removed the non-specific background, however, no specific bands were seen.

Altering the concentrations of the primary and secondary antibodies was unsuccessful in visualising proteins, hence, the incubation buffer was altered from Tris-buffered saline (TBS) to phosphate buffered saline (PBS) which is a more effective buffer at pH 7.4; this however failed to improve the blots. Other methodological alterations attempted including reducing the number and duration of washing, removing Tween-20 from the wash buffers, re-introducing Tween-20 into the antibody diluents. None of these enabled protein visualisation.

Lysing cells by sonication rather than using RIPA (Pierce, containing 25 mM Tris-HCl pH 7.6, 150 mM NaCl, 1% NP-40, 1% Sodium deoxycholate and 0.1 % SDS) buffer was also attempted without success. Finally harvesting cells by addition of 2% SDS directly to the cells rather than trypsinisation enabled protein-specific bands to be seen on the blots. The effect of SDS lysis rather than trypsinisation and sonication is illustrated in figure 2-1, where clearer specific bands are observed with cells lysed in SDS. Lastly re-introducing Tween-20 into the antibody diluents improved the intensity of the blots.

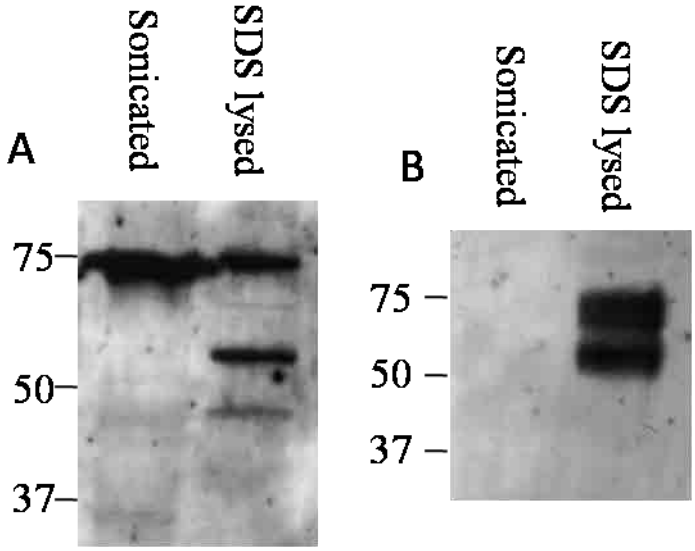

Figure 2-1 - Comparison of Two methods of Cell Harvest and Lysis

A. Human Schwann cells were treated with 50 μM H_2O_2 for 6hrs and run on western blots probed with an antibody for 4HNE adducts

B. Human Schwann cells were treated for 2hrs with 50 μM peroxynitrite and the run on a western blot, probed with an antibody for 3NT.

2.4 Assay of ROS Generation

For measurement of ROS, OxyBurst fluorogenic OxyBurst green 2'7'-dichlorodihydrofluorescein diacetate (H_2DCFDA) (Invitrogen) dye was used. The dye contains lipophilic acetate groups that enable diffusion into the cell. Cleavage of acetyl groups by intracellular esterases results in much greater cell retention and exposes the dihydrocalcein which is oxidised to green-fluorescent calcein and can be monitored by fluorescence microscopy with excitation λ =492-495nm emission 517-527nm

For measurement of intracellular ROS generation, human Schwann cells were grown for 7 days in treatment conditions. On day 5 cells were plated onto poly-L-lysine coated slides. After culture for 2 further days, cells were washed twice in Dulbecco's PBS and incubated in HBSS containing 10 µM OxyBurst green 2'7'-dichlorodihydrofluorescein diacetate (H_2DCFDA) reagent for 1h at 37^{o}C. Cells were mounted on microscope slides and imaged on a fluorescence microscope at λ = 518nm

2.5 Superoxide Dismutase Activity Assay

Human Schwann cells were grown for 7 days in experimental conditions, washed twice in PBS, harvested, by scraping in cold Hank's balanced salt solution (HBSS) and ruptured by sonication 3 x 10 sec at 30W on ice. Protein content was measured using the BCA method and total cellular SOD activity kit was measured using superoxide dismutase activity assay kit (bioassay systems). Cell lysate was incubated with a tetrazolium salt (WST-1 ((2-(4-Iodophenyl)-3-(4-nitrophenyl)-5-(2,4-disulfophenyl)-2H-tetrazolium, monosodium salt)) and xanthine oxidase (XO) (figure 2-2). Upon reduction by the superoxide anion WST-1 produces a formazan dye with peak absorption at 450nm. The rate of reduction is proportional to the activity of XO which is inhibited by SOD. Hence, the activity of SOD can be measured indirectly by the rate of inhibition of formazan production.

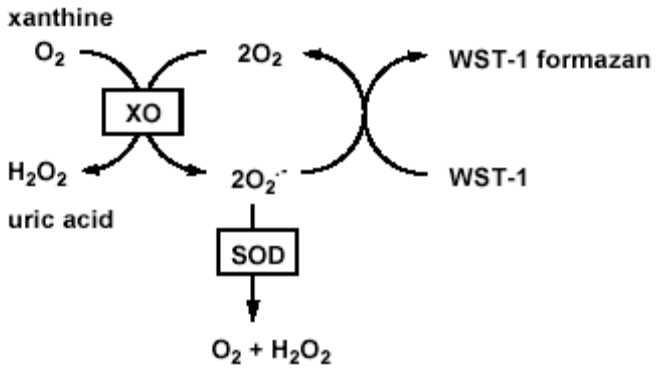

Figure 2-2 – SOD Assay

SOD activity was measured indirectly by the xanthine oxidase system. A tetrazolium salt (WST-1) is reduced by superoxide to produce a formazan dye, with peak absorbance at 450nm. The rate of reduction of WST1 is linearly proportional to the activity of xanthine oxidase, which is inhibited by the activity of superoxide dismutase. Hence, the activity of SOD can be measured by the inhibition of the formazan dye production, which is inversely proportional to SOD activity.

2.6 Catalase Activity Assay

Human Schwann cells were grown for 7 days in experimental conditions, washed twice in PBS, harvested in cold HBSS and lysed by sonication 3 x 10 sec at 30W on ice. Protein content was measured using the BCA method and total catalase activity measured using a catalase activity kit (Cayman chemicals). With an optimal concentration of H_2O_2, catalase reacts with methanol to form formaldehyde. The formaldehyde produced can be measured by incubation with Purpald (4-amino-3-hydrazino-5-mercapto-1,2,4-triazole) forming a bicyclic heterocycle. Upon oxidation the bicyclic heterocycle changes from a colourless compound to a purple colour which can be measured spectrophotometrically at 540nm.

2.7 Reduced Glutathione Concentration

Human Schwann cells were grown for 7 days in experimental conditions, washed twice in PBS, harvested in cold (HBSS) containing 50 mM 2-(N-morpholino)ethanesulphonic acid (MES) and lysed by sonication 3 x 10 sec at 30W on ice. Protein content was measured using the BCA method and reduced glutathione was measured using a commercial kit (Bioassay Systems). Total GSH was measured by incubation with DTNB (5,5'-dithiobis2-nitrobenzoic acid) which forms a yellow 5-thio-2-nitrobenzoic acid (TNB) when it reacts with GSH which can be measured at 412nm.

2.8 Measurements of Cell Viability

Propidium iodide (PI) is a fluorogenic molecule with an excitation wavelength of 544 nm and emission of 612 nm. PI binds DNA in a similar manner to ethidium bromide, intercalating between DNA bases with little or no sequence specificity. Once bound the fluorescence emitted is enhanced 20-30 fold.

PI is permeable to dead cells, but not live, hence PI staining is an accurate and highly sensitive method of assaying cell death. In this study human Schwann cells were grown for 7 days in experimental conditions, on day 5 cells were plated onto poly-L-lysine coated wells. After culture for 7 days propidium iodide (PI) (final concentration 10 µg/ml) was added, incubated at 37^{o}C, 5% CO_2 for 10mins. A reading was taken to quantify dead cells. For total cell DNA content cells were lysed by addition of 0.1% Triton X-100 containing 10 µg/ml PI for 10min at 37^{o}C, 5% CO_2 and assayed at excitation 544 nm emission of 612 nm.

2.9 Quantitative Reverse Transcription Polymerase Chain Reaction

2.9.1 RNA Extraction

Human Scwhann cells were harvested by trypsinisation and frozen in liquid nitrogen. RNA was extracted using Invitrogen micro to midi total RNA purification system. Cells were lysed in lysis buffer containing 1% β-mercaptoethanol, to reduce disulphide bonds and guanidinium isothiocyanate, which destroys all protein-protein interactions. Together these inactivate RNases, protecting the RNA from degradation. The lysate was added to a homogenisation spin column (Invitrogen) to reduce the viscosity, removing DNA from the sample. RNA was precipitated from the eluate by the addition of ethanol to 70% and added to the spin column (Invitrogen) which contains a silica-based membrane that binds the RNA. The impurities are removed by washes with wash buffers provided with the kit. RNA was eluted in RNase free water.

Quantitation and purity of RNA was measured by dissolving a sample of RNA in Tris-EDTA (TE) buffer and measuring absorbance at 260 and 280nm. DNA and RNA absorb ultraviolet light, with an absorption peak at 260nm. Aromatic amino acids in protein absorb at 280nm. The ratio of 260:280 nm reading can be used to asses RNA purity, and the absorption at 260nm to assess RNA quantity.

2.9.2 Principles of PCR

PCR was first described by Saiki et al., 1988 (300). A thermostable DNA polymerase isolated from Thermus aquaticus was used to amplify DNA at high temperatures. Taq polymerase is used for the exponential amplification of very small quantities of DNA isolated from cells or tissues. The principles are further described in appendix 1.

2.9.3 Reverse Transcription PCR (RT-PCR)

This technique is based upon traditional PCR, but utilising RNA-dependent DNA polymerase (reverse transcriptase) isolated from dsRNA viruses, to form complementary DNA (cDNA) from the mRNA template thus enabling gene expression to be measured. The first step is for target specific primers to bind to the mRNA and for reverse transcriptase to synthesise the cDNA strand from the mRNA template. After completion of this reaction, standard PCR is conducted using the target-specific DNA primers, which amplify the cDNA of interest.

2.9.4 Hot Start PCR

Thermophilic DNA polymerases have small, but measurable polymerase activity at room temperature. Hence, at room temperature DNA polymerase activity will catalyse the extension of annealed 3` ends, resulting in non-specific amplification. In addition the 5`-3` exonuclease activity of DNA polymerase degrades free 5` ends, potentially destroying annealed primer and template, resulting in lower yield. Hot start PCR inhibits the polymerase activity, by using a wax barrier, reducing this non-specific polymerase activity and increasing the yield.

2.9.5 Quantitative PCR

Traditional methods of quantitation are either by Northern (mRNA), Southern (DNA) blots or ethidium bromide staining on an agarose gel. However, Northern and Southern blots are time-consuming and require large samples for analysis and measurements using agarose gels are only semi-quantitative , therefore I chose to use quantitative PCR. Over the typical PCR the amount of product plateaus, hence at this point only large changes in starting mRNA can be measured. The development of quantitative PCR (qPCR) systems have removed these limits in end-point detection. qPCR enables accurate quantitation, high throughput processing as

well as multiplexing of samples. In qPCR the levels of newly synthesised DNA is traced (using fluorophores) as they rise above background levels to the plateau, the increase in fluorescent signal being proportional to the amount of DNA synthesised at each cycle. A threshold is defined above the background level and the cycle at which the fluorescence for a particular sample crosses the threshold is determined as Ct. The lower the Ct value, the earlier the fluorescence passes above the threshold and hence the more abundant the initial target.

There are three major types of fluorescent dyes used for q-PCR, intercalating dyes (e.g. SYBR-green) and hybridisation probes (e.g. Taq-man) are discussed in appendix 1. In this study Lux (light upon extension) primers were used. Lux primers have one standard primer and one primer labelled with a fluorophore. The fluorescent label is located near the 3` hairpin structure, which intrinsically quenches the fluorophore. When the primer becomes DNA bound, the hairpin structure is unravelled and the fluorescence is unquenched, resulting in an increase in fluorescent signal (figure 2-3). Since LUX primers do not require a separate probe, the primers are cheaper than Taq-man, however, the lack of this separate probe makes them less sensitive.

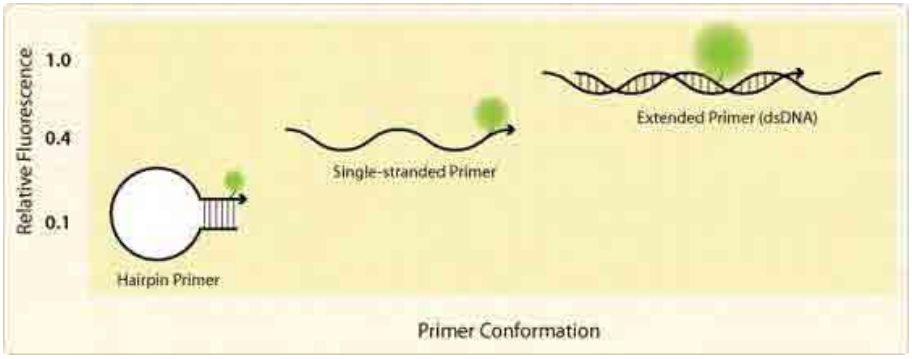

Figure 2-3 - Lux Primers

The fluorophore is attached near the 3` hairpin structure that intrinsically quenches the fluorescence. When the primer becomes DNA bound, the hairpin structure unravels, unquenching the fluorescence increasing the emitted fluorescence.

2.9.6 Relative Quantitation

The most common quantitation for qPCR is relative quantitation, where the treated sample is compared to not only a normal sample run on the same plate, but an internal control as well. During the exponential phase of PCR the quantity of DNA doubles with every cycle, hence, if one target has a Ct value 4 cycles earlier than another, it has 2^4 = 16 times more initial template. This premise is used to quantify the initial amount of target quantified relative to a reference gene (normally a housekeeping gene such as β-actin or 18S). The difference between the Ct of the reference and target gene is calculated and known as ΔCt. The relative quantity (RQ) of the treated sample can then be calculated comparing the ΔCt of the treated sample to a control sample (known as ΔΔCt) from this the relative quantity (RQ) can be calculated.

Relative quantity = $2^{-(\Delta \text{ CT sample} - \Delta \text{ Ct control})}$

qPCR is performed using fluorescence probes meaning multiplex assays can be performed with both target and reference gene amplified in the same tube or well. The use of a reference gene in the same well reduces potential error caused by slight differences in the contents of each well, i.e. template or primer concentrations. Traditionally housekeeping genes such as GAPDH, or β-actin were used as reference gene; however, more recently the use of ribosomal RNA such as 18S is more common. Whichever housekeeping gene is used with relative quantitation, it is necessary to demonstrate the expression of the reference gene is not altered by any of the treatment groups. In addition the ΔΔCt method assumes both the internal control and target are amplified with similar efficiency. It is necessary to demonstrate this is the case by running ΔCt over different RNA concentrations. If the amplification efficiency is similar the gradient of the trend line will be less than 0.1 (301).

In this project primers Fam-labelled LUX primers for TauT, nNOS and iNOS were used to measure gene expression of these targets. TauT primers were designed and optimised by Dr Wei Zeng at the boundary between exons 1 and 2 (5'TCTTGGAGATCATCATAGG'3 and 3'CGGCATTACAACGGAGG'5) producing a 200bp target, the size confirmed by agarose gel electrophoresis from the qPCR product (figure 2-4A). nNOS and iNOS primers were certified primers (Invitrogen) nNOS in exon 12, producing a produce 50-100bp product, iNOS between exons 18 and 19 producing a 50-100bp product. Again these targets were confirmed by agarose gel electrophoresis from the qPCR product (figure 2-4B).

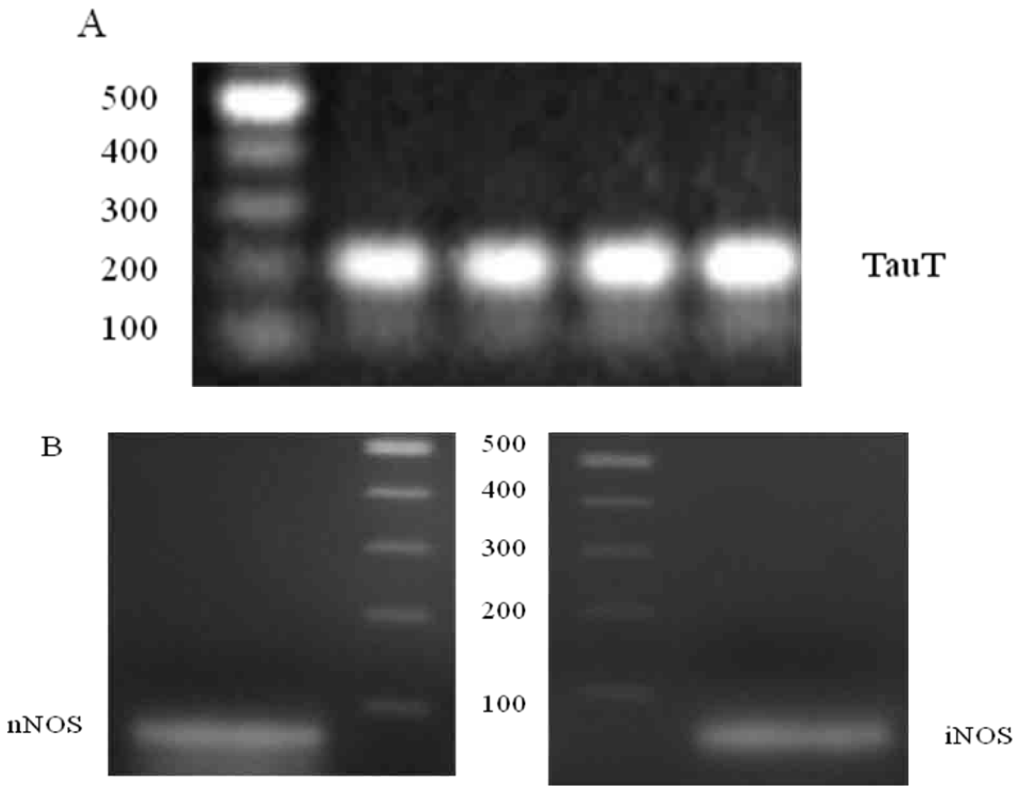

Figure 2-4 - Confirmation of PCR products

1.5% agarose gels confirming q-PCR products

A. 200bp TauT product multiplexed with 100bp actin – performed by Dr W Zeng

B. 50-100bp nNOS and iNOS products. Samples not multiplexed with actin

2.9.7 Method Development for nNOS and iNOS

Initial PCR using the NOS primers were performed using the same cycling conditions as used for TauT (insert cycling conditions), using tenfold dilutions of RNA concentration, 200ng, 20ng, 2ng and 0.2ng RNA. The nNOS curves were clear, but with little differentiation between RNA concentration, they also came up a little too late, with 200ng being measurable, demonstrating low expression. No iNOS fluorescence was visible.

The first strand cDNA synthesis stage was altered, by reducing the temperature from 50^{o}C – 45^{o}C and increasing synthesis time from 25- 30mins. This improved the nNOS curves slightly, and reduced the Ct values to approx 30, for the 20ng RNA (figure 2-5A); however, the differentiation at the lower RNA concentration was still not sufficiently clear. These changes also enabled iNOS fluorescence to be observed with differentiation observed between different RNA concentrations (figure 2-5B).

To increase primer binding, the primer binding and elongation steps were split into two. The primer binding temperature was reduced from 68^{o}C to 60^{o}C with the extension temperature remaining at 68^{o}C. Lastly, to further improve primer binding, the $MgSO_4$ concentration was increased from 3 mM to 5 mM and lastly to reduce the chances of interference between actin and the NOS primer, the amount of actin primer was reduced, by half (to 0.1 μM), which improved both NOS and actin. Further reduction of actin primer had no effect on NOS and had a detrimental effect on the actin curves. Final amplification plots for iNOS and nNOS are shown in figure 2-6. Final cycling parameters are shown in table 2.

Table 2-2 - q-RT-PCR Cycling Parameters

	TauT	**iNOS/nNOS**
	50°C 30 min	45°C 30 min
repeat 40 cycles	95°C 2 min 95°C 15 sec 60°C 1 min	95°C 2 min 95°C 15 sec 55°C 30 sec 68°C 30 sec

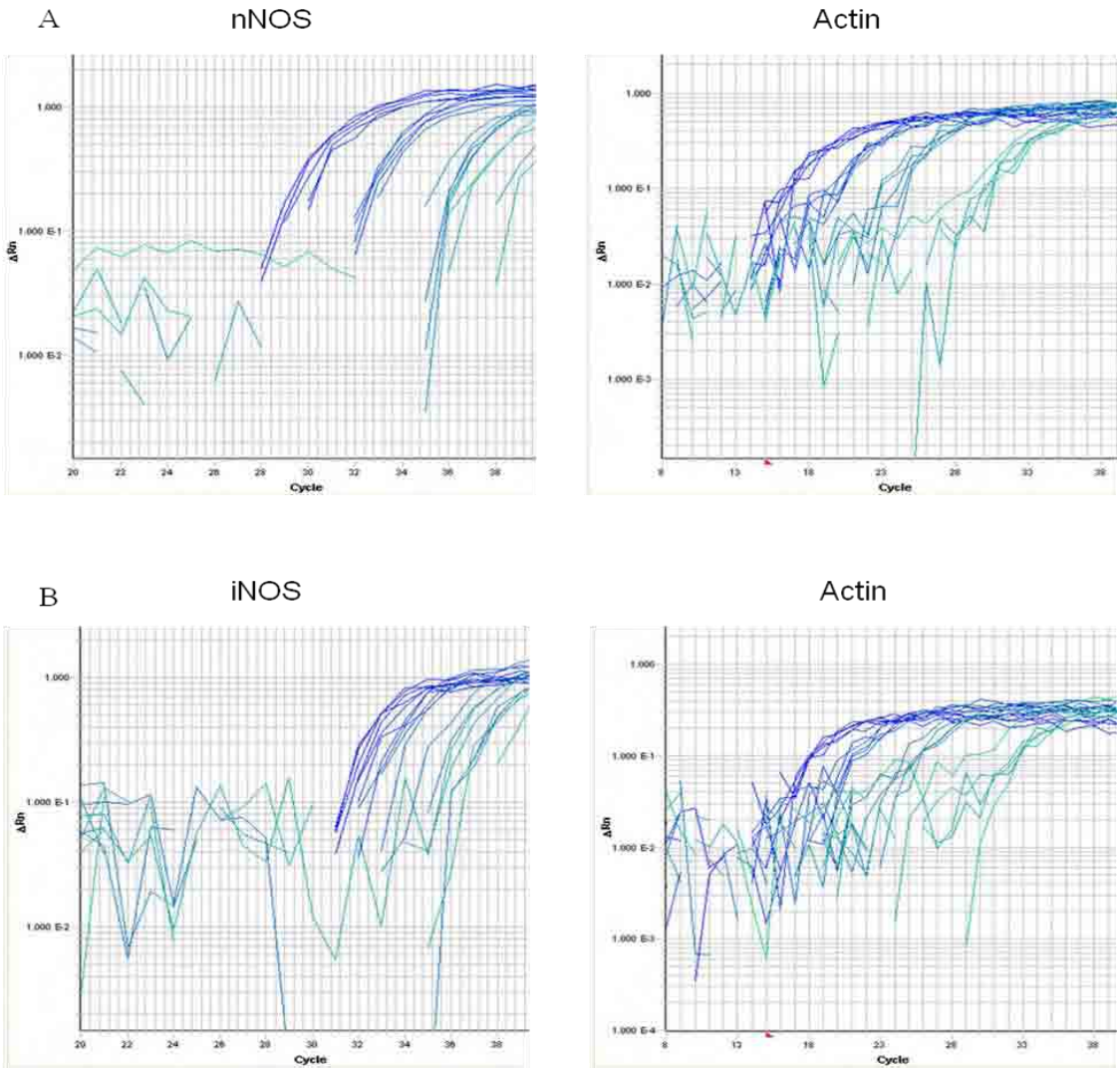

Figure 2-5 – Initial NOS qPCR Amplification Curves

Early PCR cycles for A. nNOS and B. iNOS along with the corresponding actin curves

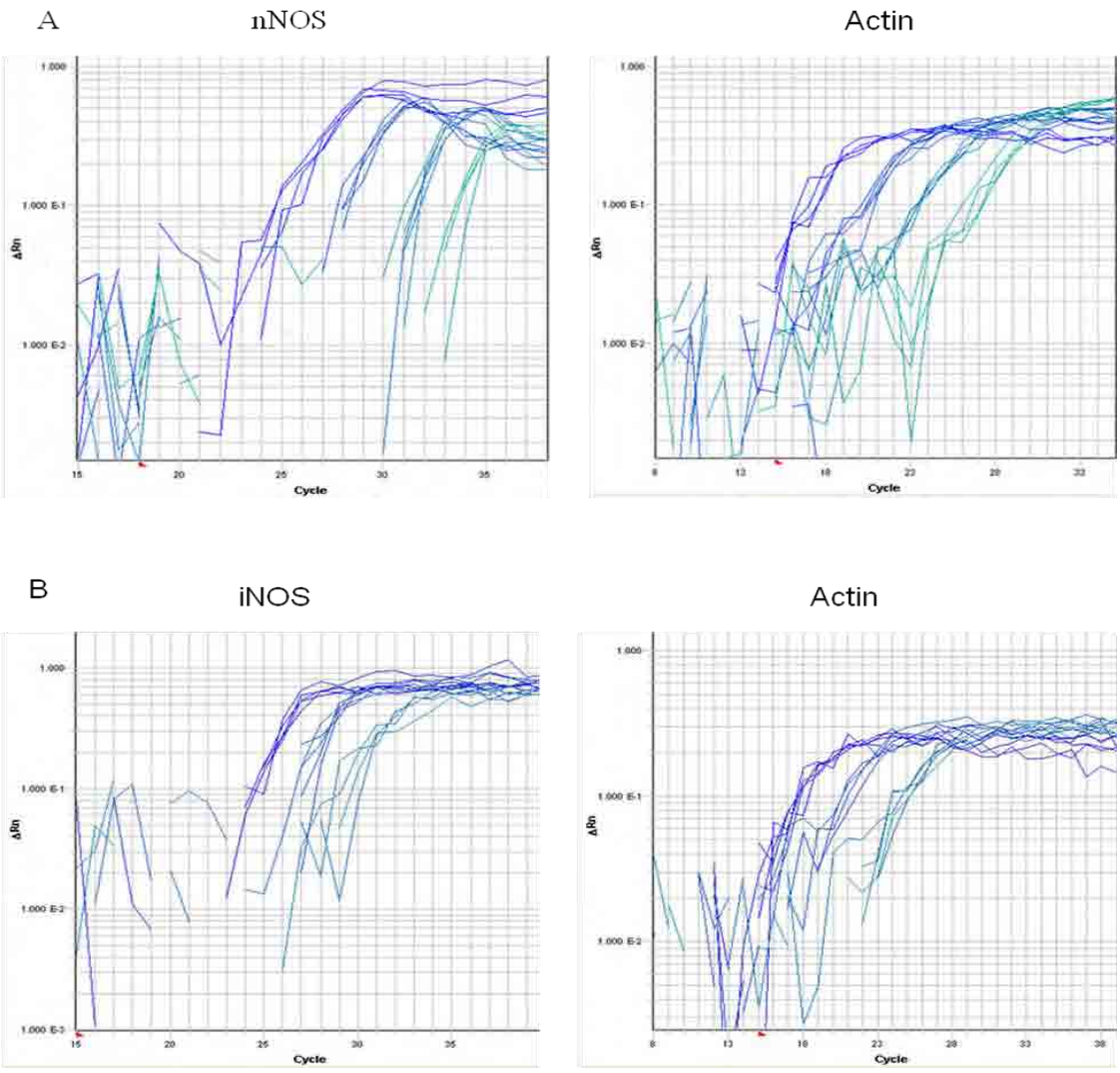

Figure 2-6 – Final NOS Amplification Curves

Final q-RT-PCR for A. nNOS and B. iNOS along with the corresponding actin curves

2.9.8 Final PCR Method

RNA was extracted from treated human Schwann cells using the micro-midi RNA extraction kit (Invitrogen). RNA 20ng was treated with 1 unit of DNase I (Invitrogen) for 15min. DNase I was heat-inactivated by incubation for 10mins with 2.5 mM EDTA and q-RT-PCR was conducted using the Invitrogen superscript® III Platinum® One-Step q-RT-PCT kit following

manufacturer's instructions and run on an ABI 7000 machine. Results were analysed using SDS software as recommended by the manufacturer. Data are expressed as cycle threshold (Ct) values (the cycle number at which the exponential fluorescence increase crosses a calculated threshold) and were used to calculate the ΔCt value (ΔCt = Ct of target gene (TauT) – Ct of endogenous control (actin)). ΔΔCt is calculated as the difference between the sample ΔCt and that of the internal control (i.e. control cells cultured in 5 mM glucose). Data are expressed as relative quantity (RQ) which is calculated as $2^{-(\Delta\Delta Ct)}$. In each assay triplicate conditions were run and the sample was run on at least 4 different independent cell treatments. Fam-labelled TauT lux primers were custom-made by Invitrogen nNOS and iNOS FAM-labelled LUX primers as well as Joe- labelled actin (used as an endogenous control) were certified primers from Invitrogen.

2.10 Taurine Uptake Studies

2.10.1 Liquid Scintillation Counting

Liquid scintillation counting is used to measure low energy β emitters. The liquid scintillation cocktail absorbs the energy emitted by the radioisotope and re-emits them as flashes of light. These light emissions pass into a photomultiplier tube that emits an electrical pulse proportionate to the number of photons, corresponding to the number of individual β emissions.

If the efficiency of conversion of the β energy emitted into light was 100% the number of disintegrations per minute (DPM) would be the same as converted into light and counted on the scintillation counter, expressed as counts per minute (CPM). This is not the case due to quenching and the efficiency of counting (CPM/DPM) needs to be taken into account. This is

normally done by the counter itself, by reading a standard of known activity through the sample to determine the quenching in the sample.

2.10.2 Transporter Kinetics

Michaelis-Menten kinetics describes the kinetics of simple enzymes or transporters. The activity of the enzyme (E) can be described as the rate of product (P) formation from the enzyme substrate (S) (see below). These equations can be equally used to describe the activity of transporters (such as TauT) in the same manner, where the substrate is extracellular taurine and the product is intracellular taurine.

$$E + S \leftrightarrow ES \rightarrow E + P$$

In simple systems the rate of conversion of ES to P is rapid and this reaction is dependent upon the substrate concentration, the maximum velocity of the enzyme (Vmax) and the affinity the enzyme has for the product, denoted by the Michaelis-Menten constant (Km).

A saturation curve of velocity of reaction (V) versus substrate concentration [S] will result in a hyperbolic curve, described by the Michaelis-Menten equation (see below) and enable derivation of the Vmax and Km.

$$V = \frac{Vmax[S]}{Km + [S]}$$

The Vmax is the asymptote of the graph, where the rate of product formation reaches saturation; the Km is the substrate concentration at half Vmax. An enzyme with a low affinity will have a high Km, a high affinity enzyme having a low Km. In biological systems perturbations in Vmax are generally due to either changes in expression or non-competitive inhibition. Whereas changes in Km are generally due to competitive inhibition (as a higher

substrate concentration is needed to reach enzyme saturation) or due to protein modification such as phosphorylation affecting enzyme-substrate interaction.

2.10.3 Final Taurine Uptake Method

For measurements of taurine uptake human Schwann cells were grown for 7 days in treatment conditions. On day 5 cells were plated onto 24 well plates cultured for a further 24 hours to reach 80% confluence. Cells were washed twice in serum-free DMEM pre-warmed at 37^{o}C. Uptake was initiated by adding warmed serum-free media containing 6.9 nM [^{3}H] taurine and increasing concentrations of unlabelled taurine (1-50 µM). At the time of these studies tritium was the only available label for taurine. Since tritium is a low energy isotope, 15 minutes incubation was used for uptake in all experiments. At the end of the incubation the medium was aspirated and cells washed twice in ice-cold HBSS. Cells were lysed by addition of 200µl 2% SDS, and transferred to 2ml of scintillation cocktail (Ecoscint) for liquid scintillation counting. Data are expressed as uptake in picomoles of taurine per milligram of protein per minute.

Active taurine transport via TauT is dependent upon both Na^{+} as well as Cl^{-}; hence the influence of Na^{+}- independent uptake was assessed by a time-course and saturation curve and compared to Na^{+}-dependent uptake. This was performed in uptake buffer containing 20 mM HEPES, 140 mM NaCl, 5.4 mM KCl, 1.8 mM $CaCl_2$, 0.8 mM $MgSO_4$ and 5 mM glucose (pH 7.4). For Na^{+}-independent uptake, choline chloride replaced NaCl.

2.11 Statistical analysis

All data were analysed using Gaphpad Prism software. For comparison within the same treatment group a one way analysis of variance (ANOVA) was performed. For comparison between different treatment groups, a two-way ANOVA wsa performed.In both cases the

Bonferroni correction was used. The Bonferroni correction uses a stricter confidence threshold which safeguards against type I error incurred by using repeated T-tests.

Chapter 3 - Taurine Transporter Dysregulation in High Glucose-Exposed Human Schwann Cells

3.1 Introduction

Increased oxidative/nitrosative stress has been implicated as a key pathogenetic pathway (4; 7; 111; 112) in microvascular complications of diabetes. Intracellular taurine depletion may result in wide-ranging metabolic perturbations including impaired cellular response to oxidative/nitrosative stress with resultant cytotoxicity.

Intracellular taurine concentration is maintained by the $Na^{+}Cl^{-}$ -dependent taurine transporter (TauT) which, in Madin-Darby Canine Kidney (MDCK) cells and retinal pigment epithelial cells (RPE) (236), is known to be regulated by glucose, oxidative stress and changes in osmolarity. Disruption of taurine transport has been identified as the important pathway leading to its intracellular depletion (73; 261). Flux through the enzyme aldose reductase at key sites for diabetes complications has been viewed as a critical link between hyperglycaemia, oxidative stress and the cell dysfunction seen in diabetes (4; 73). This pathway increases intracellular fructose, sorbitol, protein glycation and oxidative/nitrosative stress (4; 32). Increased sorbitol production can contribute to osmotic imbalance resulting in a compensatory reduction of other osmolytes such as myoinositol and taurine (73; 261; 302). Deficiency of these "compatible osmolytes" may result in their becomeing rate-limiting for normal metabolic functions (73; 303).

Covalent protein tyrosine nitration due to increased production of reactive nitrogen species (RNS) has been observed in models of both diabetes, such as in Schwann cells, neurons and epineurial blood vessels (304). Tyrosine nitration impairs tyrosine phosphorylation and as such affects many intracellular signaling pathways. However, the role of nitrosative stress on TauT regulation has never been explored.

I have examined the effects of hyperglycaemia on the effect of glucose on TauT regulation in human Schwann cells. I have also studied the effect of oxidative stress, nitrosative stress and increased polyol pathway flux.

3.2 Methods

Methods used are as described in Chapter 2 with the following additions.

3.2.1 Taurine Transporter Western Blot

Two separate polyclonal TauT antibodies were used, i.e. an affinity purified antibody made by the laboratory of Martin Stevens (75) and a commercial TauT antibody (Millipore) (305; 306). Both identified a 69kDa TauT band (figure 3-1), identified as the size of TauT. The staining from the commercial antibody was clearer and hence was used for all subsequent studies.

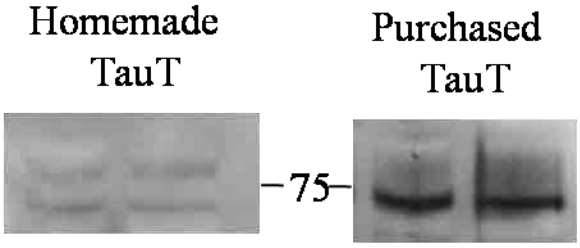

Figure 3-1 – Comparison of Two TauT Antibodies

Western blots using homemade and purchased (Millipore) TauT antibodies. In both blots the same 69 kDa band was seen, however, in the homemade antibody the band was considerably fainter and there was a band slightly higher at 80 kDa.

3.2.2 Validation of Actin mRNA as an Internal Control

Actin was chosen as an endogenous control and commercial certified actin primers (Invitrogen, Carlsbad, USA) were utilised. To validate its use, the amplification efficiency of actin vs. target primers were checked (figure 3-2) over 10 fold dilutions of RNA between 0.2ng and 200ng. The trend-line gradients from these were all less than 0.1, demonstrating similar amplification efficiencies of actin compared to target primers, allowing the ΔΔCt method of analysis to be used. To further validate the use of actin, actin mRNA expression did not alter with any of the treatment groups (Figure 3-3).

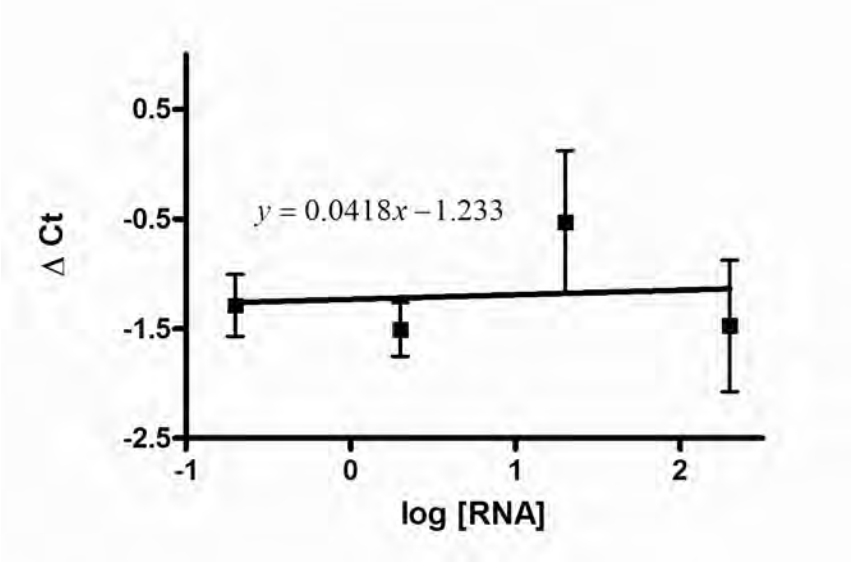

Figure 3-2 - Validation of Actin and TauT Amplification Efficiencies

q-PCR was run with 10 fold dilutions of untreated RNA from 200ng to 0.2ng. There was limited change in ΔCt over different RNA concentrations, demonstrated by the gradient of the linear regression < 0.1. Data expressed as mean ± SEM of 6 separate experiments.

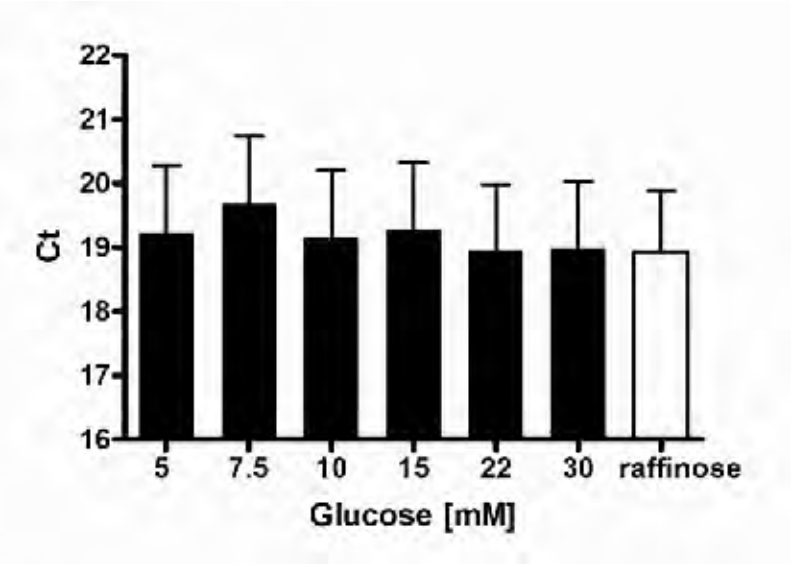

Figure 3-3 - Actin Expression with Increasing Glucose Concentrations and Raffinose

No significant changes in the actin expression (Ct) were observed in these treatments. Data expressed as mean ± SEM of 6 separate experiments.

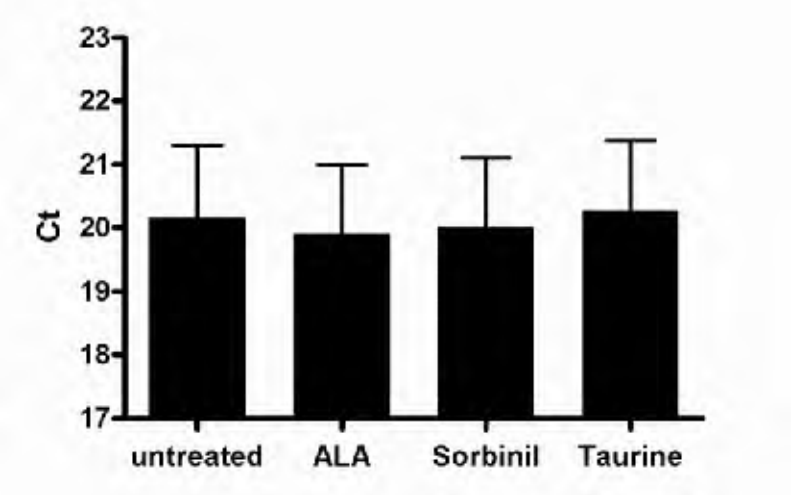

Figure 3-4 - Actin Expression with α-lipoic acid, Sorbinil and Taurine

No significant changes in the actin expression (Ct) were observed in these treatments. Data expressed as mean ± SEM of 6 separate experiments.

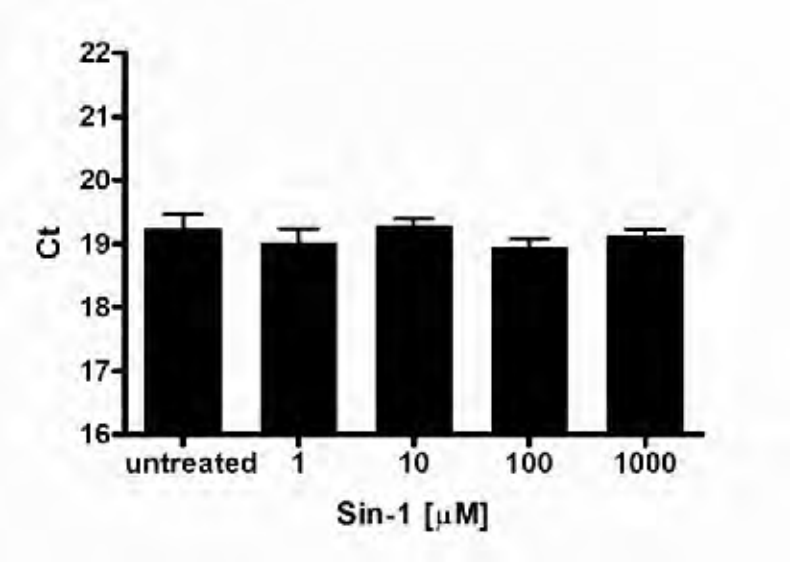

Figure 3-5 - Actin Expression with Sin-1

No significant changes in the actin expression (Ct) were observed in these treatments. Data expressed as mean ± SEM of 6 separate experiments.

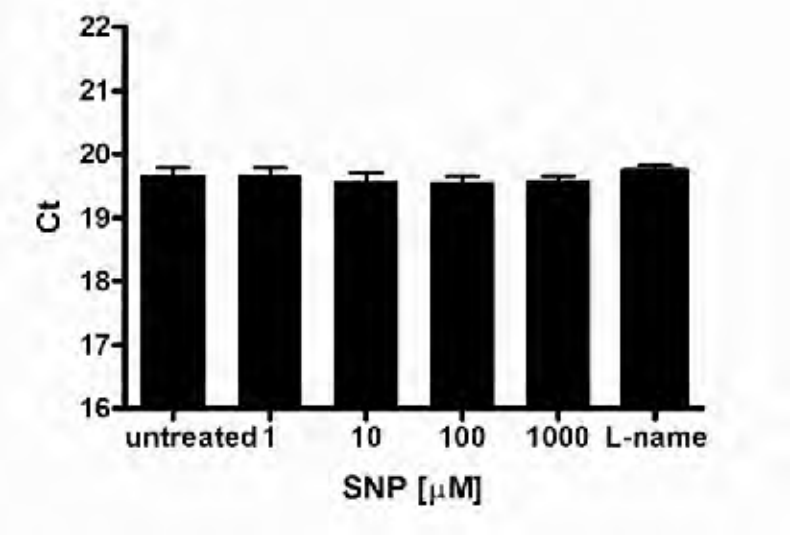

Figure 3-6 - Actin Expression with SNP and L-name

No significant changes in the actin expression (Ct) were observed in these treatments. Data expressed as mean ± SEM of 6 separate experiments.

3.2.3 Taurine Uptake

Between 1-50 µM taurine, the Na^+-independent uptake was non-saturable (figure 3-5) and uptake did not alter over time (figure 3-4), a response typical of simple diffusion. The Na^+-dependent taurine uptake was linear over 60 minutes (figure 3-4) and saturable following Michaelis-Menten kinetics with a Vmax of 54 pmole/min/mg protein and Km 8.4 µM (figure 3-5), data typical for TauT (261; 307). Intracellular taurine content is typically in the mM range, 10-50 mM (74; 236; 237) and the plasma taurine content is ~50 µM (235) hence Na^+-independent uptake accounts for very little of total taurine uptake physiologically. This was mirrored in these studies where the influence of Na^+-independent uptake was negligible (figure 3-5) and hence was not routinely taken into account in subsequent studies.

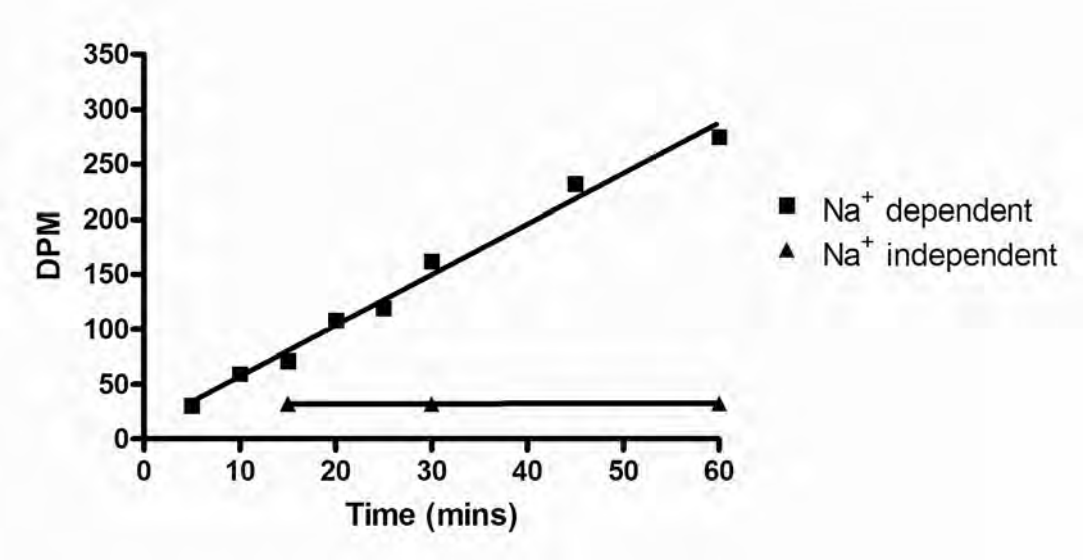

Figure 3-7 - Taurine Uptake Time-Course

A linear (R^2=0.9866) Na^+-dependent uptake is observed over 60mins. Na^+-free uptake is negligible with no alteration in DPM over time gradient 0.0061

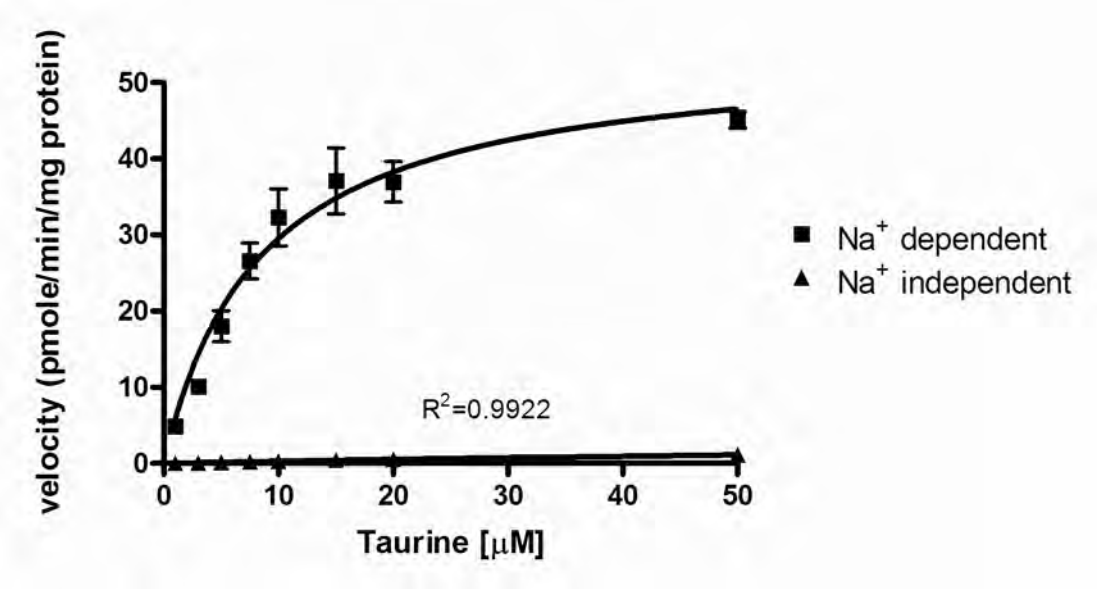

Figure 3-8 - Na^+-Dependent and Na^+-Independent Taurine Uptake Saturation Curves

Na^+-dependent taurine uptake is saturable following Michaelis-Menten kinetics with a Vmax of 54 (pmole/min/mg protein) and Km of 8.4 μM. Na^+-independent uptake is unsaturable and linear (R^2=0.9922) typical of simple diffusion.

3.3 Results

3.3.1 Effect of Hyperglycaemia on TauT Expression and Taurine Transport

Studies in RPE cells have demonstrated TauT is down regulated by high glucose concentrations (73; 261). To determine whether these effects are replicated in Schwann cells the effect of high glucose on TauT mRNA and protein expression, as well as activity in human Schwann cells were explored.

Changes in TauT mRNA expression were measured in human Schwann cells by qRT-PCR after exposure to 5, 7.5, 10, 15, 22 and 30 mM glucose for 7 days. The data shown in figure 3-6A shows the abundance of TauT mRNA declined in dose-dependent fashion with increasing glucose concentration. Expression was reduced by 14% in 10 mM glucose with maximal reduction (66 ± 6% $p<0.05$) in 30 mM glucose. No decrease was found when the osmotic control, 25 mM raffinose, was utilised in place of glucose.

The abundance of TauT protein expression in response to increases in glucose was measured by western blotting. The results are shown in figure 3-6B which demonstrate, in a similar manner to mRNA regulation, TauT protein expression decreased in a dose-dependent fashion. TauT protein levels were reduced by 63 ± 12% ($p<0.05$) in glucose concentrations above 15 mM. Again this effect was not reproduced by 25 mM raffinose.

To ascertain whether reductions of TauT expression were replicated by uptake, measurements of taurine uptake were performed and Michaelis-Menten kinetics calculated which are shown in figure 3-6C. These demonstrated that 30 mM glucose reduced TauT Vmax (maximum velocity) by 41% from 61 ± 5 pmoles/min/mg protein to 42 ± 3 pmoles/min/mg protein ($p<0.001$), while increasing the Km by 50% from 10 µM ± 2 to 16 ± 2 ($p=0.16$). Again these effects were not reproduced by 25 mM raffinose.

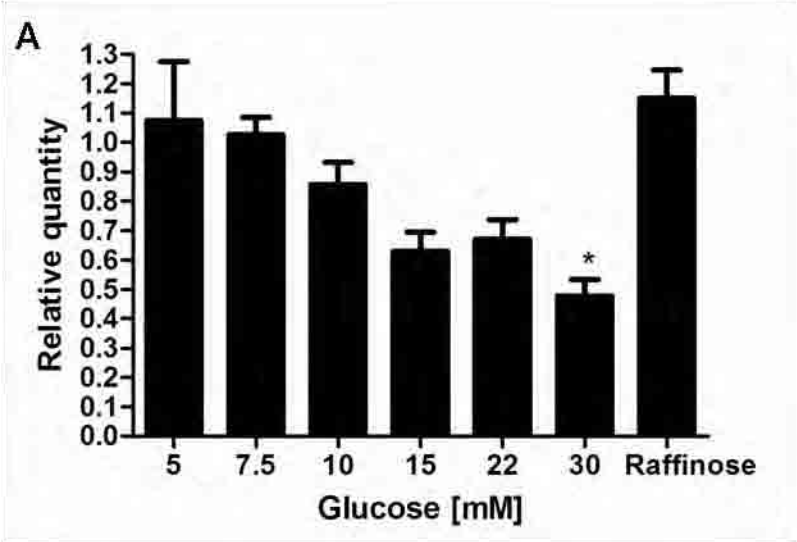
A
Relative quantity
1.3
1.2
1.1
1.0
0.9
0.8
0.7
0.6
0.5
0.4
0.3
0.2
0.1
0.0
*
5
7.5
10
15
22
30
Raffinose
Glucose [mM]

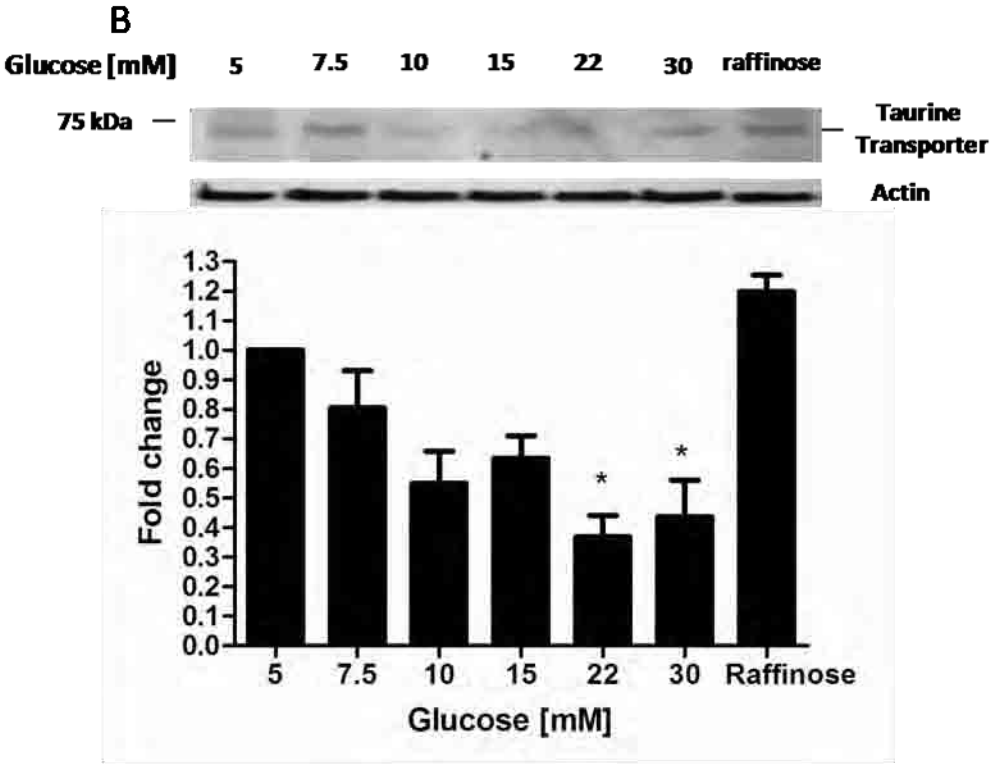
B
Glucose [mM]
5
7.5
10
15
22
30
raffinose
75 kDa
Taurine Transporter
Actin
Fold change
1.3
1.2
1.1
1.0
0.9
0.8
0.7
0.6
0.5
0.4
0.3
0.2
0.1
0.0
*
*
5
7.5
10
15
22
30
Raffinose
Glucose [mM]

C

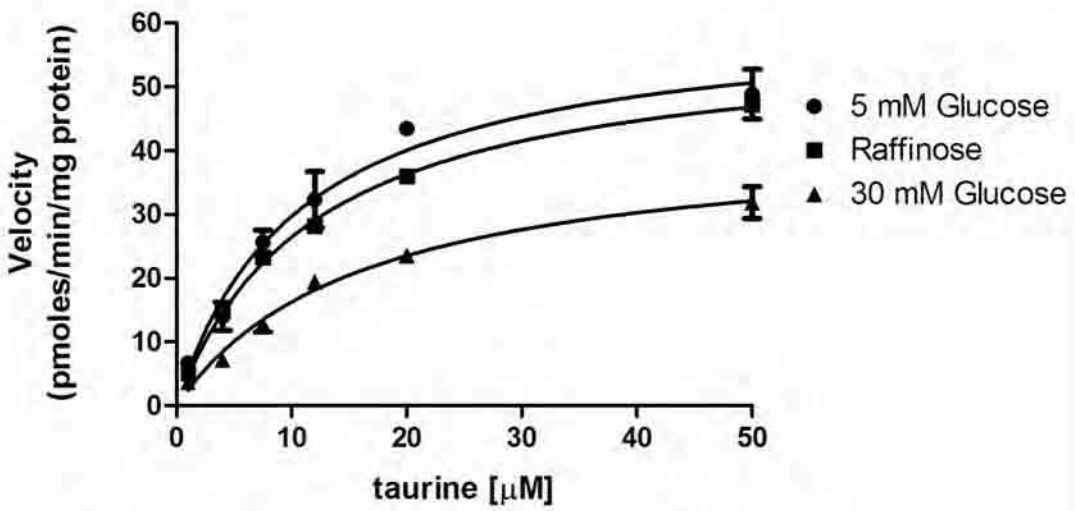

	5 mM Glucose	30 mM Glucose	Raffinose
Vmax	61.49	42.46 *	58.04 ‡
Km	10.71	16.11 †	11.96 ‡

Figure 3-9 - Concentration Dependent Effects of Chronic Glucose Exposure on the mRNA, Protein Expression and Taurine Transport

A) TauT mRNA expression was measured by q-RT-PCR using TauT specific primers. Data expressed as relative quantity of 6 separate experiments mean ± SEM $p<0.05$ (one-way ANOVA).

B) Representative western blot analysis of TauT protein expression. Equal protein loading confirmed with β-actin. Quantitation performed by densitometry 5 mM glucose is taken as 100% and data expressed as fold change vs. 5 mM glucose as mean ± SEM of 5 separate experiments *$p<0.05$ (one-way ANOVA).

C) Kinetic plots were obtained by measuring taurine uptake in cells treated in different glucose concentrations for 7 days. Michaelis-Menten plots for Na^+ dependent taurine uptake are shown at 5 and 30 mM glucose, with 25 mM raffinose as an equimolar osmotic control. Vmax and Km were obtained by non-linear regression using Prism software.*$P<0.05$ vs. 5 mM glucose †$P=0.16$ vs. 5 mM glucose ‡ $P>0.5$ vs. 5 mM glucose.

Data published – see chapter 7.3 (appendix)

3.3.2 Time-course of Effects of Glucose on TauT mRNA Expression

To ascertain the time-dependent effects of high glucose on TauT gene expression, a time-course was performed over 7 days (30 mM) and changes in TauT mRNA expression were measured. These data are shown in figure 3-7. There was a gradual downregulation of TauT mRNA expression over time in response to high glucose, with significant decreases after 4 days with a 25 ± 6% ($p<0.05$) decrease observed.

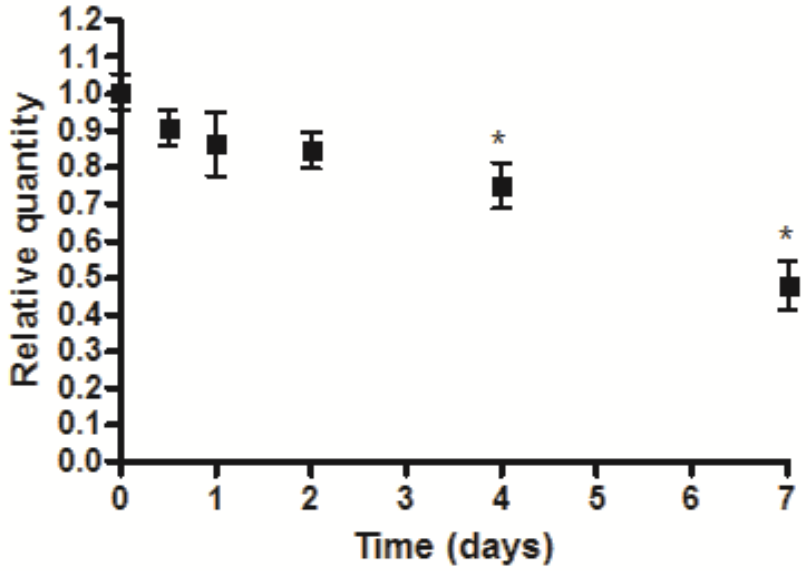

Figure 3-10 - Effect of High Glucose on TauT mRNA Expression Over 7 Days

TauT mRNA expression was measured by q-RT-PCR using TauT specific primers. Data expressed as relative quantity of 6 separate experiments mean ± SEM *$p<0.05$ (one-way ANOVA).

3.3.3 Effect of Aldose Reductase Inhibition on TauT Gene Expression and Taurine Transport

To establish the impact of aldose reductase flux on TauT downregulation, cells were co-incubated for 7 days with glucose together with the aldose reductase inhibitor sorbinil (10 μM). The effects on TauT mRNA expression are shown in figure 3-8. Inhibition of aldose reductase reversed the hyperglycaemia-induced reduction of TauT gene expression, increasing mRNA expression to levels 2.9 and 3.8 fold above 5 mM glucose in 10 and 30 mM glucose respectively (both $p<0.05$) (figure 3-8A). The effects of sorbinil on measurements of TauT kinetics are shown in figure 3-8B. Aldose reductase inhibition restored TauT Vmax, increasing it to 98% above 5 mM from 54 ± 4 pmoles/min/mg protein to 107 ± 14 pmoles/min/mg protein. There was no change in Km compared to untreated 30 mM glucose.

3.3.4 Effect of Oxidative Stress on TauT Expression and Taurine Transport

To explore the effect of oxidative stress on TauT expression and taurine transport, Schwann cells were incubated for 6 hours with the pro-oxidants, 100 μM H_2O_2 or 50 μM primaquine (PQ). The effect of pro-oxidants on TauT protein expression was measured by western blot and the results are shown in figure 3-9A. H_2O_2 and PQ increased TauT protein abundance 2 fold and 3 fold respectively ($p<0.05$ both). Co-treatment for 6 hrs with 30 mM glucose however, completely prevented this pro-oxidant-induced increase in TauT protein expression.

The functional increases in protein were confirmed by measurements of taurine transporter kinetics and the data are shown in figure 3-9B. PQ (50 μM) increased TauT Vmax by 61% from 48 ± 4 pmoles/min/mg protein to 78 ± 7 pmoles/min/mg protein ($P<0.005$). In a similar manner to protein expression, this response was almost completely abolished by co-treatment with 30 mM glucose, which reduced TauT Vmax to 57 ± 4 pmoles/min/mg protein. No

significant changes in Km were seen either with pro-oxidant treatment, or glucose co-treatment.

A

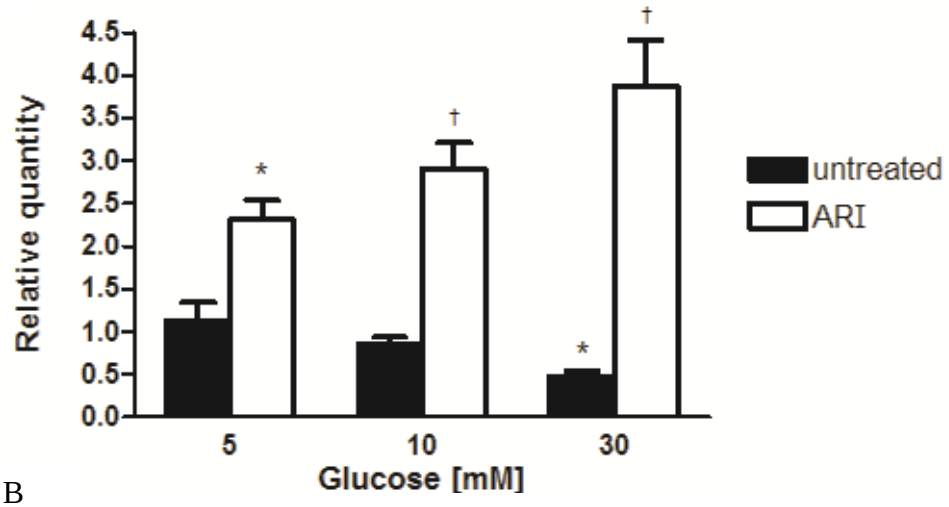

B

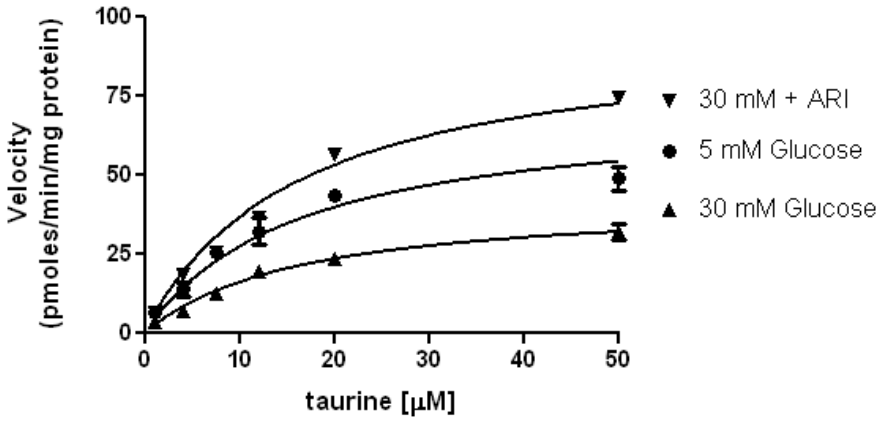

	5 mM Glucose	30 mM Glucose	30 mM + ARI
VMAX	61.49	42.46 *	107.3 *
KM	10.71	16.11	20.77

Figure 3-11 - Effect of Aldose Reductase Inhibition (ARI) with 10 µM sorbinil on TauT mRNA Expression and Kinetics

A) TauT mRNA expression was measured by q-RT-PCR using TauT specific primers. Data expressed as relative quantity of 6 separate experiments mean ± SEM *p<0.05 vs. 5 mM glucose (one-way ANOVA) †p<0.05 vs. respective glucose concentration (two-way ANOVA).

B) Kinetic plots were obtained by measuring taurine uptake in cells treated in different glucose concentrations for 7 days. Michaelis-Menten plots for Na^+ dependent taurine uptake are shown. *p<0.05 †p<0.05 vs. respective glucose concentration

Data published – see chapter 7.3 (appendix)

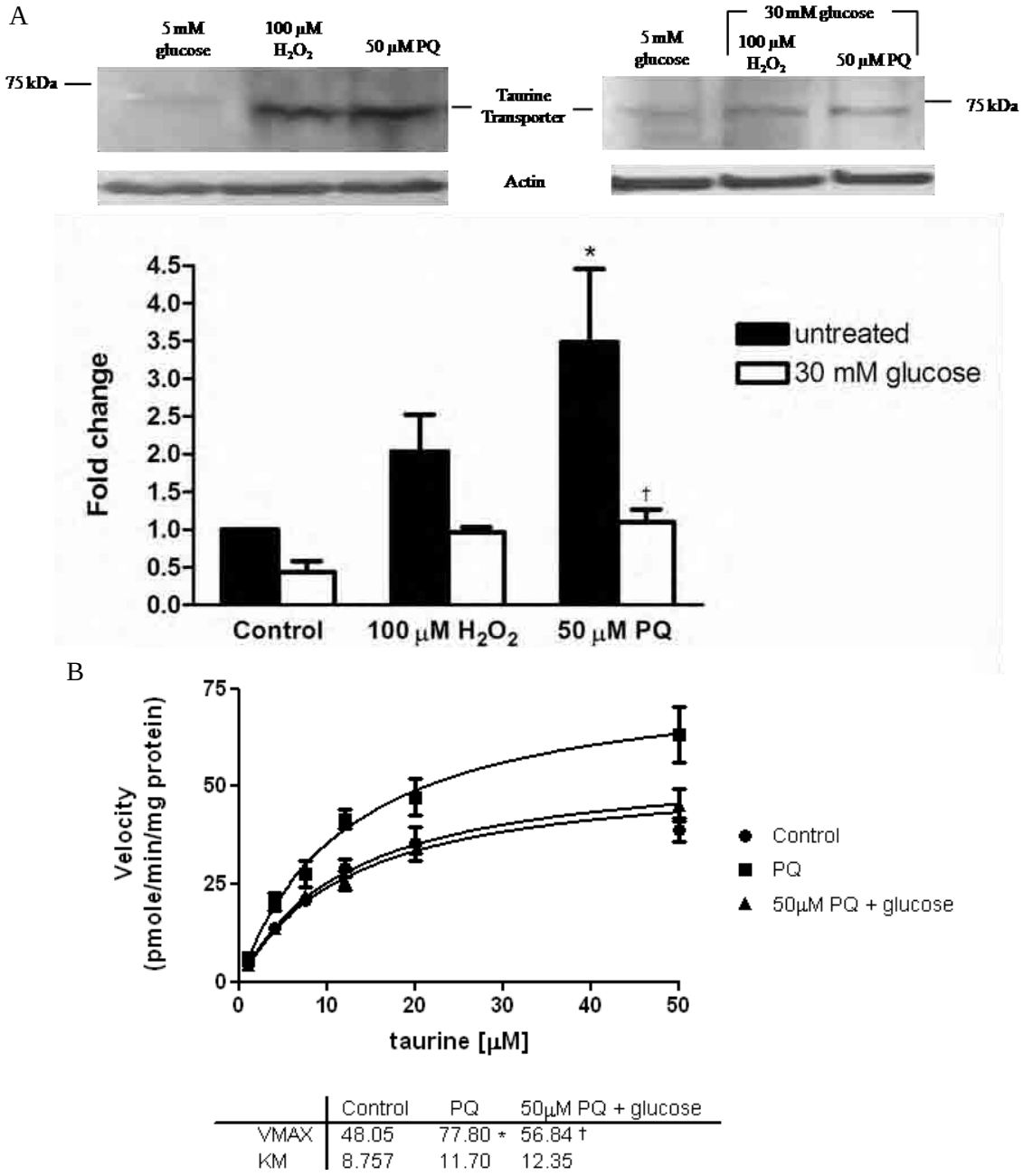

	Control	PQ	50µM PQ + glucose
VMAX	48.05	77.80 *	56.84 †
KM	8.757	11.70	12.35

Figure 3-12 – Effect of Pro-oxidants on TauT Protein Expression and Kinetics

A) Effect of pro-oxidant treatment for 6hrs with 100 µM H_2O_2 and 50 µM primaquine (PQ) on TauT protein expression in normal and high (30 mM) glucose. Representative western blot for TauT shown. Equal protein loading confirmed by β-actin. Quantitation performed by densitometry and data expressed as mean ± SEM of 5 separate experiments. * P<0.05 vs. 5mM glucose (one-way ANOVA) † p<0.05 vs. respective glucose (two-way ANOVA). (B) Treatment for 6hrs with 50 µM PQ in normal and high glucose on TauT kinetics *p<0.05 vs. normal control †p<0.05 vs. PQ

Data published – see chapter 7.3 (appendix)

3.3.5 Effect of Antioxidants on TauT Gene Expression and Taurine Transport

Treatment of STZ-D rats with the antioxidant D-L α-lipoic acid (ALA) restores nerve taurine content (115). Therefore the effect of co-treatment with glucose and ALA was performed to determine the effects of ALA and antioxidant treatment on TauT expression and kinetics. Figure 3-10A shows the effects of ALA on TauT mRNA expression. In 5 mM glucose ALA reduced TauT mRNA by 23 ± 15%, although this did not reach significance ($p=0.1$). In 10 and 30 mM glucose 100 μM ALA completely prevented the glucose-mediated reduction of TauT gene expression, with TauT mRNA increased by 15 ± 22% and 60 ± 10% ($p<0.05$) respectively over levels measured in 5 mM glucose. This effect was duplicated by treatment with 250 μM vitamin C and with 250 μM taurine, shown in figure 3-10B. Both restored TauT expression in 30 mM glucose by 94 ± 5% and 82 ± 8% respectively compared to untreated 5 mM glucose (both $p<0.05$ compared to untreated 30 mM glucose).

Similarly kinetic studies, shown in figure 3-10C, demonstrated that ALA restored the 30 mM glucose-mediated reduction of TauT Vmax, resulting in a 51% increase above 5 mM glucose from 54 ± 4 pmoles/min/mg protein to 82 ± 7 pmoles/min/mg protein ($p<0.05$) with no significant change in Km vs. untreated 30 mM glucose. Co-treatment with vitamin C also restored TauT Vmax in 30 mM glucose to 57 ± 4 pmoles/min/mg protein with no significant difference compared to untreated 5 mM glucose.

A

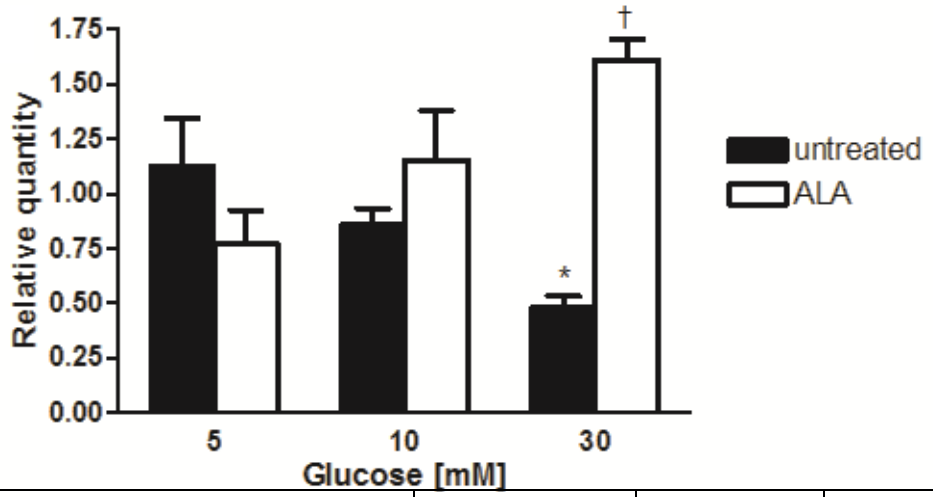

B

		untreated	vitamin C	taurine
Glucose (mM)	**5**	1.02	1.22	1.18
	10	0.86	0.93	1.15
	30	0.34	0.83†	0.94†

C

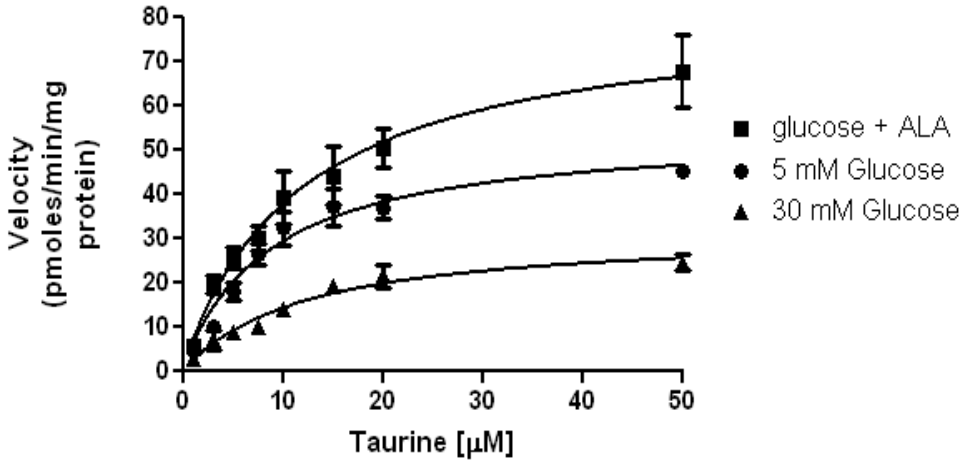

	5 mM Glucose	30 mM Glucose	glucose + ALA
Vmax	54.38	31.69*	82.03 †
Km	8.430	12.01	11.62

Figure 3-13 - Effect of Antioxidant Treatment on Taurine Transport

A) Effect of treatment with 100 µM ALA on TauT mRNA expression
B) Effect of treatment with 100 µM vitamin C and 250 µM taurine on TauT mRNA expression.. Data expressed as relative quantity of 6 separate experiments mean ± SEM *p<0.05 vs. 5 mM glucose (one-way ANOVA) †p<0.05 vs. respective glucose concentration (two-way ANOVA) C) Effect of treatment with 100 µM ALA on TauT kinetics*p<0.05 vs. 5 mM glucose †p<0.05 vs. respective glucose concentration
Data published – see chapter 7.3 (appendix)

3.3.6 Effect of NO Donors on TauT Expression and Taurine Transport

The abundance of RNS, such as peroxynitrite is increased by hyperglycaemia and nitrotyrosine is increased in both patients and models of diabetes. RNS and peroxynitrite is reduced by antioxidants. Hence, to determine whether the restorative effects of antioxidants on TauT mRNA expression and Vmax were due to changes in RNS and NO, Schwann cells were incubated for 24 hours with the nitric oxide donor, sodium nitroprusside (SNP) and the peroxynitrite donor 3-morpholinosydnonimine (SIN-1).

The effects of both SIN-1 and SNP on TauT mRNA expression are shown in figure 3-11A. Both donors reduced TauT expression. The reduction of TauT expression was maximal with 10 µM SIN-1 which resulted in a 35 ± 5% decrease in TauT mRNA expression ($p<0.05$). SNP exposure resulted in maximal reduction of TauT mRNA at 100 µM 29± 7% respectively ($p<0.05$ both).

The effects of SIN-1 and SNP on TauT kinetics are shown in figure 3-11B. 10 µM SIN-1 reduced TauT Vmax from 48 ± 4 pmoles/min/mg protein to 39 ± 2 pmoles/min/mg protein ($p<0.05$), whereas 100 µM SNP reduced TauT Vmax to 28 ± 2 pmoles/min/mg protein ($p<0.005$). No significant change in the Km was observed for either donor.

A

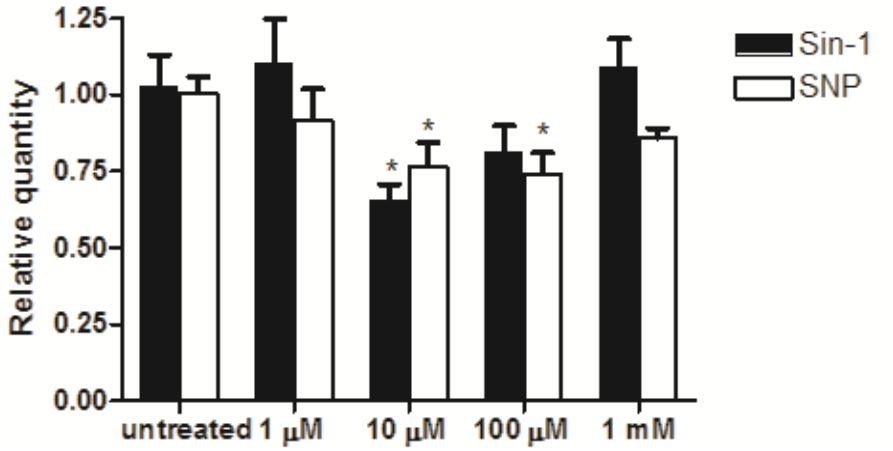

B

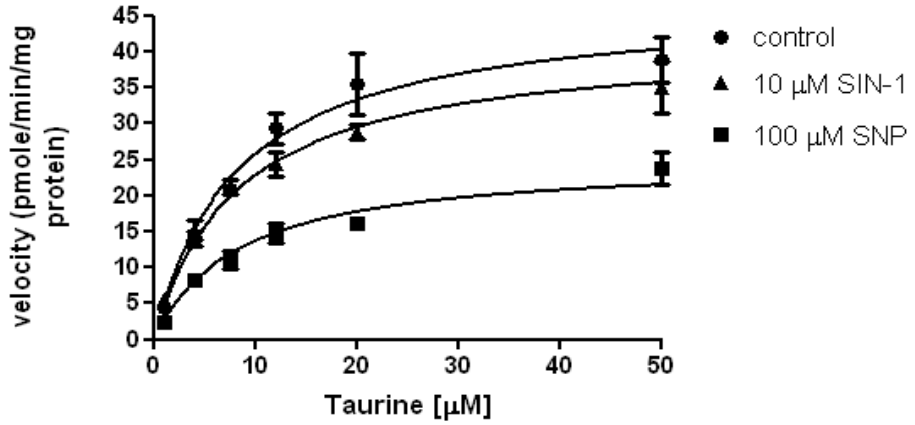

	control	100 μM SNP	10 μM SIN-1
Vmax	48.05	27.96 *	38.60*
Km	8.757	11.17	6.384

Figure 3-14 – Effects of Nitric Oxide and Peroxynitrite on TauT Expression and Taurine Uptake

A) TauT expression was measured by q-RT-PCR. Data expressed as relative quantity of 6 separate experiments mean ± SEM $p<0.05$. * $P<0.05$ vs. untreated (one-way ANOVA)

B) Kinetic plots obtained by measuring taurine uptake in Schwann cells. Michaelis-Menten plots for Na^+ dependent taurine uptake are shown. Vmax and Km were obtained by non-linear regression using Prism software* $p<0.01$ vs. untreated †$p<0.05$ vs. untreated ‡ $p>0.2$ vs. untreated

3.3.7 Effect of NOS Inhibitor on TauT Expression and Taurine Transport

To determine the effect of glucose-mediated NO generation on TauT expression, human Schwann cells were exposed for 7 days to 30 mM glucose in the presence and absence of 50 μM of the NOS inhibitor N-nitro-L-arginine methyl ester (L-NAME).

The effects of NOS inhibition on TauT mRNA are shown in figure 3-12A. Treatment with L-NAME had no effect on TauT mRNA expression in normal glucose concentrations, however in high (30 mM) glucose, L-NAME prevented the high glucose-mediated reduction, restoring TauT mRNA expression from 46 ± 6% to 93 ± 11% ($p<0.05$)

TauT kinetics are shown in figure 3-12B and demonstrate that L-NAME had no effect on TauT kinetics in normal glucose concentration, 51 ± 2 pmoles/min/mg protein in 5 mM compared to 53 ± 3 pmoles/min/mg protein treated with 50 μM L-NAME. In 30 mM glucose, however, L-NAME restored TauT Vmax from 33 ± 3 pmoles/min/mg protein to 60 ± 4 pmoles/min/mg protein ($p<0.05$) with no change in Km.

A

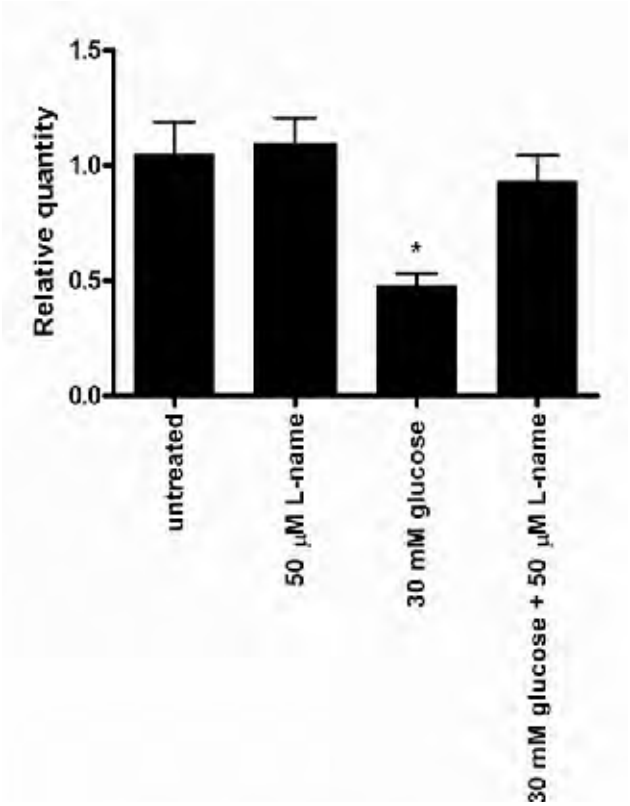

B

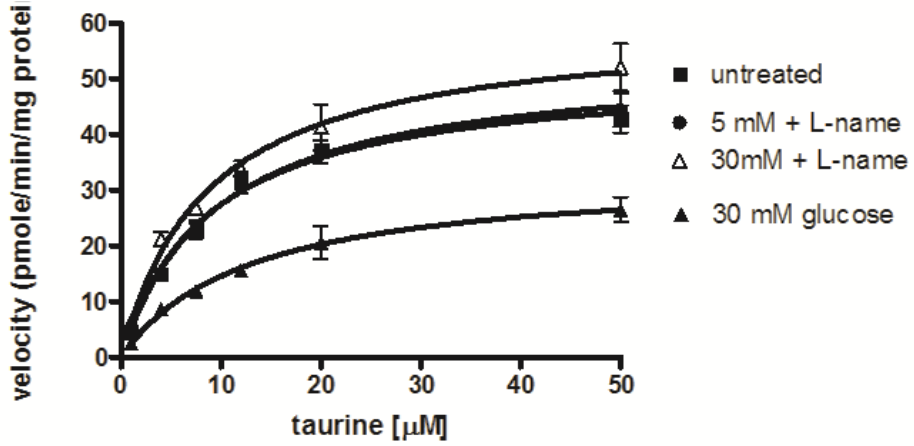

	untreated	30 mM glucose	5 mM + L-name	30mM + L-name
VMAX	51.75	33.25	53.72	60.11
KM	8.856	12.77	9.590	8.689

Figure 3-15 – Effect of NOS inhibition on TauT mRNA expression and Kinetics

A) Effects of 50 μM L-name on high glucose-induced downregulation of TauT mRNA expression. Data expressed as relative quantity of 6 separate experiments mean ± SEM *p<0.05 vs. 5 mM glucose (one-way ANOVA)

B) Effects of 50 μM L-name on high glucose-induced downregulation taurine uptake *p<0.05 vs. 5 mM glucose

3.4 Discussion

This study demonstrates for the first time that exposure of Schwann cell to pathophysiological concentrations of glucose causes a dose-dependent reduction in TauT mRNA expression, protein levels, and Vmax of TauT uptake. This is consistent with previous studies conducted in RPE cells (73; 261) and the observation of decreased circulating and intracellular taurine concentrations in diabetic models and patients. The gradual nature of the reduction illustrates the down-regulation of TauT expression is unlikely to be a direct effect of glucose, but due to a gradual build-up of intracellular metabolites or protein modification such as non-enzymatic glycation, nitrotyrosine or glycosylation by N-acetyl glucosamine.

In Schwann cells, glucose flux through aldose reductase is seen as an important link between hyperglycemia and oxidative stress in diabetic neuropathy. This study demonstrates aldose reductase inhibition reversed the glucose-induced decrease in TauT mRNA expression and Vmax in human Schwann cells. In common with other osmoregulatory genes, such as aldose reductase, TauT is transcriptionally upregulated by tonicity response element (TonE) contained in the 5` region of the gene, in response to hypertonic stress (236; 308). The 'compatible osmolyte' hypothesis suggests that organic osmolytes such as sorbitol, taurine and myoinositol respond coordinately to changes in external osmolarity (72; 73). It is thought that increases in intracellular sorbitol due to greater aldose reductase flux, may contribute to the transcriptional down regulation of TauT expression (73). Hence aldose reductase inhibition depletes intracellular sorbitol resulting in a compensatory increase in TauT expression.

Pro-oxidants alone increased TauT protein expression as well as TauT Vmax. The TauT promoter contains an antioxidant response element (ARE) which is activated in response to

pro-oxidants (73). AREs are known to be activated by pro-oxidant stress and genes known to contain ARE are involved in protecting the cell from oxidative damage. They include glutathione *S*-transferases (309), γ–glutamylcysteine transferase catalytic and regulatory subunits (310). The pro-oxidant response of TauT demonstrates the paradox whereby oxidative stress increases TauT expression, whereas high glucose (which increases oxidative and nitrosative stress by a wide range of pathways) down regulates TauT expression and taurine transport. The TauT response to pro-oxidant stimuli was blocked by co-treatment with 30 mM glucose which illustrates that a component of glucose-induced stress, other than oxidative stress is responsible for the down-regulation of TauT.

Further demonstrating the paradox of TauT down-regulation in high glucose, treatment with the antioxidant ALA restored TauT mRNA expression and Vmax. This effect was repeated with antioxidant treatment with vitamin C and taurine. Antioxidants would not be expected to alter sorbitol content; hence it appears antioxidants neutralize a component of glucose toxicity, such as glycation, 3-nitrotyrosine, or S-nitrosylation which impairs the TauT response to oxidative stress. This parallels studies in streptozotocin diabetic rats where ALA restored nerve taurine content without affecting sorbitol content (115) and in the composite nerve, taurine restored taurine content without affecting either sorbitol or myoinositol abundance (75).

To examine the nature of the antioxidant-sensitive component and to ascertain the effect of increased nitric oxide and nitrotyrosine on TauT expression, Schwann cells were incubated with SNP an NO donor and SIN-1 a peroxynitrite donor. These demonstrated that both NO and peroxynitrite reduce TauT mRNA expression and TauT Vmax to a similar extent. In 5 mM glucose, NOS inhibition had no effect on TauT expression, however, in high glucose co-treatment with the NOS inhibitor L-NAME reversed the glucose-induced decrease in TauT

expression and Vmax without affecting the Km. These demonstrates that RNS and/or NO down regulate taurine transport and increased RNS and NO in diabetes could therefore contribute to TauT downregulation. Since antioxidants reduce RNS, it is likely this is the component they affect, restoring taurine transport.

This study highlights the paradox of glucose-mediated TauT downregulation. High glucose exposure decreases taurine transport whereas pro-oxidants upregulate taurine transport. TauT expression and kinetics are restored by aldose reductase inhibition, antioxidant treatment and NOS inhibition, whilst NO and peroxynitrite alone reduced TauT expression and taurine transport. Together these data implicate intracellular sorbitol as well as nitrosative stress in glucose-induced TauT downregulation.

Chapter 4 - Effect of High Glucose and Taurine Supplementation on Oxidative Stress and the Antioxidant Defence System in Human Schwann Cells

4.1 Introduction

Increased oxidative stress, driven by glucose has been identified in the nerve (113-115), eye (71), vasculature (311), kidney (312; 313) and heart (314) in diabetic rodent models and in diabetic patients (119-122). Oxidative stress occurs due to an imbalance in the production of reactive oxygen species (ROS) in concert with impaired antioxidant defence. Excess ROS production can have many down-stream pathogenic effects within the cell including protein nitration, formation of poly(ADP-ribosyl)ated (PAR) protein polymers and apoptosis (315-320). Antioxidant approaches have been shown to prevent or reverse complications in experimental diabetes (145). Glycation of superoxide dismutase (SOD) has been hypothesised as the mechanism behind the observed reduction in SOD activity in some models, however, this, in similar fashion to increased activity of catalase (CAT) appears to be tissue-specific and has never been examined in human Schwann cells. Antioxidant defence may also be compromised because increased aldose reductase flux depletes intracellular NADPH, an essential cofactor for regenerating reduced glutathione (GSH), resulting in GSH depletion in many diabetic models (4; 32).

Hyperglycaemia-induced taurine depletion has been demonstrated in the nerve (321), lens (322) and mesangial cells (323) of diabetic rodents. Circulating taurine levels are reduced in diabetic patients (257). Intracellular taurine depletion may result in wide-ranging metabolic perturbations including impaired cellular response to oxidative/nitrosative stress with resultant cytotoxicity. Indeed taurine replacement has been shown to attenuate oxidative stress and functional deficits in these tissues (76; 145; 264), and to ameliorate thermal and mechanical hyperalgesia (225; 262) in diabetic rodents. The antioxidant mechanism of taurine

is unclear, since taurine is unable to directly scavenge classic ROS (266). Some studies have attributed the antioxidant action of taurine as an indirect effect by acting upon the antioxidant defence system, however, it is unclear whether this occurs in diabetes (76).

In this study I examined whether hyperglycaemia increases oxidative stress and PAR abundance in human Schwann cells. I also determined the activity of both SOD and CAT and the level of GSH. The effects of taurine on all these parameters were examined.

4.2 Methods

Methods used are described in Chapter 2 with the following additions.

4.2.1 Western Blot Antibody Selection

Hydroxyl radical ($OH^{\cdot}$) removes a hydrogen from polyunsaturated fatty acids producing lipid radical which reacts with O2 forming lipid peroxy radicals such as 4-hydroxy-2-noneal (4HNE). 4HNE is a highly reactive aldehyde which reacts non-enzymatically with histidine, lysine and cysteine amino-acid side-chains, forming stable adducts. The abundance of 4HNE adducts is used as a measure of ROS in biological systems. A well-characterised commercial antibody against 4HNE adducts was used in Western blots (Merck) ((64; 324; 325) and total band density was determined.

ROS and RNS are known to cause DNA strand breaks. Poly-ADP-ribose-polymerase 1 (PARP) is a nuclear enzyme known to be activated by DNA strand breaks. Upon activation PARP cleaves nicotinamide adenine dinucleotide (NAD^{+}) forming nicotinamide and ADP-ribose residues, and the latter attaches to nuclear proteins forming poly(ADP-ribosyl)ated protein polymers. The abundance of poly(ADP-ribosyl)ated proteins was measured by Western blot using a well-characterised commercial antibody (Alexis) (326-328) and total band density was determined.

4.3 Results

4.3.1 Effect of High Glucose on Oxidative Stress

The changes in oxidative stress in human Schwann cells after chronic (7 day) exposure to 5, 10 and 30 mM glucose were explored using H_2DCFDA reagent to assay ROS generation. The results are shown in figure 4-1A which demonstrate that fluorescence intensity was increased in 10 and 30 mM glucose compared to 5 mM glucose. This experiment was repeated 3 times with consistent increases

To confirm this finding, Western blotting against stable 4HNE adducts, was performed on cells treated with high glucose for 7 days, shown in figure 4-1B. 4HNE abundance was increased by 30 ± 4% and by 20 ± 5% (both $p<0.05$) on exposure to 10 and 30 mM glucose, respectively

4.3.2 Effect of High Glucose on PAR Formation

To assess the effect of high glucose on PAR formation, Western blotting of PAR proteins was performed in Schwann cells incubated in high glucose for 7 days and data are displayed in figure 4-2. PAR protein abundance was increased dose-dependently, 26 ± 7% in 10 mM and 40 ± 13% in 30 mM glucose ($p<0.05$).

A

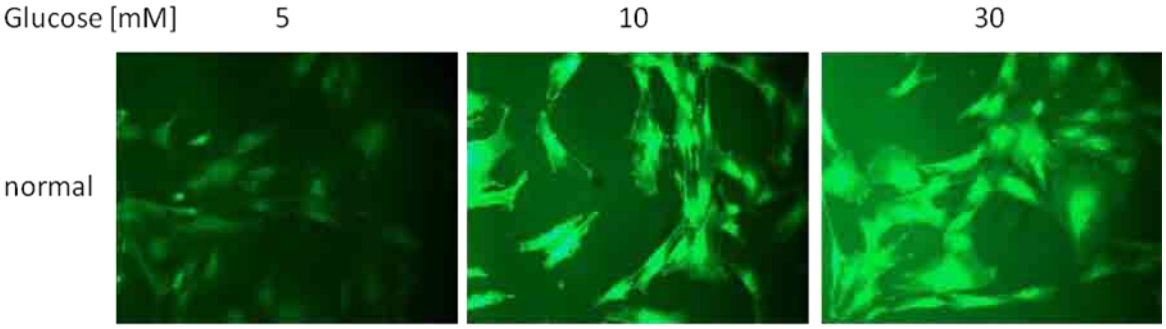

B

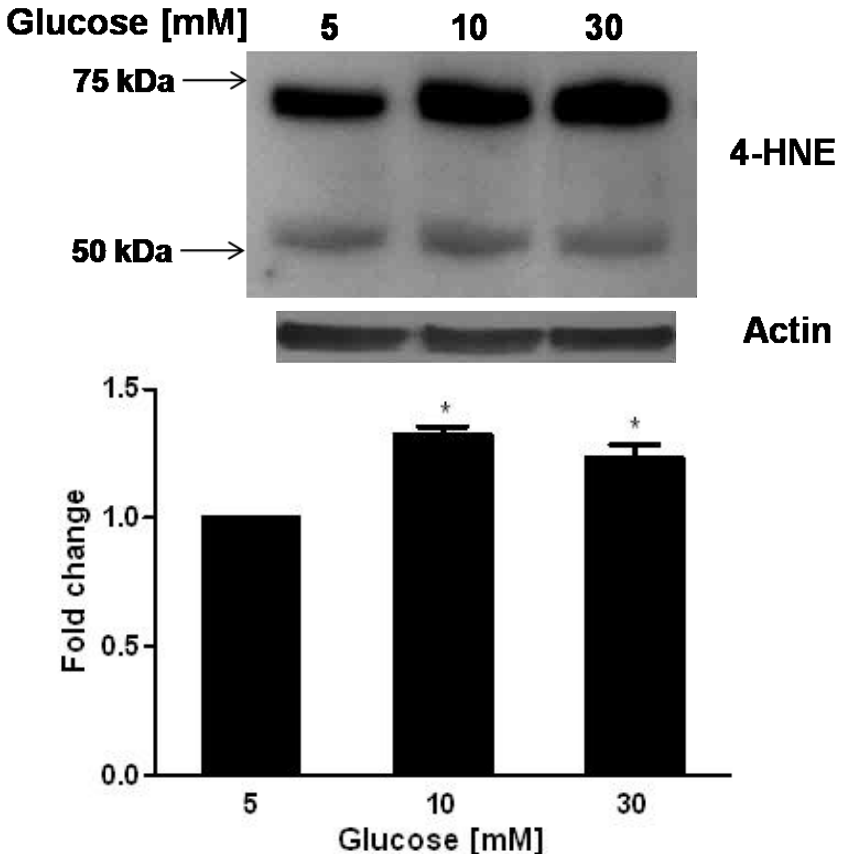

Figure 4-1 – Effect of High Glucose on Oxidative Stress

Effect of high glucose on oxidative stress (A) representative images of ROS fluorescence measured using H_2DCFDA and (B) representative western blots of 4HNE adducts. Equal protein loading confirmed by β-actin. Quantitation performed by densitometry and data expressed as mean ± SEM of 5 separate experiments. * $P<0.05$ vs. 5mM glucose (one-way ANOVA). Data published – see chapter 7.3 (appendix)

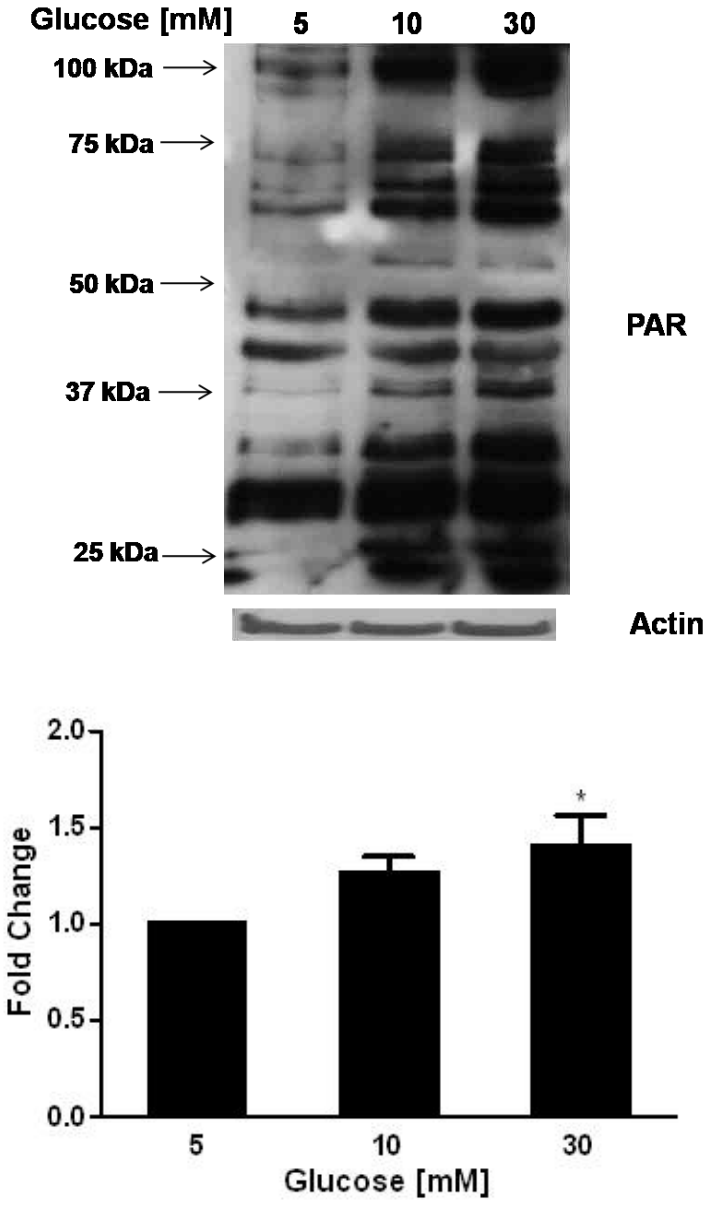

Figure 4-2 – Effect of High Glucose on Poly(ADP-ribosyl)lated Protein Abundance

Effect of high glucose on poly(ADP-ribosyl)lated protein abundance. Equal protein loading confirmed by β-actin. Quantitation performed by densitometry on total bands and data expressed as mean ± SEM of 5 separate experiments. * $P<0.05$ vs. 5mM glucose (one-way ANOVA)

Data published – see chapter 7.3 (appendix)

4.3.3 Effect of High Glucose on the Antioxidant Defence System

To determine the response of the antioxidant defence in response to glucose-induced oxidative stress, the activities of SOD and catalase were measured, along with GSH concentration in human Schwann cells after chronic (7 days) exposure to 5, 10 and 30 mM glucose.

The activity of SOD was increased by 41 ± 24% in 10 mM and 70 ± 18% in 30 mM glucose ($p<0.05$ compared with untreated), shown in figure 4-3A. As illustrated in figure 4-3B catalase activity was increased 3 fold at 10 mM and 30 mM glucose (both $p<0.05$), clearly demonstrating mobilisation of the antioxidant defence system in response to high glucose. The abundance of GSH was reduced by 16 ± 6% at 10 mM and by 28 ± 4% at 30 mM glucose ($p<0.05$), shown in figure 4-3C. No change was observed when 30 mM L-glucose was used as an osmotic control.

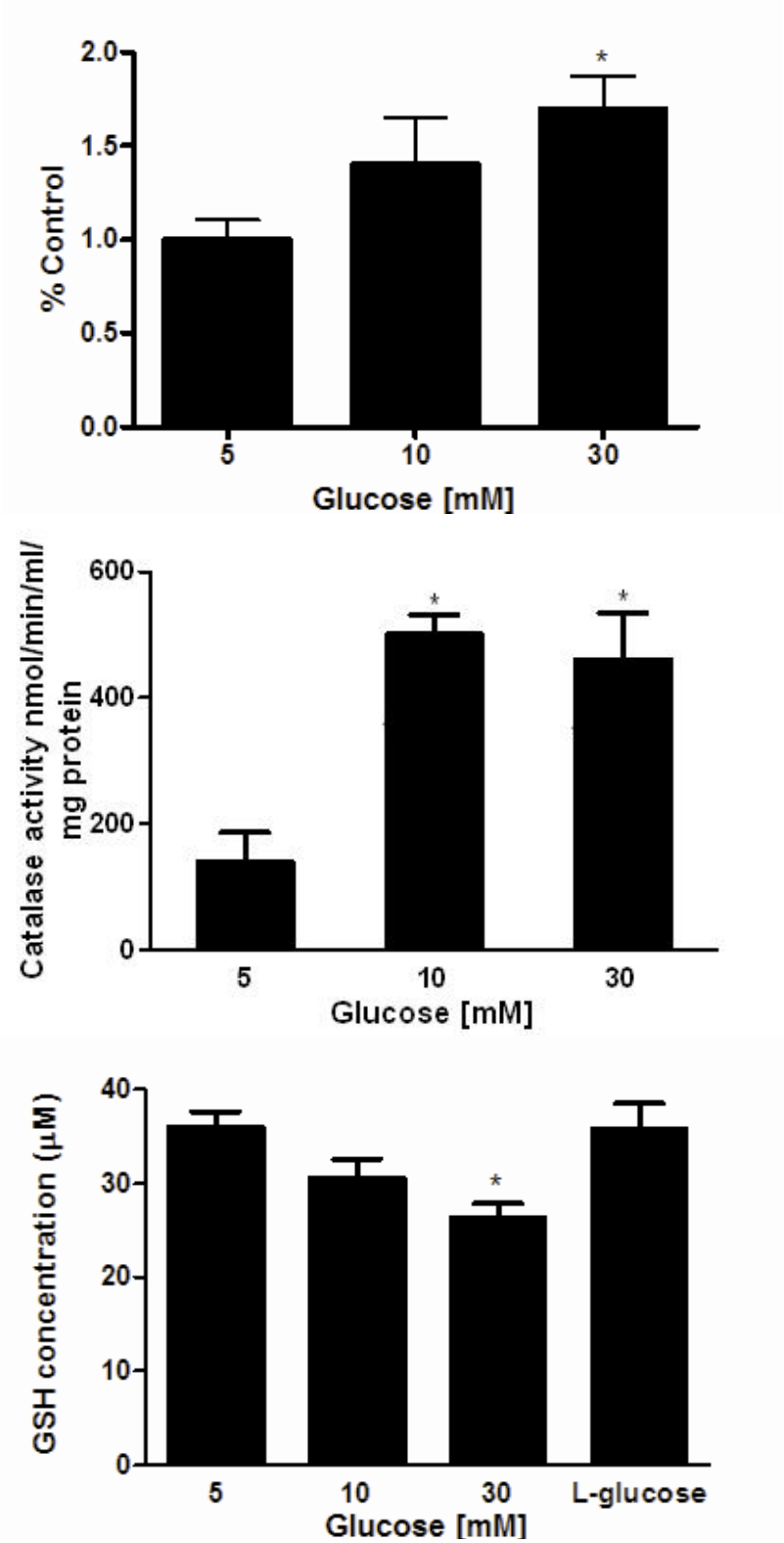

Figure 4-3 – Effect of High Gluocse on Antioxidant Defence

Effects of high glucose on SOD and catalase activity and GSH concentration. Data expressed as mean ± SEM * $p<0.05$ vs. untreated 5 mM glucose (one-way ANOVA). Data published – see chapter 7.3

4.3.4 Effect of Taurine on High Glucose-Induced Oxidative Stress

The effects of taurine on glucose-induced increases in oxidative stress were explored by co-treatment with glucose and 250 µM taurine for 7 days. As shown in figure 4-4, the increase in H_2DCFDA fluorescence induced by high glucose was abrogated by concurrent treatment with 250 µM taurine.

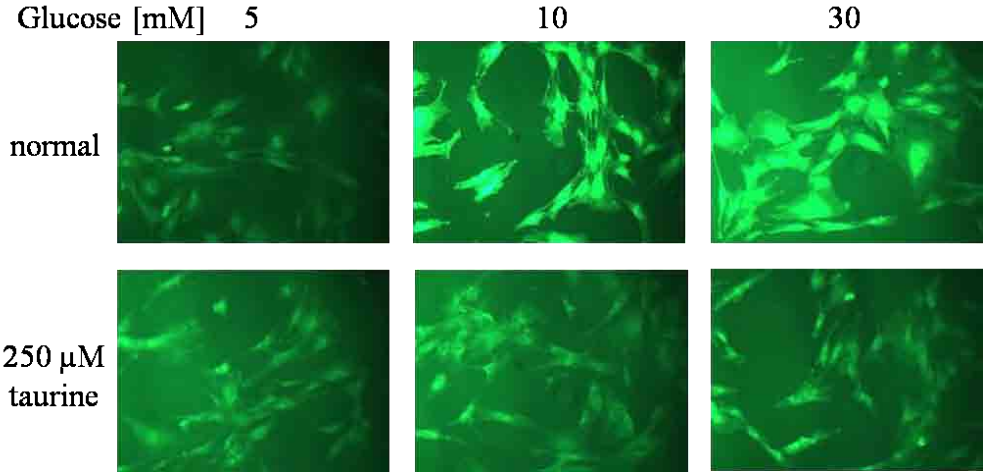

Figure 4-4 - Effect of Taurine on High Glucose-Induced Oxidative Stress

Effect of high glucose and taurine on oxidative stress. Representative images of ROS fluorescence measured using H_2DCFDA

Data published – see chapter 7.3 (appendix)

4.3.5 Effect of Taurine on High Glucose-Induced 4HNE Abundance

The effect of co-treatment with glucose and 250 µM taurine on 4HNE abundance is shown in figure 4-5. In high glucose conditions, taurine treatment reduced 4HNE abundance compared to untreated 5 mM control with a 9% reduction at both 10 and 30 mM ($p<0.05$ both vs. respective glucose concentration). At 5 mM glucose, taurine addition resulted in a similar reduction in 4HNE abundance, 9 ± 3% reduction, $p=0.2$.

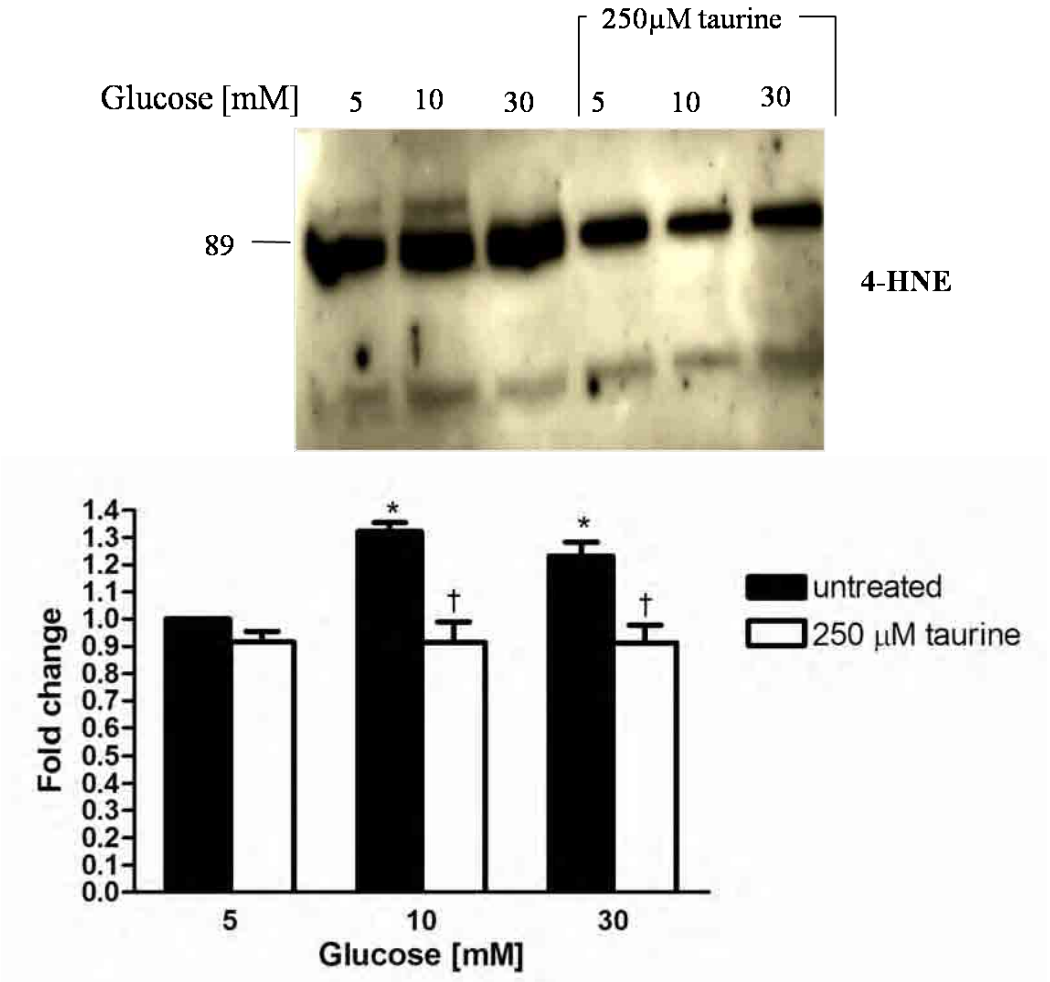

Figure 4-5 - Effect of Taurine on High Glucose-Induced 4HNE Abundance

Effect of high glucose on 4HNE abundance. Representative western blots of 4HNE adducts. Equal protein loading confirmed by β-actin. Quantitation performed by densitometry and data expressed as mean ± SEM of 5 separate experiments. * P<0.05 vs. 5mM glucose (one-way ANOVA) † p<0.05 vs. respective glucose (two-way ANOVA).

Data published – see chapter 7.3 (appendix)

4.3.6 Effect of Taurine on High Glucose-Induced PAR Abundance

The effects of taurine co-treatment on PAR protein abundance are shown in figure 4-6. Taurine reduced PAR protein abundance compared to untreated 5 mM control, with a 14 ± 2% reduction at 5 mM glucose and reductions of 12 ± 19% and 3 ± 14% in 10 and 30 mM glucose respectively ($p<0.05$ vs. respective glucose concentration)

4.3.7 Effect of Taurine Treatment on the Antioxidant Defence System

To ascertain whether the antioxidant effects of taurine were due to upregulation of antioxidant defence systems, the effects of taurine treatment in normal and high glucose were measured and compared to the antioxidant ALA and shown in Table 4-1. In 5 mM glucose taurine treatment resulted in a 3 fold increase in catalase activity ($p<0.05$), and a 50 ± 21% increase in SOD activity ($p=0.144$). ALA also increased SOD activity in 5 mM glucose by 79 ± 18% ($p<0.05$) and CAT activity 3 fold ($p<0.05$). The response of GSH to ALA, however, differed from that of taurine, since ALA increased GSH concentration at 5 mM glucose by 22 ± 10% ($p<0.05$), whereas taurine decreased GSH concentration by 23 ± 4% ($p<0.05$). In high glucose, taurine treatment had no additive effect on either SOD or catalase activity and did not restore GSH content, whereas ALA restored GSH content and had some additive effect on catalase activity, although this was not statistically significant.

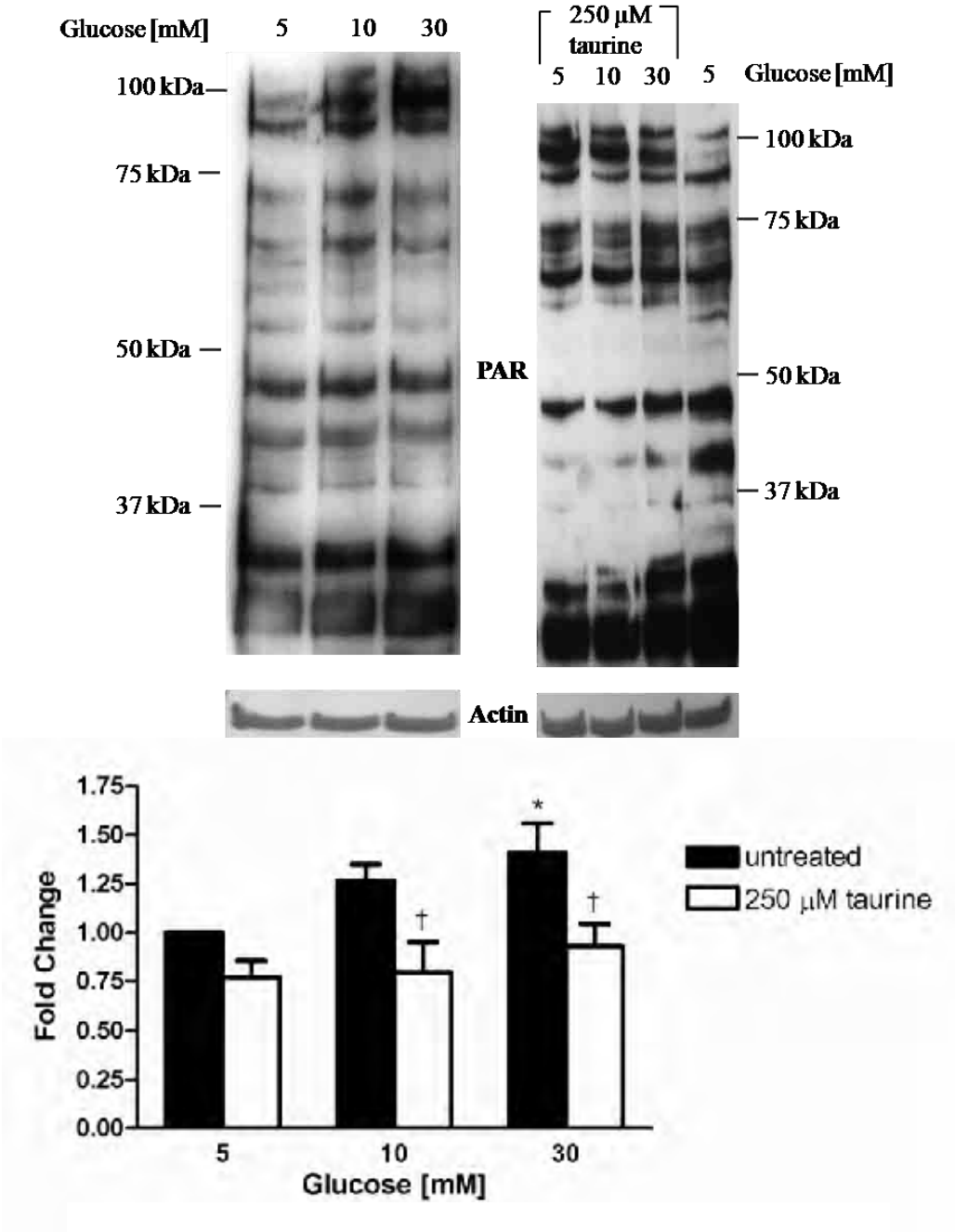

Figure 4-6 - Effect of Taurine on High Glucose-Induced PAR Abundance

Effect of high glucose and taurine on poly(ADP-ribosyl)ated protein abundance. Equal protein loading confirmed by β-actin. Quantitation performed by densitometry on total bands and data expressed as mean ± SEM of 5 separate experiments. * $P<0.05$ vs. 5 mM glucose (one-way ANOVA) † $p<0.05$ vs. respective glucose (two-way ANOVA)

Data published – see chapter 7.3 (appendix)

			SOD activity (% control)	catalase activity nmol/min/ml/mg protein	GSH [µM]
Glucose [mM]	5	**untreated**	100 ± 11	139 ± 48	36 ± 1.6
		taurine	150 ± 21	519 ± 72*	28 ± 1.4*
		ALA	179 ± 18*	444 ± 92*	44 ± 3.7*
	10	**untreated**	141 ± 24	500 ± 32*	31 ± 2.0
		taurine	142 ± 10	493 ± 78*	29 ± 1.8
		ALA	168 ± 16	606 ± 87*	32 ± 1.5
	30	**untreated**	170 ± 18*	349 ± 69*	26 ± 1.5*
		taurine	167 ± 15	504 ± 80*	29 ± 1.8
		ALA	145 ± 16	616 ± 109*	33 ± 3.0†
	25 mM L-glucose	**untreated**			36 ± 2.7

Table 4-1 - Effect of Taurine Treatment on the Antioxidant Defence System

Effects of high glucose co-treated with either 250 µM taurine or 100 µM ALA on SOD and CAT activity and GSH concentration. Data expressed as mean ± SEM * $p<0.05$ vs. untreated 5 mM glucose (one-way ANOVA) † $p<0.05$ vs. respective glucose (two-way ANOVA)

Data published – see chapter 7.3 (appendix)

4.4 Discussion

There is substantial evidence for increased oxidative/nitrosative stress in peripheral nerve of diabetic rodents (32; 304). In experimental diabetic neuropathy, increased ROS abundance and nitrotyrosine immunoreactivity have been observed in the epineurial blood vessels (304) which may be etiologically important in the development of nerve perfusion deficits. Oxidative stress, PARP activation (329) and apoptosis in dorsal root ganglion neurones have also been implicated in the development of functional and structural deficits (330). However, the effects of pathophysiological elevations of glucose on Schwann cell metabolism and function remain less well characterised. In the studies reported herein, in common with Obrosova et al., 2005 I demonstrated that high glucose increased oxidative stress, lipid peroxidation and PAR abundance in human Schwann cells. These effects demonstrate high glucose directly inducing oxidative stress within Schwann cells, independent of the nerve, or vascular deficits. It also suggests Schwann cell dysfunction in diabetes is directly due to effects of glucose on Schwann cells rather than vascular deficits.

The response of the antioxidant defence system to glucose-induced oxidative stress is tissue specific and the response in human Schwann cells is unclear. In this study in non-immortalised *human* Schwann cells the activity of both SOD and catalase increased in response to glucose-induced increases in oxidative stress. The abundance of GSH however decreased. These combined responses demonstrate some mobilisation of antioxidant defence in response to glucose-induced oxidative stress, but considering the increase in oxidative stress and PAR in high glucose, the response is insufficient.

Depletion of GSH is a common observation in models of diabetic neuropathy, seen in the sciatic nerve of diabetic rodents (75; 115) as well as immortalised mouse Schwann cells.

Changes of SOD and catalase in diabetes are much more inconsistent than those of GSH and vary depending upon both tissue and model. In the nerve of STZ-D rats the activity of both SOD and catalase tended to decrease (115). In the only previous study in Schwann cells exposed to high glucose, increased oxidative stress was associated with decreased SOD activity, while the activity of catalase remained unchanged (65). This study was performed in immortalised mouse Schwann cell and mice have lower aldose reductase expression than in humans (85; 114). Whether the differences between my study and that of Miinea et al are due to species differences known to occur in diabetes (77; 139; 331; 332), or due to the immortalization of the cells, is yet to be determined.

Taurine is known to have a potent ability to reduce ROS and lipid peroxidation but the precise mechanism(s) of its antioxidant effect remain uncertain. Aruoma et al., 1988 (333) established that taurine is incapable of directly scavenging superoxide anion, hydroxyl radical and hydrogen peroxide, although, it is known to scavenge hypochlorite produced by morphonuclear leukocytes and eosinophils (76). While of relevance in whole animal models, in isolated cell culture, this mechanism does not account for the antioxidant effect observed and many authors cite indirect mechanisms of ROS scavenging by taurine, e.g. by increasing the activities of other members of the antioxidant defence system (76).

This study demonstrates that in normal glucose concentrations (5 mM) taurine has an indirect affect on SOD and catalase, increasing the activity of both in a similar manner to ALA. Taurine however, decreased GSH abundance in normal glucose, which was increased by ALA. The mechanism of this effect is unclear however; since taurine and GSH are both synthesized from cysteine, depletion of GSH may reflect reduced synthesis, due to decreased cysteine uptake (334), or structural differences between the antioxidants or varying targets of antioxidant activity.

The effect of taurine on markers of oxidative stress has previously been explored in animal models of diabetes, where taurine has been found to reduce lipid peroxidation in the plasma (263), heart, muscle, liver, kidney (264) and sciatic nerve (145) and decrease superoxide formation in β-islet cells from rats infused with high glucose (265). My study demonstrates for the first time the ability of taurine to reduce glucose-induced ROS generation and lipid peroxidation in Schwann cells. I also demonstrated for the first time that taurine can completely prevent the accumulation of PAR proteins. The effect of taurine on PAR protein abundance is consistent with that observed for aldose reductase inhibitors (80-82) and direct PAR inhibition (64). The mechanism of this effect is unknown, however, a mechanism involving the attenuation of oxidative or nitrosative stress is likely to be involved. PARP inhibition reduces oxidative stress and 4HNE abundance in human Schwann cells (64) and in STZ-D rats restores nerve conductivity (203), effects similar to taurine treatment. Considering the effect of taurine on PAR in 5 mM glucose, it is possible that taurine-mediated effects are through actions on this pathway.

Increased oxidative stress and PAR accumulation are signatures of glucose-induced cell dysfunction and normalisation of these abnormalities demonstrates the ability of taurine to reduce diabetes-induced Schwann cell dysfunction. These effects would likely improve nerve growth factor and myelin deficits observed in diabetes due to Schwann cell dysfunction. This reversal would also affect oxidative stress in the peripheral nerve and endoneurium.

In high glucose, taurine treatment had no additive effect on SOD or catalase activity and did not restore GSH content, whereas ALA restored GSH content. In experimental diabetic neuropathy in the rat, taurine treatment was found to reduce lipid peroxidation, attenuate deficits of nerve conduction, dorsal root ganglion neuron calcium signalling, endoneurial blood flow and hyperalgesia (225). In this animal model in the composite nerve, no changes

in SOD activity or GSH abundance (145) were observed with taurine treatment, with taurine being found to selectively impact only the ascorbate/dehydroascorbate system.

These effects are indicative of direct antioxidant actions. It is possible this is due to the effects of taurine on Ca^{2+} signalling or AGE scavenging, or through PARP inhibition, therefore reducing ROS generation by normalising these deficits. Another possibility, is based around work from Suzuki (335; 336) and Kirino (337) who found that taurine forms conjugates with uridines of mammalian mitochondrial tRNA and in certain mitochondrial diseases these taurine modifications were lacking. This raises the possibility that taurine may be important in synthesis of mitochondrial proteins, such as those in the electron transport chain. Deficiency in synthesis of these proteins may lead to diversion of electrons from respiratory transport to oxygen, increasing formation of superoxide anion and resulting in back-up glycolytic metabolites, increasing flux through pathways associated with diabetic complications, such as polyol pathway (76). This suggests that rather than a direct antioxidant effect of taurine, taurine supplementation reverses the pro-oxidant effect of taurine depletion, brought about by TauT down regulation.

In conclusion in a key site for diabetic complications, glucose increased oxidative stress and PAR abundance, SOD and catalase activity, while disrupting the glutathione system. Taurine supplementation restored ROS, 4HNE and PAR back to levels found in normal glucose. This action was achieved without changes in classic antioxidant defence systems demonstrating direct antioxidant taurine actions.

Chapter 5 - Effect of Taurine on Nitrosative Stress and NO Regulation in High Glucose

5.1 Introduction

Reactive nitrogen species (RNS) are produced by the reaction between nitric oxide (NO) and superoxide (O_2^-) (178) to form the highly reactive peroxynitrite ($ONOO^-$). This can further react with CO_2, or H^+ to form other RNS such as nitrosoperoxycarbonate ($ONOOCO_2^-$) and nitrogen dioxide (NO_2^-) (177). RNS are known to induce DNA damage, poly(ADP-ribose) polymerase activation and nitration of amino acids on proteins (178), which is known to modify protein function. For many receptor tyrosine kinases, e.g. the insulin receptor, phosphorylation of tyrosines is an important signalling event, and thus tyrosine nitration can prevent its phosphorylation and can block growth factor and insulin actions (190). Increased nitrotyrosine has been observed in the peripheral nerve, spinal cord and dorsal root ganglion in animal models of both type 1 and type 2 diabetes mellitus (32) and is associated with increased levels of nitrate and nitrite in the serum of patients with both Type 1 (176) and Type 2 diabetes (142; 144) as well as increased expression of both iNOS and nNOS in various tissues.

In this study I therefore examined the effect of glucose and taurine co-treatment on iNOS and nNOS expression along with nitrotyrosine abundance. Akt plays a critical role in insulin signalling and is activated by insulin binding to receptor tyrosine kinases (8). Akt activation is reduced by oxidative and nitrosative stress and also in models of diabetes (8; 190). Whether this reduction is due to reduced insulin secretion and/or hyperglycaemia is controversial (8). Therefore in the isolated Schwann cell model I examined the effect of high glucose on Akt protein expression and activation.

In results Chapter 4, I demonstrated that taurine supplementation reduced glucose induced oxidative stress, lipid peroxidation, and poly(ADP-ribose) accumulation. Some of the MAPK pathways are activated by oxidative/nitrosative stress and have been seen as transducers of glucose-induced cellular stress (6; 59). Therefore I examined the effects of high glucose and taurine co-treatment on activation and protein expression on p38 MAPK, p42/44MAPK and JNK/SAPK.

5.2 Methods

5.2.1 Actin Validation

To validate the use of actin as an endogenous control in mRNA quantitation, the amplification efficiency of actin vs. iNOS and nNOS primers were checked over 10 fold dilutions of RNA between 0.2ng and 200ng (figure 5-1). The trend-line gradients from these were all less than 0.1, demonstrating similar amplification efficiencies of actin compared to target primers, allowing the ΔΔCt method of analysis to be used.

5.2.2 Antibody Selection

The levels of nitrotyrosine were measured by Western blot using a well-characterised commercial antibody against nitrotyrosine, which is used as a marker of RNS and can also be used as a marker of NO production (Millipore) and inflammation (338-341). Densitometry was used for quantitation, total band density being determined. Although this antibody is specific for nitrotyrosine and will not recognise S-nitrosylation of cysteine on amino acids, it should reflect NO production from NOS.

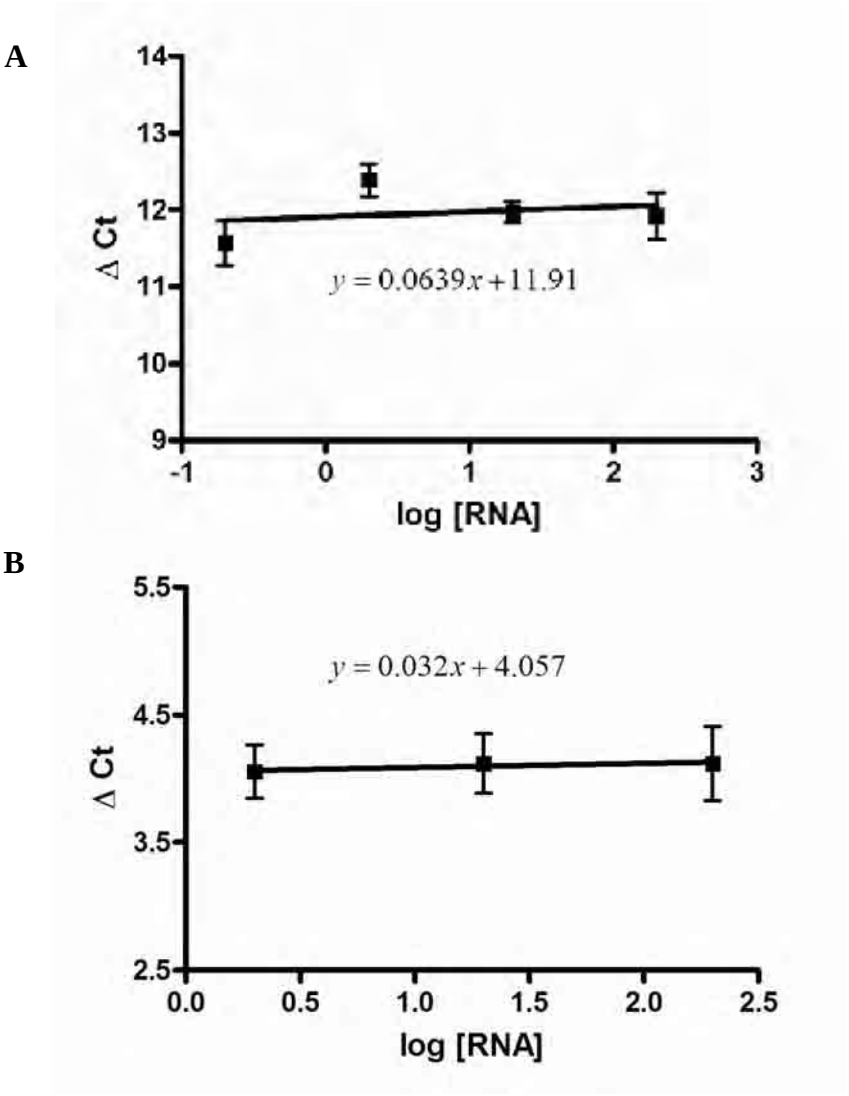

Figure 5-1 - Validation of Amplification Efficiencies of Actin and Target A) nNOS B) iNOS.

q-PCR was run with 10 fold dilutions of untreated RNA from 200ng to 0.2ng, except with iNOS where there was no detectable target with 0.2ng RNA. For each primer there was limited change in ΔCt with different RNA concentrations, demonstrated by the gradient of the linear regression < 0.1. Data expressed as mean ± SEM of 6 separate experiments.

5.3 Results

5.3.1 Effect of High Glucose on nNOS and iNOS mRNA Expression

In order to determine the effect of high glucose on iNOS and nNOS mRNA expression analysis by qRT-PCR after exposure of human Schwann cells to 5, 7.5, 10, 15, 22 and 30 mM glucose was examined. The data are shown in figure 5-2.

The expression of iNOS was significantly increased at glucose concentrations >15 mM, with a 77 ± 25% and 55 ± 20% increase at 22 and 30 mM glucose respectively ($p<0.05$ both vs. 5 mM glucose). nNOS expression was increased at glucose concentrations >10 mM with dose-dependent increases of 60 ± 14%, 89 ± 20% and 120 ± 24% in 15, 22 and 30 mM respectively ($p<0.05$ all). No increase was found when the osmotic control, 25 mM raffinose, was used in place of glucose, iNOS 10 ± 9% increase, nNOS 5 ± 7% decrease.

5.3.2 Effect of High Glucose on Protein Nitrotyrosine Content

To determine the effect of sustained high glucose levels on the formation of nitrotyrosine, Western blotting was performed against nitrotyrosine. A representative blot and pooled densitometry data are shown in figure 5-3. The abundance of nitrotyrosine was increased by 46 ± 16% in 10 mM and by 56 ± 11% in 30 mM glucose ($p<0.05$) compared to 5 mM glucose. These experiments were repeated 4 times with consistent increases observed.

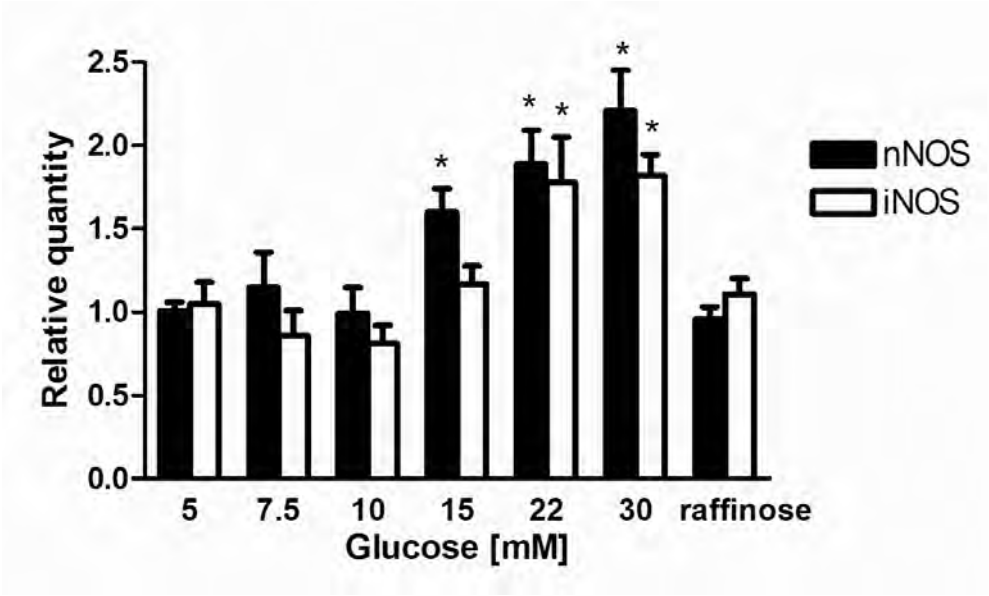

Figure 5-2 - Concentration Dependent Effects of Chronic Glucose Exposure on the Expression of iNOS and nNOS mRNAs

iNOS and nNOS mRNA expression was measured by q-RT-PCR using TauT specific primers. Data expressed as relative quantity of 6 separate experiments mean ± SEM $p<0.05$. * $p<0.05$ vs. 5 mM glucose (one-way ANOVA).

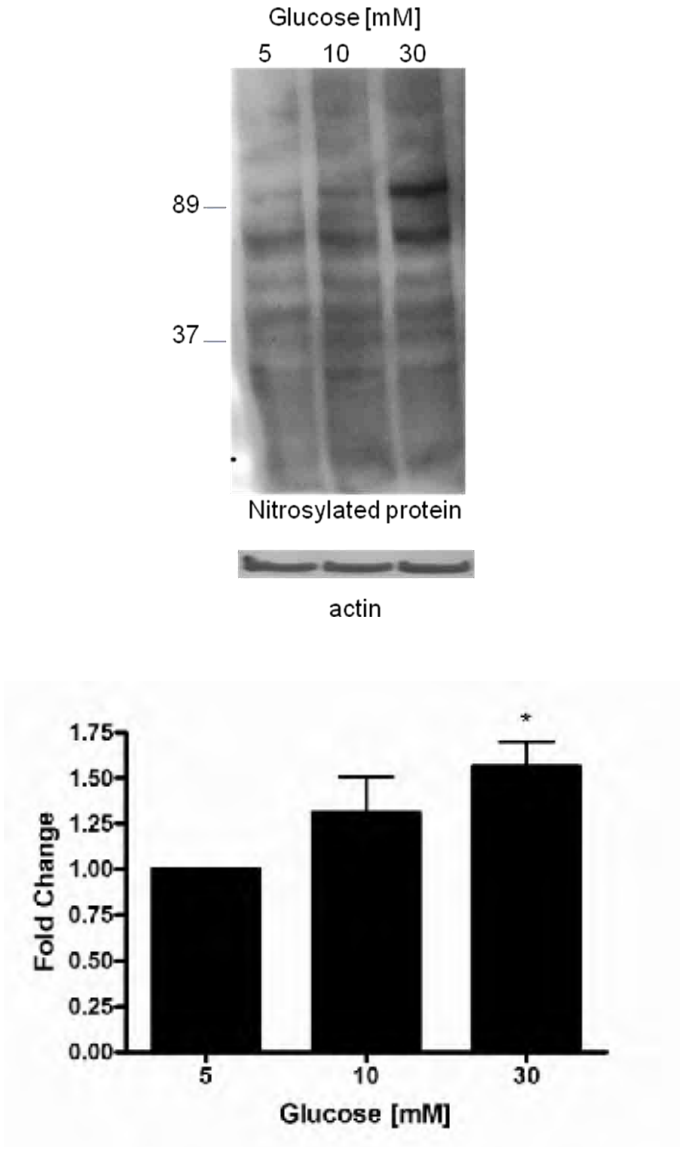

Figure 5-3 - Effect of High Glucose on Protein Nitrosylation

A representative Western blot of nitrosylated proteins is shown. Equal protein loading confirmed by β-actin. Quantitation was performed by densitometry and data expressed as mean ± SEM of 5 separate experiments. * $p<0.05$ vs. 5 mM glucose (one-way ANOVA)

5.3.3 Effect of Taurine on iNOS and nNOS mRNA Expression

To further document the effect of taurine supplementation on glucose-mediated events, the effect of taurine co-treatment on iNOS and nNOS mRNA expression was performed in human Schwann cells exposed to normal (5 mM) and high (10-30 mM) glucose. To determine whether the effects of taurine on NOS were antioxidant-mediated, they were compared to the antioxidant ALA. The data are shown in figure 5-4

In 5 mM glucose, neither taurine nor ALA affected iNOS mRNA expression (figure 5-4A) In 10 mM glucose, taurine treatment increased iNOS mRNA expression 45 ± 5% ($p<0.05$), whereas the 12 ± 7% increase observed with ALA, was not statistically significant. In 30 mM glucose, co-treatment with either taurine or ALA entirely prevented glucose-mediated upregulation of iNOS with 50 ± 15% and 40 ± 5% reductions in iNOS expression compared to untreated 30 mM glucose ($p<0.01$ both).

The corresponding changes in nNOS expression are shown in figure 5-4B. In normal glucose (i.e. 5 mM) both taurine and ALA increased nNOS expression compared to control by 130 ± 43% and 81 ± 18% respectively ($p<0.05$ both). In 10 mM glucose, neither co-treatment with taurine, nor ALA had any significant effect on nNOS expression compared with untreated 10 mM. In 30 mM glucose the effects of ALA and taurine differed: Taurine decreased nNOS expression by 44 ± 18% to levels similar to 5 mM glucose, whereas ALA co-treatment did not affect nNOS expression.

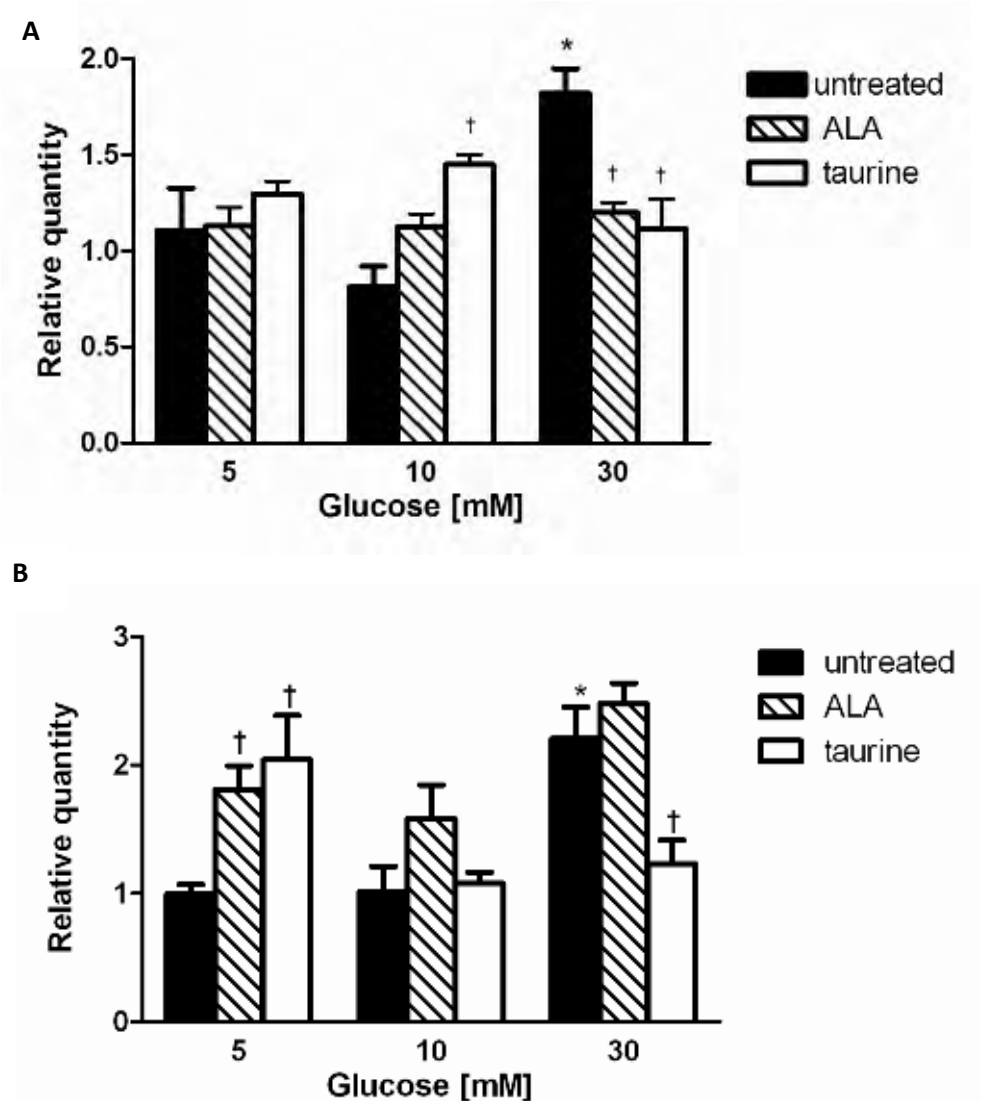

Figure 5-4 - Effect of Taurine and ALA on iNOS and nNOS mRNA Expression

Effect of treatment with 100 µM ALA and 250 µM taurine on (A) iNOS and (B) nNOS mRNA expression in normal and high glucose. Data expressed as relative quantity of 6 separate experiments mean ± SEM * $p<0.05$ vs. 5mM glucose (one-way ANOVA) †$p<0.05$ vs. respective glucose (two-way ANOVA)

5.3.4 Effect of Taurine on Nitrotyrosine

In Chapter 4, I demonstrated that taurine reduces oxidative stress in glucose-exposed human Schwann cells. To determine whether taurine also reduces nitrosative stress, I measured the effect of taurine co-treatment in normal (5 mM) and high (10 and 30 mM) glucose on nitrotyrosine. In response to co-treatment with 250 μM taurine, the abundance of nitrotyrosine, measured by densitometry of nitrotyrosine on Western blots, was significantly reduced to levels below 5 mM untreated glucose, with reductions at 5, 10 and 30 mM glucose of 50 ± 10%, 54 ± 7% and 56 ± 11% respectively ($p<0.05$ all) figure 5-5.

5.3.5 Effect of Polyol Pathway Flux on iNOS and nNOS mRNA Expression

Flux through the polyol pathway increases oxidative/nitrosative stress and depletes intracellular taurine. To explore the effect of increased polyol pathway flux on iNOS and nNOS expression, human Schwann cells were co-treated with 5, 10 and 30 mM glucose, along with the aldose reductase inhibitor, sorbinil (10 μM).

The response of iNOS expression to sorbinil is shown in figure 5-6A, demonstrating that sorbinil increased iNOS expression in normal glucose media (5 mM) and in 10 mM glucose by 74 ± 20% and 72 ± 13% respectively ($p<0.05$ both). In 30 mM glucose however, sorbinil reduced glucose-stimulated iNOS expression from 181 ± 12% to 130 ± 10%, a reduction of 22 ± 10% ($p<0.05$). As shown in figure 5-6B, sorbinil increased nNOS expression by 45 ± 10% at 5 mM glucose ($p<0.05$). In 10 mM glucose sorbinil had no effect on nNOS expression. In 30 mM glucose sorbinil, in parallel with taurine, prevented the glucose-mediated increase of nNOS expression, with a 59 ± 7% reduction from 220 ± 24% to 91 ± 7.5% compared to untreated 30 mM glucose.

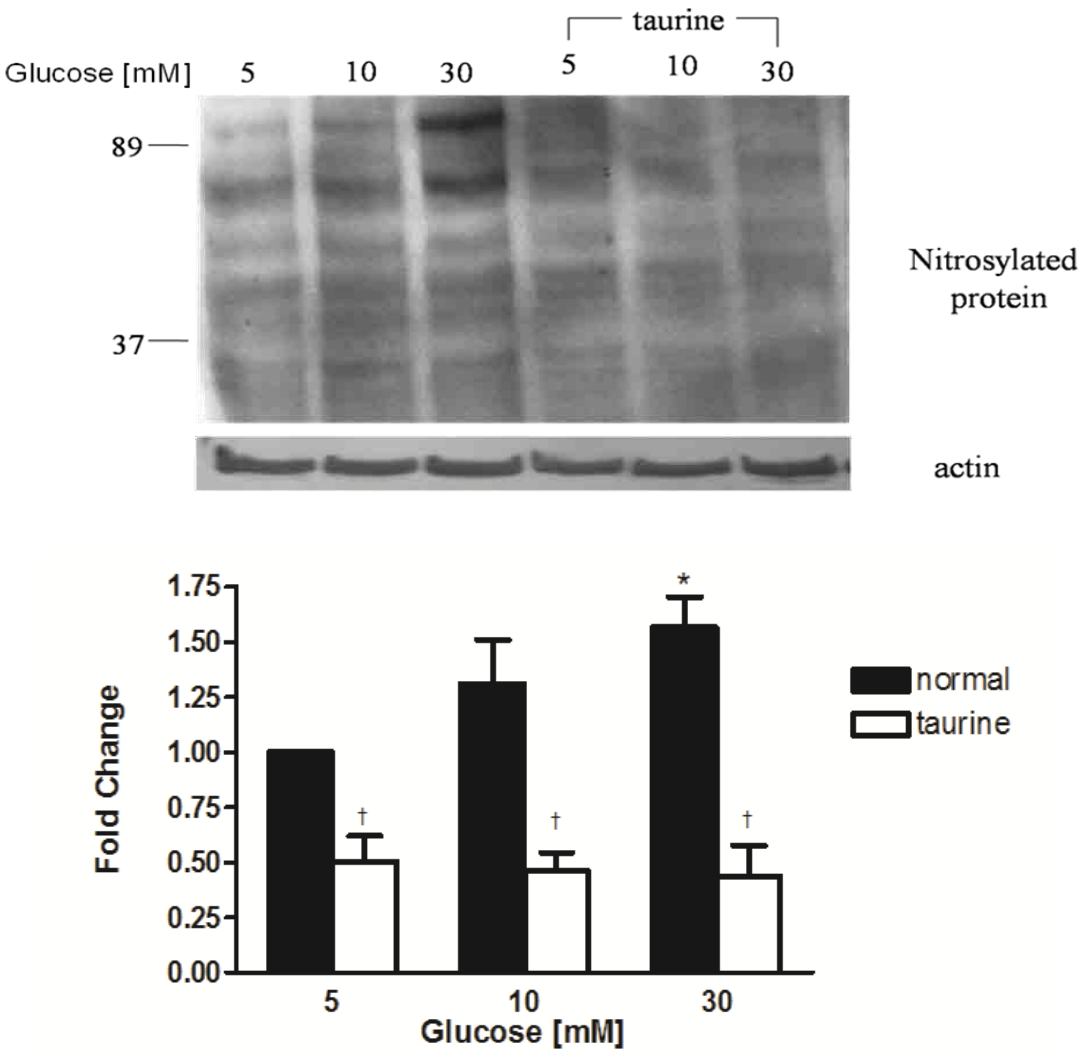

Figure 5-5 - Effect of High Glucose and Taurine Treatment on Tyrosine Nitration

Representative western blots of 3NT protein shown. Equal protein loading confirmed by β-actin. Quantitation was performed by densitometry and data expressed as mean ± SEM of 5 separate experiments. * $p<0.05$ vs. 5mM glucose (one-way ANOVA) †$p<0.05$ vs. respective glucose (two-way ANOVA)

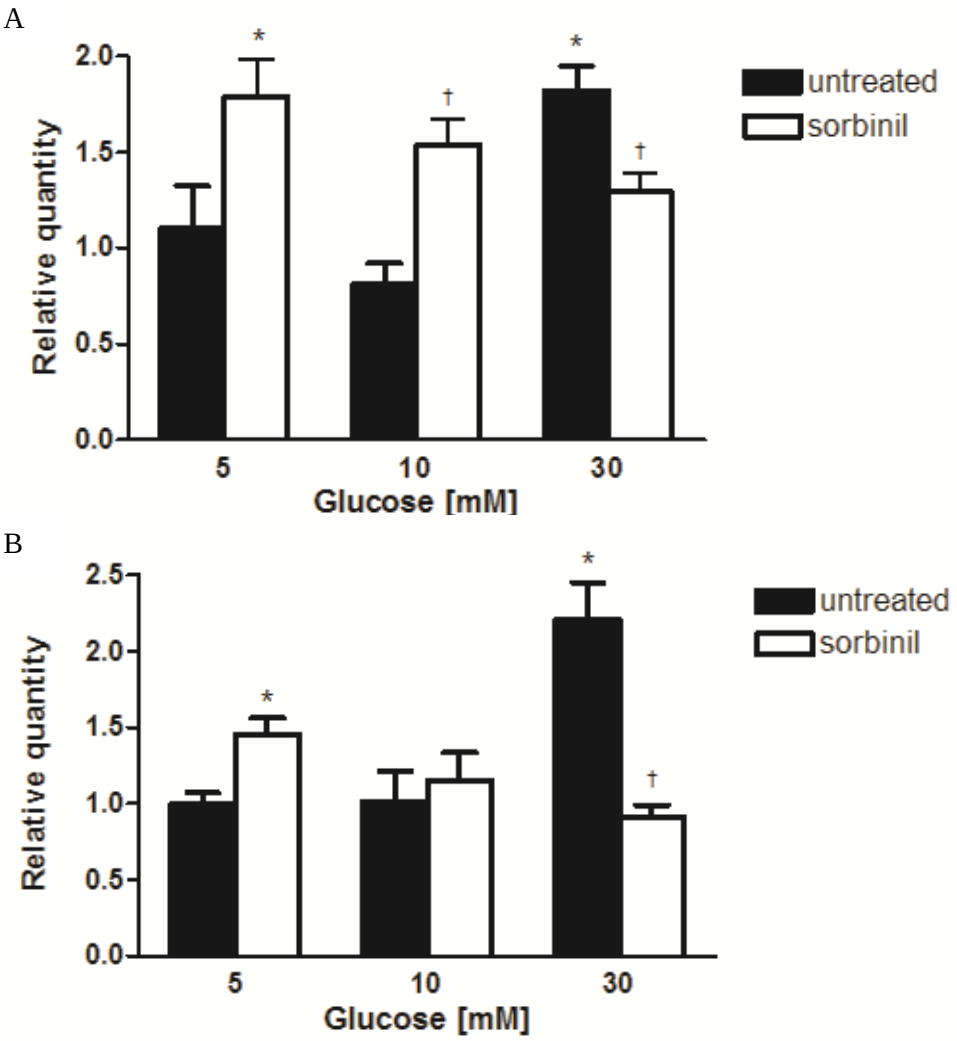

Figure 5-6 - Effect of Polyol Pathway Flux on iNOS and nNOS mRNA Expression

Effect of the aldose reductase inhibition with 10 µM Sorbinil on (A) iNOS and (B) nNOS mRNA expression. Data expressed as relative quantity of 6 separate experiments mean ± SEM * $p<0.05$ vs. 5mM glucose (one-way ANOVA) †$p<0.05$ vs. respective glucose (two-way ANOVA)

5.3.6 Effect of High Glucose on p38, p42/44, JNK/SAPK and Akt

To determine the effect of high glucose and taurine supplementation on the transduction pathways involved in diabetic complications in particular those activated by cellular stress i.e. p38 and SAPK and those mediating cell growth and survival i.e. p42/44 MAPK and Akt, levels of total and phosphorylated kinases, were examined by Western blot in response to 10 mM and 30 mM glucose and co-treatment with 250 µM taurine. In order to determine whether the taurine effects were mediated by an antioxidant mechanism, they were compared with those mediated by ALA. The responses are shown in figure 5-7.

Phospho-p38 MAPK was increased by 50 ± 16% and 32 ± 14% in 10 and 30 mM glucose respectively ($p<0.05$). Taurine reduced phospho-p38 expression by 50% in 5, 10 and 30 mM glucose, a finding similar to those of ALA. There were no detectable changes in the abundance of total JNK/SAPK or phospho-JNK/SAPK either by high glucose or co-treatment with taurine or ALA. Phospho-SAPK was not detectable in any of the treatment groups.

The abundance of phosphorylated p42/44 MAPK and Akt were reduced in 10 and 30 mM glucose to below the level of detection, with no changes in total p42/44 MAPK or Akt. Taurine co-treatment in 5 mM glucose also reduced phospho-p42/44 MAPK and phospho-Akt expression to undetectable levels and at higher glucose concentrations in the presence of taurine, expression remained undetectable. ALA in 5 mM glucose had no discernable effect on phospho-p42/44 MAPK but in higher glucose concentrations ALA restored levels of both phospho-p42/44 MAPK and Akt to levels observed in 5 mM glucose.

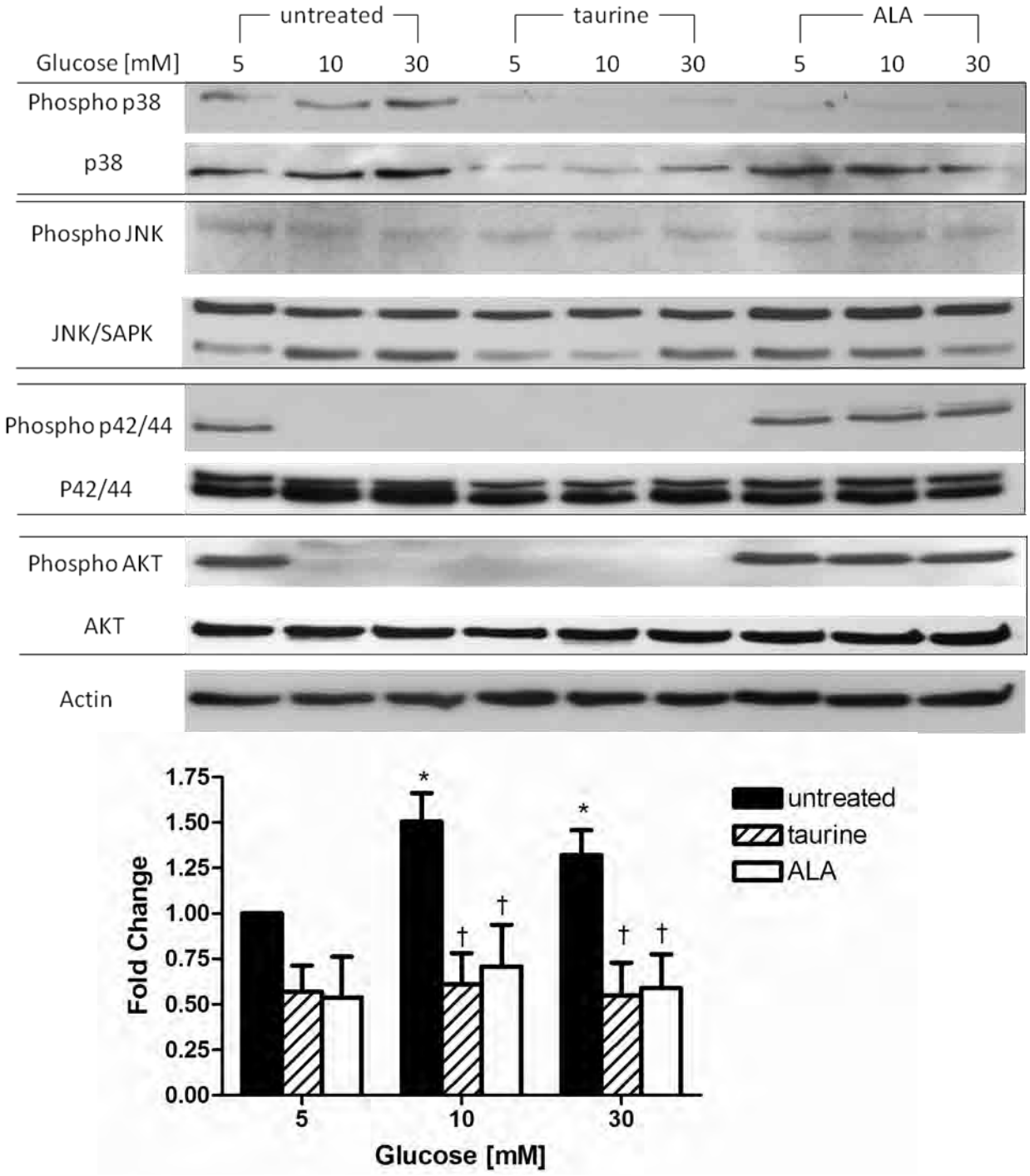

Figure 5-7 - Effect of High Glucose and Treatment with Taurine and ALA on MAPK Family Members and Akt

(A) Representative western blots shown, equal protein loading confirmed by β-actin. Quantitation of phospho-p38 (B) performed by densitometry and normalised by β-actin. Data expressed as mean ± SEM of 5 separate experiments * $p<0.05$ vs. 5 mM glucose (one-way ANOVA) † $p<0.05$ vs. respective glucose (two-way ANOVA).

5.3.7 Effect of High Glucose on Schwann Cell Growth and Death

Hyperglycaemia reduces growth and induces apoptosis in neuropathic models (342). To determine the effect of hyperglycaemia on Schwann cell growth and apoptosis, Schwann cell growth was measured using propidium iodide in 5, 10 and 30 mM glucose and the effects are shown in Table 5-1. Elevation of glucose to 10 mM and 30 mM glucose did not increase the proportion of dead cells in the culture. Assessment of DNA content in the cell layer however, showed that glucose reduced Schwann cell growth dose-dependently by 6 ± 2% ($p=0.132$) and 11 ± 2% ($p<0.05$) at 10 and 30 mM glucose respectively.

To determine whether effects of taurine on Schwann cell growth and apoptosis could be antioxidant-mediated, they were compared to the antioxidant ALA. These measurements demonstrated that neither treatment affected the proportion of dead cells in the culture. Measurements of DNA content however, showed that both taurine and ALA restored the glucose-induced reduction in Schwann cell growth with a 0 ± 1% and 4 ± 2% increase respectively compared to untreated 5 mM glucose.

A

Glucose [mM]		% dead cells relative to control
5	untreated	100.0 ± 3.2
	taurine	100.0 ± 2.0
	ALA	100.0 ± 3.7
10	untreated	98.2 ± 2.3
	taurine	102.7 ± 2.0
	ALA	104.0 ± 1.6
30	untreated	101.8 ± 1.1
	taurine	101.5 ± 1.2
	ALA	102.9 ± 2.0

B

Glucose [mM]		Schwann cell growth % control
5	untreated	100.0 ± 3.5
	taurine	100.0 ± 1.5
	ALA	100.0 ± 3.6
10	untreated	94.4 ± 1.8
	taurine	101.1 ± 1.8
	ALA	102.4 ± 1.6
30	untreated	89.0 ± 1.8 *
	taurine	100.4 ± 1.3 †
	ALA	103.7 ± 2.1 †

Table 5-1 - Effects of High Glucose, Taurine and ALA on Cell Death and DNA Content

Total levels of DNA were measured using the PI method. A) the relative proportion of dead cells within the culture compared to 5 mM control which is fixed at 100%. B) total number of cells within the cultures. Data expressed as relative quantity of sextuplicate experiments mean ± SEM $p<0.05$. * $p<0.05$ vs. untreated 5 mM glucose (one-way ANOVA) †$p<0.05$ vs. respective glucose (two-way ANOVA)

5.4 Discussion

Accumulation of nitrotyrosine along with increased iNOS expression have been seen as key pathogenic markers in diabetes complications and are increased in the sciatic nerve of STZ-D rats (82). In this study in isolated human Schwann cells I have shown that high glucose increased nitrotyrosine and iNOS mRNA expression, in agreement with data from Obrosova *et al.*, 2005. I further demonstrated that high glucose increases nNOS mRNA expression. Due to the role of NO in vasodilation, RNS injury is thought of in conjunction with vascular deficits; however, this study in isolated cells demonstrates RNS injury in Schwann cells independent of the vasculature. Considering the cell permeability of RNS this suggests that glucose-induced RNS produced within Schwann cells, could directly damage the vasculature and nerve. The linked role of iNOS, RNS and inflammation also show that glucose can induce production of inflammatory stimulators within isolated Schwann cells. NO production is spatially regulated and NO production from nNOS is thought to affect neuronal signalling. The glucose-induced increase in nNOS mRNA suggests this may impact upon neuronal signalling, possibly affecting pain response.

Taurine reduced nitrotyrosine abundance by 50% in Schwann cells at all glucose concentrations. A similar effect of taurine has been observed in endotoxin-exposed hepatocytes (343). RNS is generated from NO and O_2^-, therefore a reduction in either NO, or O_2^- will decrease RNS. In 5 and 10 mM glucose, the taurine-mediated nitrotyrosine reduction was accompanied by an increase in nNOS. At these levels of glucose, the reduction in nitrotyrosine by taurine therefore probably reflects an antioxidant action, reducing O_2^- production rather than by decreasing NO production. Further to the effect of taurine against oxidative stress shown in Chapter 4, the reduction of nitrotyrosine by taurine demonstrates a

protective affect against nitrosative stress. RNS causes DNA damage, resulting in PARP activation so the effect of taurine on nitrotyrosine demonstrates a potential mechanism by which taurine reduces glucose-mediated PAR accumulation which was shown in Chapter 4. This effect also suggests taurine could prevent dysregulation of tyrosine phosphorylation which occurs due to RNS.

In very high glucose (30 mM), taurine restored iNOS mRNA expression to levels observed in 5 mM glucose. The response of iNOS to taurine was similar to that of ALA, consistent with an antioxidant effect. Taurine reduces inflammation by scavenging hypochlorite (HOCl) (74; 270). The combined effects of taurine on nitrotyrosine and iNOS suggest another mechanisms by which taurine can reduce inflammatory mediators or signalling in diabetes.

Interestingly the response of nNOS to taurine differed from ALA, because although taurine prevented high-glucose mediated nNOS upregulation, ALA treatment was without effect. This suggests that the effect of taurine on nNOS is unlikely to be mediated by an antioxidant action, but could be mediated by carbonyl scavenging or by restoring Ca^{2+} signalling. Ca^{2+} influx mediated by glutamate binding to NMDA receptors activates nNOS (165; 166) and since taurine has been shown to attenuate excessive Ca^{2+} flux in diabetes (225; 344), normalization of Ca^{2+} signalling by taurine in human Schwann cells may underpin its effect on nNOS expression.

As shown in Chapter 3, aldose reductase inhibition prevents deficits of taurine transport in human Schwann cells and is also able to restore intracellular taurine in complications-prone diabetic tissues such as the nerve and retina (261; 345). I found that the aldose reductase inhibitor sorbinil ablated the high (30 mM) glucose-induced increase in both iNOS and nNOS expression, suggesting the increase in NOS expression is at least in part, mediated by aldose

reductase. In lower glucose concentrations however, only iNOS expression was significantly increased by aldose reductase inhibition. Although the mechanisms of the effect of aldose reductase inhibition on nNOS are unclear, the close parallelism of these effects and taurine suggest that restoration of intracellular taurine could be an important component of this response.

The effects of taurine and ALA were compared on glucose-induced changes in MAPK family members and Akt. MAPKs have been identified as transducers linking high glucose to biochemical deficits in diabetes. P38 mediates responses to osmotic stress including the regulation of genes such as aldose reductase and taurine. Together with SAPK/JNK these are activated by oxidative stress, RNS and increased polyol pathway flux in the peripheral nerves of diabetic rodents and patients (208). Aldose reductase-sensitive phosphorylation and nuclear migration of p38 MAPK has been demonstrated in DRG sensory neurons of diabetic rodents and specific inhibition of p38 prevents Na^+ channel phosphorylation and NCV slowing (346). This study demonstrates a clear increase in phospho-p38 MAPK in response to increasing glucose, and a trend to an increase in total p38. Consistent with the report of Yuan et al 2009 (219) no changes were seen in SAPK/JNK and only phospho-JNK was detectable. To my knowledge, this is the first communication to demonstrate that taurine reduced phospho-p38. Activation of sensory neuron's p38 MAPK has been invoked in the development of hyperalgesia and thus the salutary effect of taurine to prevent hyperalgesia in diabetic rodents could be mediated via this mechanism (211).

Phosphorylation of both Akt and p42/44 MAPK signalling intermediates were inhibited by incubation with 10 mM and 30 mM glucose compared with 5 mM glucose. ALA prevented the glucose-mediated reduction of phospho-p42/44 MAPK and phospho-Akt suggesting that ROS are responsible for this inhibition. This is compatible with the increases in nitrotyrosine I

documented earlier, that can block tyrosine phosphorylation and thus insulin signalling. Taurine treatment however failed to restore either phospho-p42/44 MAPK or phospho-Akt and reduced levels in 5 mM glucose. These data are compatible with an effect of taurine, reported in other cell lines, to increase phosphatase activities. Taurine increased activities of p42/44 MAPK phosphatase in human retinal pigment epithelial cells and protein tyrosine phosphatase in rat vascular smooth muscle cells which are responsible for the dephosphorylation of MAPK and Akt respectively (347; 348). These results show that taurine does not restore high glucose-induced signalling deficits and the results on Akt may, in part explain the inconsistent results in relation to taurine and glucose uptake in animal models discussed in the introduction. Despite the inability of taurine to maintain Akt and MAPK phosphorylation at control levels in high glucose-treated cells, the small reductions in cell growth and survival mediated by high glucose, were reversed by treatment with taurine or ALA. Whether other means to promote cell survival have been activated, remains to be determined.

In conclusion, taurine can abrogate high glucose-mediated accumulation of nitrotyrosine, p38 activation, impaired growth and increased NOS expression in human Schwann cells. Taurine appears to play an important role in the regulation of nNOS in particular, with a mechanism of action which is at least partially independent of an antioxidant effect.

Chapter 6 - Discussion and Future Work

Increased oxidative/nitrosative stress in key sites is critical in the pathogenesis of diabetic complications, linking high glucose to cell dysfunction. Crucial to this is the role of the antioxidant defence system, the response of which is tissue specific (77). In Chapter 4, I have demonstrated that in response to pathophysiological elevations of glucose, activities of SOD and catalase are increased, demonstrating mobilization of antioxidant defence in Schwann cells however, GSH is depleted. Consistent with other reports (4; 32) GSH depletion is most likely due to NADPH depletion caused by increased flux through aldose reductase. In contrast to the increase in SOD and catalase, the mRNA and protein expression of TauT as well as the Vmax of taurine uptake were reduced in a dose-dependent manner. The response of TauT to glucose-induced oxidative stress is not found with the 'clean' pro-oxidants such as primaquine or H_2O_2. These increased the TauT protein expression and Vmax. This is consistent with the findings of Nakashima *et al*.,(73) who showed an antioxidant response element contained within the TauT promoter region. A panel of pro-oxidants, H_2O_2, primaquine, artemisinin, diethyl maleate and buthionine sulfoximine, also all increased TauT protein expression (73). Paradoxically however, as I show in Chapter 3, elevated glucose increases oxidative stress, yet decreases TauT expression and taurine uptake, and actually inhibits the response of TauT to oxidative stress.

Figure 6-1 illustrates potential mechanisms behind this downregulation. Previous studies have suggested increased polyol pathway flux as the primary driver behind glucose-induced TauT downregulation (73; 261; 349). Increased intracellular concentration of the osmolyte sorbitol results in compensatory depletion of other organic osmolytes such as myoinositol and taurine to restore osmotic balance. This has been previously demonstrated in retinal pigment epithelial cells by inhibiting aldose reductase as well as over-expression of the enzyme (73).

In Chapter 3 I further emphasised the link and showed that inhibition of aldose reductase increases TauT expression and Vmax both in normal and high glucose. Previous studies have also shown roles for reduced Na^+K^+ATPase activity and increased PKC activity in TauT downregulation (261). I also demonstrated increased NO and nitrosative stress in diabetes plays a role in TauT downregulation. To establish the potential role played by nitrosylative stress, cells can be treated with a nitrosylating agent such as S-nitrocysteine and TauT expression, Km and Vmax measured. It is likely that reversal of these stresses is the explanation for the reversal of TauT downregulation by antioxidants demonstrated in Chapter 3 and by Stevens et al., (115).

Other potential mechanisms of TauT dysregulation in high glucose could be explored and the contribution of AGE or N-acetyl glucosamine determined. N-acetyl glucosamine is increased in diabetes and induces increases in non-enzymatic glycation and glycosylation, which can result in modification of transcription factors which affects protein expression. Indeed the activity of Sp1, which regulates TauT transcription, is increased by N-acetyl glucosamine. Assessment of TauT expression and activity after incubation of Schwann cells with precursors of these pathways, such as 3-methoxyglucose and glucosamine, as well as inhibitors of these pathways, such as aminoguanidine and Benfotiamine, may resolve their roles.

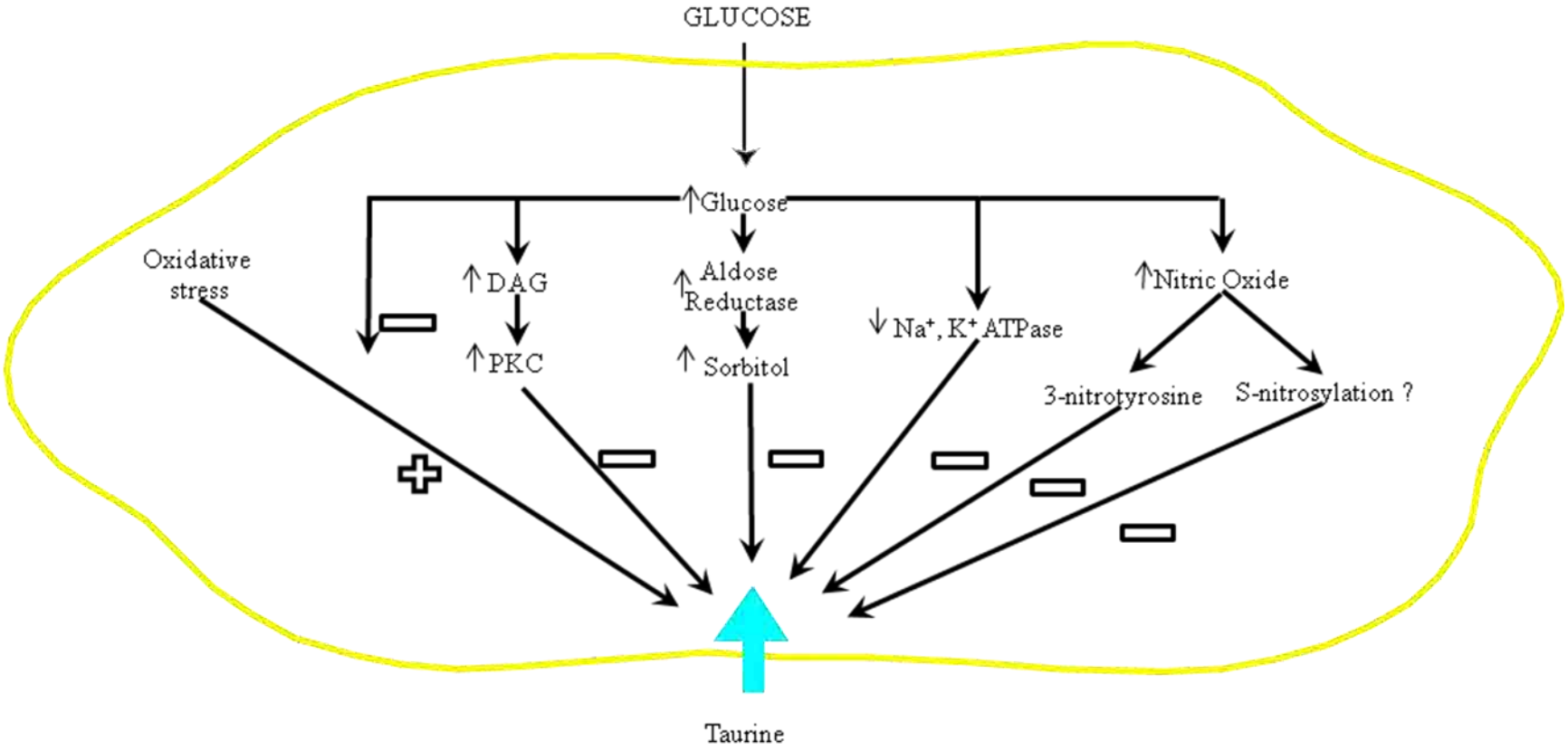

Figure 6-1- Potential Mechanisms of Taurine Depletion

Glucose-induced dysregulation of taurine uptake. Oxidative stress increases taurine uptake, an effect inhibited by glucose. Reduced taurine uptake is influenced by glucose-induced increases in PKC activity, increased aldose reductase flux, reduced Na^+K^+ATPase activity and increased NO, possibly due to increased nitrotyrosine or nitrosylation.

In diabetes taurine is depleted intracellularly and in plasma and hence beneficial effects of taurine supplementation have been explored in my in vitro studies as well as in *in vivo* models. Plasma and cellular taurine content inversely regulated TauT. Despite this and glucose-induced TauT downregulation, in human and animal models, dietary taurine supplementation restores plasma and intracellular taurine content. Similarly in cell culture models exogenous taurine supplementation restores intracellular taurine content (278). Due to the low levels of taurine supplement and high intracellular content, this restoration cannot be explained by Na^+ independent uptake, which is passive. In these studies I demonstrated that antioxidants including taurine restore TauT mRNA expression, however, taurine supplementation also restores Na^+K^+ATPase activity, which maintains the Na^+ gradient down which taurine is transported (278). A combination of these factors could explain how exogenous taurine uptake restores taurine flux into the cell, therefore restoring intracellular taurine content in diabetes and also explains how relatively modest elevations in extracellular taurine can have dramatic effects on intracellular function.

In these studies I have demonstrated that in human Schwann cells, hyperglycaemia increases oxidative stress, nitrosative stress and PAR abundance. I used specific antibodies and Western blotting to detect and quantify these modifications. While this method requires multiple steps, any of which is subject to technical variation, the data I obtained were consistent with those observed in similar studies using Schwann cells (64). Immunohistochemical techniques would enable subcellular distribution to be determined, but quantification is even more difficult. Other methods exist for measuring protein nitrosylation, such as an enzyme-linked immunosorbent assay but these also require the use of antibodies and concerns of specificity exist. Nitrotyrosine is measurable by HPLC with electrochemical detection (343) following

acid hydrolysis of the protein regrettably was not available to me but additional data using this technique would substantiate my results.

In Chapters 4 and 5 I demonstrated that taurine has many of the beneficial effects typical of an antioxidant. Figure 6-2 illustrates the taurine mediated effects reducing hyperglycaemia induced cellular dysfunction. The taurine mediated reduction of oxidative stress has been observed in many models of diabetes, but in these studies I also showed that taurine also reduces nitrosative stress and PAR. In addition by comparing other effects with the antioxidant ALA, I demonstrated other antioxidant actions, restoring iNOS expression and phospho-p38 abundance. The data suggest that taurine down regulates p38 expression, resulting in decreased phospho-p38. This effect could be further explored by examining the effect of taurine on p38 mRNA expression in comparison to treatment with other antioxidants such as ALA, N-acetyl cysteine or vitamin C.

In diabetic models, PAR has been observed as a key determinant in complications and has been suggested as a unifying mechanism of diabetic complications (2). Treatment with PARP inhibitors reduces nitrotyrosine, iNOS expression and oxidative stress in human Schwann cells (64) and reversed nerve blood flow and conduction deficits in STZ-D rats (203). Since there are similarities between the response of direct PARP inhibition and taurine treatment it is possible that taurine could act directly inhibiting PARP, subsequently resulting in the beneficial effects seen. To establish whether this is occurring direct measurements of PARP expression, which is increased in diabetes as well as activity can be measured.

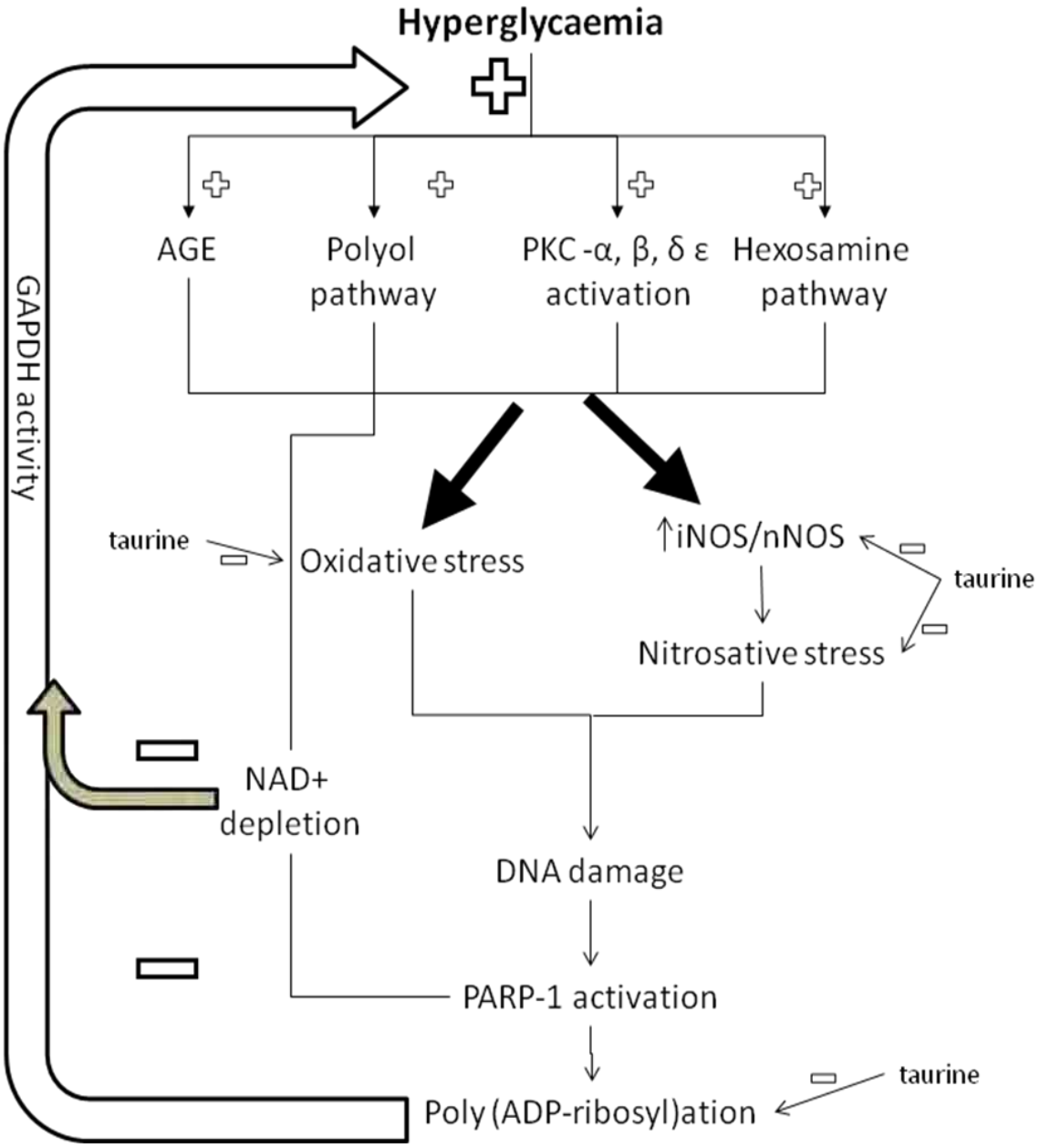

Figure 6-2 - The Effects on the Pathway of Glucose-Mediated Cellular Dysfunction by Taurine

Taurine reduces oxidative stress, iNOS and nNOS expression, nitrosative stress and poly(ADP-ribosyl)ation.

The increases in nitrotyrosine were correlated with increases in iNOS and nNOS expression. Increases in iNOS and nNOS protein and mRNA expression have been previously seen in models of diabetes and both iNOS and nNOS knockout STZ-D mice demonstrate improved nerve conduction velocity compared to wild-type STZ-D mice. However, the relative impact of increased iNOS and nNOS expression on either nitrosative stress, or other aspects of neuropathy have not been determined either in animal models or in my *in vitro* work. This could be elucidated by using selective inhibitors of iNOS and nNOS, (BYK402750 and 1-(2-trifluoromethylphenyl)-imidazole (TRIM) respectively) on glucose-induced Schwann cell dysfunction. Interestingly, in STZ-D rats, NOS inhibition with L-NAME (which inhibits all NOS enzymes) failed to improve nerve conduction velocity (52). Conceivably L-NAME exacerbates the vascular deficits by inhibition of eNOS rather than the potential positive effects gained by iNOS of nNOS inhibition. Therefore examination of the effect of non-selective NOS inhibition, i.e. with L-NAME on oxidative/nitrosative stress and poly(ADP-ribosyl)ation , in isolated Schwann cell cultures would identify potential beneficial effects independent of the vascular component. These data could also be compared with selective iNOS or nNOS inhibition enabling the relative components of each to be measured.

In these studies I examined the effects of high glucose and taurine on 3-nitrotyrosine. However, S-nitrosylation also results from NO production and is increased in diabetes (192; 350). Aberrant 3-nitrotyrosine and S-nitrosylation both occur due to reactions between NO and superoxide resulting in RNS generation (350). The relative change in 3-nitrotyrosine and S-nitrosylation due to high glucose would therefore be predicted to be similar. However, it is possible that different mechanisms of RNS scavenging exist, or turn-over of nitrated or nitrosylated proteins occur at different rates, which would result in relatively different abundance. Measurement of S-nitrosylation in high glucose would confirm this. In a similar

way that 3-nitrotyrosine affects tyrosine signalling, S-nitrosylation affects protein signalling dependent upon cysteine. Both impair insulin signalling, 3-nitrotyrosine directly affecting the insulin receptor which is a receptor tyrosine kinase, S-nitrosylation affecting downstream pathways of IRS and Akt signalling (192). Since, 100 proteins are currently known to be S-nitrosylated (351; 352) and it is likely more will be identified, aberrant S-nitrosylation could have many downstream consequences.

Taurine reduces iNOS and nNOS mRNA expression as well as oxidative stress. Taurine should reduce S-nitrosylation in the same way as 3-nitrotyrosine. However the failure of taurine to reverse high-glucose induced Akt downregulation could be due to a failure of taurine to affect S-nitrosylation. Measuring the effect of taurine treatment on S-nitrosylation would further explore this. Technically, measurement of S-nitrosylation is more difficult than that of 3-nitrotyrosine. The most common method used is the biotin switch method. The biotin switch method is a three stage technique. Firstly free cysteine thiol residues are blocked with methyl methane thiosulfonate (MMTS), the remaining cysteine thiol residues are converted to thiols by transnitrosation by ascorbic acid before being labelled by S-biotinylation and detected by immunoblotting. By immunoprecipitating with the target protein prior to the biotin switch, it is also possible to detect S-nitrosylation on specific target proteins (351-354).

The mechanism behind the taurine-mediated down-regulation in iNOS expression is unclear. Considering the response of iNOS to taurine mirrored that of ALA, it is likely to be antioxidant-mediated although further confirmation of these using different antioxidants such as ascorbic acid and N-acetyl cysteine should be sought. Increases in iNOS expression in diabetes have been linked to mobilisation of the immune response, due to oxidative stress and AGE binding to RAGE. These increase NFκB and TNF-α, both of which regulate iNOS

expression. To further explore whether taurine is affecting this mechanism the response of AGE, RAGE and NFκB to taurine supplementation could be measured. Taurine is known to react with hypochlorite HOCl forming taurine chloramines, which reduces expression of TNF-α and NFκB. Measuring the response of these factors to taurine treatment in high glucose would determine whether this occurs in high glucose in a manner similar to that observed with aldose reductase inhibition (160), which also increases TauT expression and taurine transport.

Taurine's antioxidant activity is well established, but since taurine itself is unable to directly scavenge the major pro-oxidants (266) the mechanism of this action is unclear. Some authors cite indirect actions, by increasing the activity of the antioxidant defence system. In chapter 4 taurine, like ALA increased SOD and catalase activities in 5 mM glucose, however, like ALA there were no measurable effects in 10 mM or 30 mM glucose. These observations have been repeated by Dr Zeng in our laboratory studying SOD and catalse mRNA expression in human fibroblast cells in response to both taurine and 30 mM glucose (unpublished observations). Both taurine and high glucose independently increased SOD and catalase mRNA expression, but there was no additive effect when combined. These data demonstrate that the antioxidant effects of taurine in hyperglycaemic conditions are not achieved by mediating actions on the antioxidant defence system.

Some authors have cited direct actions of taurine that could induce an antioxidant effect e.g. effects on mitochondrial superoxide production, AGE, Ca^{2+} signalling or restoration of mitochondrial protein synthesis. To explore whether these mechanisms could be responsible, studies examining the impact of high glucose with and without taurine supplementation on AGE formation, Ca^{2+} signalling and on mitochondrial superoxide generation would be revealing

Taurine derivatives are found in uridine in mitochondrial tRNAs (335; 336) and Schaeffer et al., 2009 suggested that due to this role taurine depletion in diabetes could reduce mitochondrial protein synthesis. Reduced synthesis of proteins involved the ETC would result in back-up metabolites, resulting in production of superoxide, rather than ATP formation, thereby increasing mitochondrial superoxide generation. These authors suggest restoration of intracellular taurine concentration would restore mitochondrial protein synthesis and therefore reduce oxidative stress. This hypothesis could be tested by measuring the impact of hyperglycaemia on mitochondrial protein synthesis and RNA abundance. It could be further explored whether taurine supplementation restored mitochondrial protein synthesis or RNA abundance.

Not all the actions of taurine appear to be antioxidant-mediated. In Chapter 5, I demonstrated that taurine increased nNOS expression in 5 mM glucose. NO production from nNOS is regulated by Ca^{2+} influx, resulting in calmodulin binding and it is also regulated by Akt phosphorylation at Ser 1412 (148), phosphorylated Akt was reduced by taurine. Therefore, increased nNOS expression will not necessarily result in increased NO production. Measuring NO production from nNOS is technically difficult. The half-life of NO is very short, 1-40 seconds, so indirect methods are often employed measuring levels of NO_2^- and NO_3^- ions using the Greiss reaction. However, NO production in Schwann cells is also very low, making this difficult. Measuring nNOS phosphorylation and Ca^{2+} signalling, using Fura 2 in response to high glucose and taurine supplementation would help to further establish whether these treatments affect NO production from nNOS. In these studies taurine increased nNOS expression in normal glucose. NO production from nNOS is thought to regulate nerve conduction and in diabetic animals taurine increased nerve conduction velocity. Therefore measuring nerve conductivity in non-diabetic animal models would ascertain whether taurine

can increase nerve conductivity in normal animals. However, in non-diabetic rats, no change was observed in sensory or motor nerve conduction velocity following taurine supplementation (262).

One of the major factors associated with the pathogenesis of diabetic neuropathy is vascular deficits. Reduction in nerve blood flow exacerbates neuropathy creating periods of ischaemia and reducing the purging of pro-oxidants from the nerve, both of which increase oxidative stress. Reduced NO production from eNOS partly reflects increased NADPH utilisation following increased polyol pathway flux (see section 1.4.1.5) which is required as a cofactor for NO generation by eNOS (52; 53). In a similar manner to nNOS, NO production from eNOS is dependent upon its phosphorylation by Akt as well as Ca^{2+} influx. In STZ-D treated rats, taurine restores nerve blood flow deficits but discrimination of whether this is a neural or an endothelial effect has not been determined. Whether taurine regulates eNOS expression and NO production from endothelial cells is unknown. To elucidate this, I would perform a similar set of experiments as in Chapter 3, but in endothelial cells such as human vascular endothelial cells (HUVECs). I would measure eNOS expression and phospho-eNOS. In addition I would also measure Akt and phospho-Akt as well as Ca^{2+} signalling in response to both high glucose and taurine supplementation. Were taurine to increase NO production from eNOS, this could be a mechanism by which taurine improves blood flow deficits, which would not only be important in neuropathy, but also in diabetic ulceration and potentially diabetic autonomic neuropathy as well.

In Chapter 5, I examined the response of MAPK and Akt to hyperglycaemia and taurine supplementation. Signalling via MAPK phosphorylation is transient, with phosphorylation/dephosphorylation occurring rapidly within minutes. The studies contained herein were all designed to represent chronic hyperglycaemia and were undertaken following

7 days incubation in high glucose. In animal models of diabetic neuropathy p38 MAPK inhibitors (FR167653 or CNI-1493) were found to improve neuropathic pain (355) and SB239063 was found to improve nerve conduction velocity (356) and aldose reductase inhibition reduced expression of phospho-p38 MAPK (209). Although the impact of hyperglycaemia on p42/44 MAPK are more varied, use of p38 and p42/44 inhibitors and activators (such as 4-(2-Aminoethyl)benzenesulfonylfluoride hydrochloride or N-Arachidonoylethanolamine(all-Z)-N-(2-Hydroxyethyl)-5,8,11,14-eicosatetraenamide) would demonstrate the impact of these signalling pathways on high-glucose induced Schwann cell dysfunction and further explore the effects found within these studies.

Inhibition of p38 MAPK with SB203580 reduces taurine uptake in a murine macrophage cell line (357), however, the effect of p38 or p42/44 MAPK inhibition on taurine transport in diabetes has not been explored. The use of p38 MAPK and p42/44 MAPK inhibitors and activators in Schwann cells in normal and high glucose would also enable the impact of these cell-signalling systems on TauT regulation in normal and high glucose to be measured.

Taurine supplementation reduced the stress kinase phospho-p38 MAPK in high glucose, a response similar to that evoked by ALA, indicating an antioxidant effect. However, both taurine and glucose reduced phospho-p42/44 MAPK and phospho-Akt a response which differed from ALA, hence this change was not antioxidant-mediated. Studies in other cell culture systems have shown that taurine increases the activity of p42/44 MAPK phosphatase in human retinal pigment epithelial cells and protein tyrosine phosphatase in vascular smooth muscle cells which are responsible for the dephosphorylation of MAPK and Akt respectively [18, 48]. Studies on the activity of MAPK phosphatase and tyrosine phosphatase in response to both concentrations of high glucose as well as taurine treatment would resolve whether this also occurred in Schwann cells.

Most of the effects of taurine appear to be antioxidant effects, but other such as restoration of nNOS expression, phospho- p42/44 MAPK and phospho-Akt seem independent of antioxidant mechanisms. The mechanisms of action of taurine supplementation are still unclear with three major actions regularly cited, being that of i) an antioxidant, ii) scavenger of carbonyl compounds and iii) restoration of Ca^{2+} signalling.

The studies herein have demonstrated many beneficial effects of taurine supplementation; however, the effects of taurine are not entirely beneficial. In STZ-D rats, taurine supplementation further depletes myoinositol (75) and high taurine doses can slow nerve conduction velocity and result in hyperexcitability (145). Potential side-effects of taurine administration are also suggested by the data on p42 MAPK and Akt where taurine failed to restore phosphorylation in high glucose and reduced phosphorylation in 5 mM glucose.

In patients with diabetes there is a reduction in circulating taurine as well as a deficiency in intracellular taurine (257). It is possible the effects of taurine in diabetic neuropathy are due to correcting taurine deficiency. To determine this, models of taurine deficiency can be used. Taurine deficiency can be induced by either incubating Schwann cells in serum free media, deficient of taurine or using siRNA to partially or totally knock out TauT expression. By repeating the experiments set out in Chapters 4 and 5 using taurine deficient cell-culture systems, these models would enable comparison between the impact of taurine deficiency and hyperglycaemic insult on Schwann cells.

TauT knockout mice suffer from renal, retinal and olfactory dysfunction along with reduced exercise capacity, a reduction in taurine-evoked synaptic enhancement and neuroceptor expression. Additionally increased $GABA_A$, AMPA and kainite receptor densities were observed in the brain (239; 358). There are, however, no published studies on the effects on

peripheral nerves in the TauT knockout mouse. The effects of taurine depletion on cats have focused on the retinal degradation (238) and in a similar manner to the TauT knockout mouse there are no studies examining the effect of taurine deficiency on peripheral nerve function in cats. Examining nerve conduction velocity, nerve blood flow and oxidative stress within the peripheral nerve in either taurine deficient model and comparing these data with the equivalent diabetic animal models, may delineate the extent to which taurine depletion is responsible for the nerve conduction deficits observed in diabetic neuropathy.

From these studies it is clear taurine supplementation has many benefits in isolated cell models. These findings add to those already performed in diabetic animal models, demonstrating significant benefits of taurine supplementation (75; 145; 225; 262) . In all these studies taurine content was increased by oral taurine supplementation, something that has also been effective in human patients (257). However, demonstrated in these studies and in others involving STZ-D rats, taurine content can be restored by aldose reductase inhibition (261), ALA treatment (115) and potentially by prevention of 3-NT accumulation or a direct TauT agonist. This illustrates that rather than restoration of taurine content per se being the end goal, it can be observed as part of a global therapeutic strategy encompassing many factors of the condition. For example taurine restoration could be achieved by inhibition of iNOS. Applying this strategy would encompass the benefits from two targets into one therapy and may also remove potential side-effects of taurine supplementation, such as myoinositol depletion.

Chapter 7 - Appendix

7.1 Principles of PCR

Traditional PCR consists of 3 distinct phases, denaturation, annealing and elongation (figure 6).

Denaturation

Heating the mixture to 94-96^{o}C for 20-30 seconds causes the DNA template and primers to melt by disrupting the hydrogen bonds between the complementary strands, yielding single DNA strands and enabling primer binding.

Annealing

Lowering the temperature to 45-65^{o}C allows primer binding to the complementary sequence of the DNA template. The specificity of primer binding will depend upon the annealing temperature (the higher the annealing temperature the more specific the primer binding), salt content and magnesium concentration.

Extension/elongation

The temperature is then increased to that optimum for the DNA polymerase used, normally taq polymerase, generally at 72^{o}C. Taq polymerase synthesises a new complementary strand from the template in a 5` to 3` direction.

These steps are then repeated. Denaturing the newly formed dsDNA enables formation of new templates for the second-round of annealing and extension steps. These cycles are repeated between 20 and 40 times depending upon what is required.

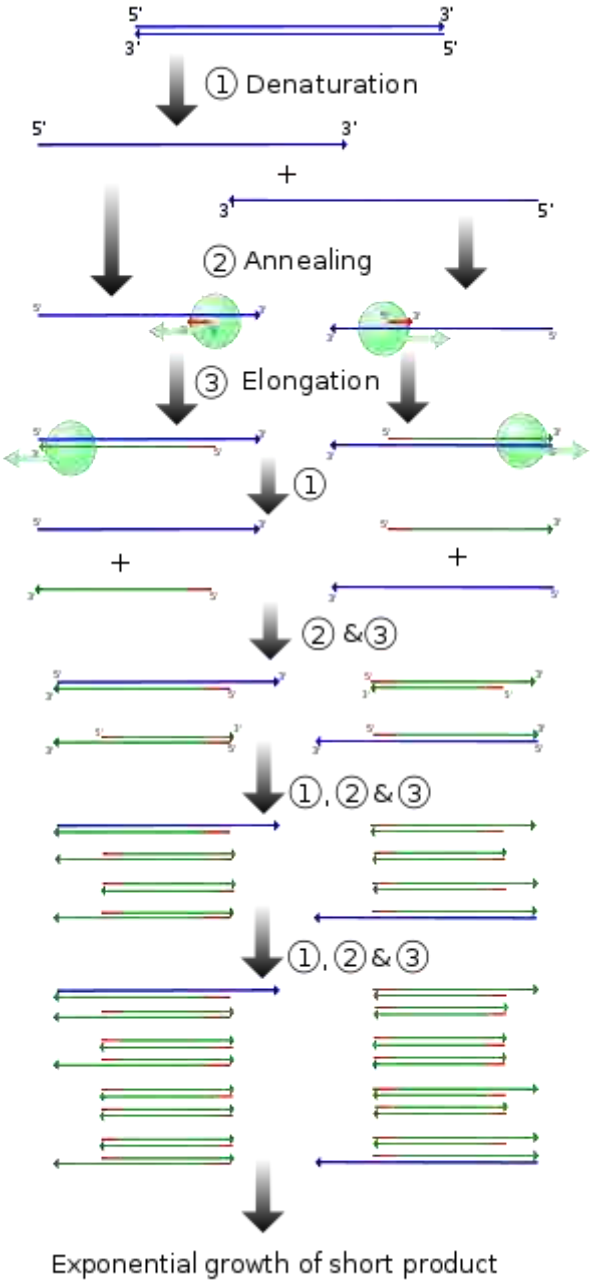

7-1 - Schematic of polymerase chain reaction

http://en.wikipedia.org/wiki/Polymerase_chain_reaction

7.2 Alternative q-PCR dyes

7.2.1 Intercalating dyes (e.g. SYBR-Green)

Intercalating dyes bind to double stranded DNA, upon which the dye fluorescence increases over a hundred fold. Hence, as the DNA is amplified the emitted fluorescence increases. These dyes are cheap, sensitive and since the dye binds to any dsDNA, no further optimisation is required over standard PCR. The only disadvantage they have over other systems is that the dye will bind any dsDNA, making it less selective than other systems and with potential problems of primer:dimers resulting in fluorescence.

7.2.2 Hybridisation-Probes e.g. taq-man

Hybridisation probes work using the forster energy resonance transfer system (FRET). As well as two primers, a separate probe that binds to the target sequence with a fluorescent reporter dye and quencher attached is used. Whilst the probe is still intact the quencher greatly reduces the fluorescence emitted by the reporter dye. During PCR the probe anneals downstream of one of the primers and is cleaved during extension by the 5` to 3` exonuclease activity of taq polymerase. This cleavage separates reporter and quencher increasing the fluorescence signal from the reporter dye.

This system has an advantage in that in addition to the specific primer binding, binding of the probe to the target sequence is also required. This means that unlike intercalating dyes, the fluorescence emitted is specific for the target, ensuring the result is more specific for the target sequence.

7.3 Publication reference

Askwith T, Zeng W, Eggo MC and Stevens MJ. Oxidative Stress and Dysregulation of the Taurine Transporter in High Glucose-Exposed human Schwann Cells: Implications for Pathogenesis of Diabetic Neuropathy. Am J Physiol Endocrinol Metab 2009.

Chapter 8 - References

1. **Vinik AI, Holland MT, Le Beau JM, Liuzzi FJ, Stansberry KB and Colen LB**. Diabetic neuropathies. *Diabetes Care* 15: 1926-1975, 1992.

2. **Brownlee M**. The pathobiology of diabetic complications: a unifying mechanism. *Diabetes* 54: 1615-1625, 2005.

3. **Edwards JL, Vincent AM, Cheng HL and Feldman EL**. Diabetic neuropathy: Mechanisms to management. *Pharmacol Ther* 120: 1-34, 2008.

4. **Brownlee M**. Biochemistry and molecular cell biology of diabetic complications. *Nature* 414: 813-820, 2001.

5. **Hansen SH**. The role of taurine in diabetes and the development of diabetic complications. *Diabetes Metab Res Rev* 17: 330-346, 2001.

6. **Cavaletti G, Miloso M, Nicolini G, Scuteri A and Tredici G**. Emerging role of mitogen-activated protein kinases in peripheral neuropathies. *J Peripher Nerv Syst* 12: 175-194, 2007.

7. **Vincent AM, Russell JW, Low P and Feldman EL**. Oxidative stress in the pathogenesis of diabetic neuropathy. *Endocr Rev* 25: 612-628, 2004.

8. **Zdychova J and Komers R**. Emerging role of Akt kinase/protein kinase B signaling in pathophysiology of diabetes and its complications. *Physiol Res* 54: 1-16, 2005.

9. **Turner H and Wass J**. Diabetes: classification and diagnosis. In: Oxford Handbook of Diabetes, edited by Turner H and Wass J. Oxford: Oxford University Press, 2007, p. 1-10.

10. **Harris RA and Crabb DW**. Metabolic Interrelationships. In: Textbook of Biochemistry with Clinical Correlations, edited by Devlin TM. New York: Wiley-Liss, 2001, p. 861-902.

11. **J.Denis McGarry**. Lipid Metabolism 1: Ultilization and Storage of Energy in Lipid Form. In: Textbook of Biochemistre with Clinical Correlations, edited by Thomas M Devlin. New York: Wiley-Liss, 2002, p. 693-725.

12. **Riste L, Khan F and Cruickshank K**. High prevalence of type 2 diabetes in all ethnic groups, including Europeans, in a British inner city: relative poverty, history, inactivity, or 21st century Europe? *Diabetes Care* 24: 1377-1383, 2001.

13. **Robbins JM, Vaccarino V, Zhang H and Kasl SV**. Socioeconomic status and type 2 diabetes in African American and non-Hispanic white women and men: evidence from

the Third National Health and Nutrition Examination Survey. *Am J Public Health* 91: 76-83, 2001.

14. The effect of intensive treatment of diabetes on the development and progression of long-term complications in insulin-dependent diabetes mellitus. The Diabetes Control and Complications Trial Research Group. *N Engl J Med* 329: 977-986, 1993.

15. Intensive blood-glucose control with sulphonylureas or insulin compared with conventional treatment and risk of complications in patients with type 2 diabetes (UKPDS 33). UK Prospective Diabetes Study (UKPDS) Group. *Lancet* 352: 837-853, 1998.

16. **Turner HE and Wass JAH**. Diabetic Eye Disease. In: Oxford Handbook of Diabetes, edited by Turner HE and Wass JAH. New York: Oxford University Press, 2007, p. 30-40.

17. **Madsen-Bouterse SA and Kowluru RA**. Oxidative stress and diabetic retinopathy: pathophysiological mechanisms and treatment perspectives. *Rev Endocr Metab Disord* 9: 315-327, 2008.

18. **Caldwell RB, Bartoli M, Behzadian MA, El-Remessy AE, Al-Shabrawey M, Platt DH and Caldwell RW**. Vascular endothelial growth factor and diabetic retinopathy: pathophysiological mechanisms and treatment perspectives. *Diabetes Metab Res Rev* 19: 442-455, 2003.

19. **Turner HE and Wass JAH**. Diabetic Renal Disease. In: Oxford Handbook of Diabetes, edited by Turner HE and Wass JAH. New York: Oxford University Press, 2007, p. 41-50.

20. **Jerums G, Premaratne E, Panagiotopoulos S, Clarke S, Power DA and MacIsaac RJ**. New and old markers of progression of diabetic nephropathy. *Diabetes Res Clin Pract* 82 Suppl 1: S30-S37, 2008.

21. **Vinik AI, Maser RE, Mitchell BD and Freeman R**. Diabetic autonomic neuropathy. *Diabetes Care* 26: 1553-1579, 2003.

22. **Ziegler D**. Diagnosis and treatment of diabetic autonomic neuropathy. *Curr Diab Rep* 1: 216-227, 2001.

23. **Turner HE and Wass JAH**. Diabetic Neuropathy. In: Oxford Handbook of Diabetes, edited by Turner HE and Wass JAH. New York: Oxford University Press, 2007, p. 51-61.

24. **Said G**. Focal and multifocal diabetic neuropathies. *Arq Neuropsiquiatr* 65: 1272-1278, 2007.

25. **Said G**. Diabetic neuropathy--a review. *Nat Clin Pract Neurol* 3: 331-340, 2007.

26. **Boulton AJ, Vinik AI, Arezzo JC, Bril V, Feldman EL, Freeman R, Malik RA, Maser RE, Sosenko JM and Ziegler D**. Diabetic neuropathies: a statement by the American Diabetes Association. *Diabetes Care* 28: 956-962, 2005.

27. **Booya F, Bandarian F, Larijani B, Pajouhi M, Nooraei M and Lotfi J**. Potential risk factors for diabetic neuropathy: a case control study. *BMC Neurol* 5: 24, 2005.

28. **Yagihashi S, Yamagishi S and Wada R**. Pathology and pathogenetic mechanisms of diabetic neuropathy: correlation with clinical signs and symptoms. *Diabetes Res Clin Pract* 77 Suppl 1: S184-S189, 2007.

29. **Hong S, Morrow TJ, Paulson PE, Isom LL and Wiley JW**. Early painful diabetic neuropathy is associated with differential changes in tetrodotoxin-sensitive and -resistant sodium channels in dorsal root ganglion neurons in the rat. *J Biol Chem* 279: 29341-29350, 2004.

30. **Chung JM and Chung K**. Importance of hyperexcitability of DRG neurons in neuropathic pain. *Pain Pract* 2: 87-97, 2002.

31. **Kapur D**. Neuropathic pain and diabetes. *Diabetes Metab Res Rev* 19 Suppl 1: S9-15, 2003.

32. **Obrosova IG**. Diabetes and the peripheral nerve. *Biochim Biophys Acta* 1792: 931-940, 2008.

33. **Yagihashi S**. Pathology and pathogenetic mechanisms of diabetic neuropathy. *Diabetes Metab Rev* 11: 193-225, 1995.

34. **Mizisin AP, Shelton GD, Wagner S, Rusbridge C and Powell HC**. Myelin splitting, Schwann cell injury and demyelination in feline diabetic neuropathy. *Acta Neuropathol* 95: 171-174, 1998.

35. The effect of intensive treatment of diabetes on the development and progression of long-term complications in insulin-dependent diabetes mellitus. The Diabetes Control and Complications Trial Research Group. *N Engl J Med* 329: 977-986, 1993.

36. **UK Prospective Diabetes Study (UKPDS) Group**. Effect of intensive blood-glucose control with metformin on complications in overweight patients with type 2 diabetes (UKPDS 34). *Lancet* 352: 854-865, 1998.

37. Intensive blood-glucose control with sulphonylureas or insulin compared with conventional treatment and risk of complications in patients with type 2 diabetes (UKPDS 33). UK Prospective Diabetes Study (UKPDS) Group. *Lancet* 352: 837-853, 1998.

38. The effect of intensive treatment of diabetes on the development and progression of long-term complications in insulin-dependent diabetes mellitus. The Diabetes Control and Complications Trial Research Group. *N Engl J Med* 329: 977-986, 1993.

39. The effect of intensive treatment of diabetes on the development and progression of long-term complications in insulin-dependent diabetes mellitus. The Diabetes Control and Complications Trial Research Group. *N Engl J Med* 329: 977-986, 1993.

40. **Duby JJ, Campbell RK, Setter SM, White JR and Rasmussen KA**. Diabetic neuropathy: an intensive review. *Am J Health Syst Pharm* 61: 160-173, 2004.

41. **Deshpande AD, Harris-Hayes M and Schootman M**. Epidemiology of diabetes and diabetes-related complications. *Phys Ther* 88: 1254-1264, 2008.

42. **Tesfaye S, Chaturvedi N, Eaton SE, Ward JD, Manes C, Ionescu-Tirgoviste C, Witte DR and Fuller JH**. Vascular risk factors and diabetic neuropathy. *N Engl J Med* 352: 341-350, 2005.

43. **Aaberg ML, Burch DM, Hud ZR and Zacharias MP**. Gender differences in the onset of diabetic neuropathy. *J Diabetes Complications* 22: 83-87, 2008.

44. **Lanting LC, Joung IM, Mackenbach JP, Lamberts SW and Bootsma AH**. Ethnic differences in mortality, end-stage complications, and quality of care among diabetic patients: a review. *Diabetes Care* 28: 2280-2288, 2005.

45. **Vague P, Brunetti O, Valet AM, Attali I, Lassmann-Vague V and Vialettes B**. Increased prevalence of neurologic complications among insulin dependent diabetic patients of Algerian origin. *Diabete Metab* 14: 706-711, 1988.

46. **Abbott CA, Chaturvedi N, Malik RA, Salgami E, Yates AP, Pemberton PW and Boulton AJ**. Explanations for the lower rates of diabetic neuropathy in Indian Asians versus Europeans. *Diabetes Care* 33: 1325-1330, 2010.

47. **Gary SR and Woo KY**. The biology of chronic foot ulcers in persons with diabetes. *Diabetes Metab Res Rev* 24 Suppl 1: S25-S30, 2008.

48. **Turner HE and Wass JAH**. Diabetic Foot. In: Oxford Handbook of Diabetes, edited by Turner HE and Wass JAH. New York: Oxford University Press, 2007, p. 75-82.

49. **Bowering CK**. Diabetic foot ulcers. Pathophysiology, assessment, and therapy. *Can Fam Physician* 47: 1007-1016, 2001.

50. **Papanas N, Mavridis G, Karavageli E, Symeonidis G and Maltezos E**. Peripheral neuropathy is associated with increased mean platelet volume in type 2 diabetic patients. *Platelets* 16: 498-499, 2005.

51. **Stevens MJ, Feldman EL and Greene DA**. The aetiology of diabetic neuropathy: the combined roles of metabolic and vascular defects. *Diabet Med* 12: 566-579, 1995.

52. **Stevens MJ, Dananberg J, Feldman EL, Lattimer SA, Kamijo M, Thomas TP, Shindo H, Sima AA and Greene DA**. The linked roles of nitric oxide, aldose reductase and, (Na+,K+)-ATPase in the slowing of nerve conduction in the streptozotocin diabetic rat. *J Clin Invest* 94: 853-859, 1994.

53. **Stevens MJ**. Nitric oxide as a potential bridge between the metabolic and vascular hypotheses of diabetic neuropathy. *Diabet Med* 12: 292-295, 1995.

54. **Schemmel KE, Padiyara RS and D'Souza JJ**. Aldose reductase inhibitors in the treatment of diabetic peripheral neuropathy: a review. *J Diabetes Complications* 24: 354-360, 2009.

55. **Quarles RH**. Myelin sheaths: glycoproteins involved in their formation, maintenance and degeneration. *Cell Mol Life Sci* 59: 1851-1871, 2002.

56. **Roglio I, Giatti S, Pesaresi M, Bianchi R, Cavaletti G, Lauria G, Garcia-Segura LM and Melcangi RC**. Neuroactive steroids and peripheral neuropathy. *Brain Res Rev* 57: 460-469, 2008.

57. **Dowling JE**. Cells and Synapses. In: Neurons and Networks: An Introduction to Behavioural Neuroscience, edited by Dowling JE. Massachusetts: Harvard University Press, 2001, p. 32-57.

58. **Figueroa-Romero C, Sadidi M and Feldman EL**. Mechanisms of disease: The oxidative stress theory of diabetic neuropathy. *Rev Endocr Metab Disord* 9: 301-314, 2008.

59. **Tomlinson DR and Gardiner NJ**. Diabetic neuropathies: components of etiology. *J Peripher Nerv Syst* 13: 112-121, 2008.

60. **Ludvigson MA and Sorenson RL**. Immunohistochemical localization of aldose reductase. I. Enzyme purification and antibody preparation--localization in peripheral nerve, artery, and testis. *Diabetes* 29: 438-449, 1980.

61. **Maekawa K, Tanimoto T, Okada S, Suzuki T, Suzuki T and Yabe-Nishimura C**. Expression of aldose reductase and sorbitol dehydrogenase genes in Schwann cells isolated from rat: effects of high glucose and osmotic stress. *Brain Res Mol Brain Res* 87: 251-256, 2001.

62. **Suzuki T, Mizuno K, Yashima S, Watanabe K, Taniko K and Yabe-Nishimura C**. Characterization of polyol pathway in Schwann cells isolated from adult rat sciatic nerves. *J Neurosci Res* 57: 495-503, 1999.

63. **Eckersley L**. Role of the Schwann cell in diabetic neuropathy. *Int Rev Neurobiol* 50: 293-321, 2002.

64. **Obrosova IG, Drel VR, Pacher P, Ilnytska O, Wang ZQ, Stevens MJ and Yorek MA**. Oxidative-nitrosative stress and poly(ADP-ribose) polymerase (PARP) activation in experimental diabetic neuropathy: the relation is revisited. *Diabetes* 54: 3435-3441, 2005.

65. **Miinea C, Kuruvilla R, Merrikh H and Eichberg J**. Altered arachidonic acid biosynthesis and antioxidant protection mechanisms in Schwann cells grown in elevated glucose. *J Neurochem* 81: 1253-1262, 2002.

66. **Suzuki T, Sekido H, Kato N, Nakayama Y and Yabe-Nishimura C**. Neurotrophin-3-induced production of nerve growth factor is suppressed in Schwann cells exposed to high glucose: involvement of the polyol pathway. *J Neurochem* 91: 1430-1438, 2004.

67. **Ohi T, Saita K, Furukawa S, Ohta M, Hayashi K and Matsukura S**. Therapeutic effects of aldose reductase inhibitor on experimental diabetic neuropathy through synthesis/secretion of nerve growth factor. *Exp Neurol* 151: 215-220, 1998.

68. **Leinninger GM, Vincent AM and Feldman EL**. The role of growth factors in diabetic peripheral neuropathy. *J Peripher Nerv Syst* 9: 26-53, 2004.

69. **Obrosova IG and Stevens MJ**. Effect of dietary taurine supplementation on GSH and NAD(P)-redox status, lipid peroxidation, and energy metabolism in diabetic precataractous lens. *Invest Ophthalmol Vis Sci* 40: 680-688, 1999.

70. **Obrosova IG, Fathallah L, Lang HJ and Greene DA**. Evaluation of a sorbitol dehydrogenase inhibitor on diabetic peripheral nerve metabolism: a prevention study. *Diabetologia* 42: 1187-1194, 1999.

71. **Obrosova IG, Stevens MJ and Lang HJ**. Diabetes-induced changes in retinal NAD-redox status: pharmacological modulation and implications for pathogenesis of diabetic retinopathy. *Pharmacology* 62: 172-180, 2001.

72. **Burg MB and Kador PF**. Sorbitol, osmoregulation, and the complications of diabetes. *J Clin Invest* 81: 635-640, 1988.

73. **Nakashima E, Pop-Busui R, Towns R, Thomas TP, Hosaka Y, Nakamura J, Greene DA, Killen PD, Schroeder J, Larkin DD, Ho YL and Stevens MJ**. Regulation of the human taurine transporter by oxidative stress in retinal pigment epithelial cells stably transformed to overexpress aldose reductase. *Antioxid Redox Signal* 7: 1530-1542, 2005.

74. **Franconi F, Di Leo MA, Bennardini F and Ghirlanda G**. Is taurine beneficial in reducing risk factors for diabetes mellitus? *Neurochem Res* 29: 143-150, 2004.

75. **Pop-Busui R, Sullivan KA, Van HC, Bayer L, Cao X, Towns R and Stevens MJ**. Depletion of taurine in experimental diabetic neuropathy: implications for nerve metabolic, vascular, and functional deficits. *Exp Neurol* 168: 259-272, 2001.

76. **Schaffer SW, Azuma J and Mozaffari M**. Role of antioxidant activity of taurine in diabetes. *Can J Physiol Pharmacol* 87: 91-99, 2009.

77. **Maritim AC, Sanders RA and Watkins JB, III**. Diabetes, oxidative stress, and antioxidants: a review. *J Biochem Mol Toxicol* 17: 24-38, 2003.

78. **Obrosova IG, Van HC, Fathallah L, Cao XC, Greene DA and Stevens MJ**. An aldose reductase inhibitor reverses early diabetes-induced changes in peripheral nerve function, metabolism, and antioxidative defense. *FASEB J* 16: 123-125, 2002.

79. **Nambu H, Kubo E, Takamura Y, Tsuzuki S, Tamura M and Akagi Y**. Attenuation of aldose reductase gene suppresses high-glucose-induced apoptosis and oxidative stress in rat lens epithelial cells. *Diabetes Res Clin Pract* 82: 18-24, 2008.

80. **Drel VR, Pacher P, Stevens MJ and Obrosova IG**. Aldose reductase inhibition counteracts nitrosative stress and poly(ADP-ribose) polymerase activation in diabetic rat kidney and high-glucose-exposed human mesangial cells. *Free Radic Biol Med* 40: 1454-1465, 2006.

81. **Drel VR, Pacher P, Ali TK, Shin J, Julius U, El-Remessy AB and Obrosova IG**. Aldose reductase inhibitor fidarestat counteracts diabetes-associated cataract formation, retinal oxidative-nitrosative stress, glial activation, and apoptosis. *Int J Mol Med* 21: 667-676, 2008.

82. **Obrosova IG, Pacher P, Szabo C, Zsengeller Z, Hirooka H, Stevens MJ and Yorek MA**. Aldose reductase inhibition counteracts oxidative-nitrosative stress and poly(ADP-ribose) polymerase activation in tissue sites for diabetes complications. *Diabetes* 54: 234-242, 2005.

83. **Uehara K, Yamagishi S, Otsuki S, Chin S and Yagihashi S**. Effects of polyol pathway hyperactivity on protein kinase C activity, nociceptive peptide expression, and neuronal structure in dorsal root ganglia in diabetic mice. *Diabetes* 53: 3239-3247, 2004.

84. **Demaine AG**. Polymorphisms of the aldose reductase gene and susceptibility to diabetic microvascular complications. *Curr Med Chem* 10: 1389-1398, 2003.

85. **Yagihashi S, Yamagishi SI, Wada RR, Baba M, Hohman TC, Yabe-Nishimura C and Kokai Y**. Neuropathy in diabetic mice overexpressing human aldose reductase and effects of aldose reductase inhibitor. *Brain* 124: 2448-2458, 2001.

86. **Ho EC, Lam KS, Chen YS, Yip JC, Arvindakshan M, Yamagishi S, Yagihashi S, Oates PJ, Ellery CA, Chung SS and Chung SK**. Aldose reductase-deficient mice are protected from delayed motor nerve conduction velocity, increased c-Jun NH2-terminal kinase activation, depletion of reduced glutathione, increased superoxide accumulation, and DNA damage. *Diabetes* 55: 1946-1953, 2006.

87. **Greene DA, Arezzo JC and Brown MB**. Effect of aldose reductase inhibition on nerve conduction and morphometry in diabetic neuropathy. Zenarestat Study Group. *Neurology* 53: 580-591, 1999.

88. **Goh SY and Cooper ME**. Clinical review: The role of advanced glycation end products in progression and complications of diabetes. *J Clin Endocrinol Metab* 93: 1143-1152, 2008.

89. **Wada R and Yagihashi S**. Role of advanced glycation end products and their receptors in development of diabetic neuropathy. *Ann N Y Acad Sci* 1043: 598-604, 2005.

90. **Brownlee M**. Advanced protein glycosylation in diabetes and aging. *Annu Rev Med* 46: 223-234, 1995.

91. **Giardino I, Edelstein D and Brownlee M**. Nonenzymatic glycosylation in vitro and in bovine endothelial cells alters basic fibroblast growth factor activity. A model for intracellular glycosylation in diabetes. *J Clin Invest* 94: 110-117, 1994.

92. **Shinohara M, Thornalley PJ, Giardino I, Beisswenger P, Thorpe SR, Onorato J and Brownlee M**. Overexpression of glyoxalase-I in bovine endothelial cells inhibits intracellular advanced glycation endproduct formation and prevents hyperglycemia-induced increases in macromolecular endocytosis. *J Clin Invest* 101: 1142-1147, 1998.

93. **Vlassara H**. Advanced glycation end-products and atherosclerosis. *Ann Med* 28: 419-426, 1996.

94. **Arai K, Maguchi S, Fujii S, Ishibashi H, Oikawa K and Taniguchi N**. Glycation and inactivation of human Cu-Zn-superoxide dismutase. Identification of the in vitro glycated sites. *J Biol Chem* 262: 16969-16972, 1987.

95. **Arai K, Iizuka S, Tada Y, Oikawa K and Taniguchi N**. Increase in the glucosylated form of erythrocyte Cu-Zn-superoxide dismutase in diabetes and close association of the nonenzymatic glucosylation with the enzyme activity. *Biochim Biophys Acta* 924: 292-296, 1987.

96. **Tanaka S, Avigad G, Brodsky B and Eikenberry EF**. Glycation induces expansion of the molecular packing of collagen. *J Mol Biol* 203: 495-505, 1988.

97. **Toth C, Rong LL, Yang C, Martinez J, Song F, Ramji N, Brussee V, Liu W, Durand J, Nguyen MD, Schmidt AM and Zochodne DW**. Receptor for advanced glycation end products (RAGEs) and experimental diabetic neuropathy. *Diabetes* 57: 1002-1017, 2008.

98. **Bolton WK, Cattran DC, Williams ME, Adler SG, Appel GB, Cartwright K, Foiles PG, Freedman BI, Raskin P, Ratner RE, Spinowitz BS, Whittier FC and Wuerth JP**. Randomized trial of an inhibitor of formation of advanced glycation end products in diabetic nephropathy. *Am J Nephrol* 24: 32-40, 2004.

99. **Du XL, Edelstein D, Rossetti L, Fantus IG, Goldberg H, Ziyadeh F, Wu J and Brownlee M**. Hyperglycemia-induced mitochondrial superoxide overproduction activates the hexosamine pathway and induces plasminogen activator inhibitor-1 expression by increasing Sp1 glycosylation. *Proc Natl Acad Sci U S A* 97: 12222-12226, 2000.

100. **Kolm-Litty V, Sauer U, Nerlich A, Lehmann R and Schleicher ED**. High glucose-induced transforming growth factor beta1 production is mediated by the hexosamine pathway in porcine glomerular mesangial cells. *J Clin Invest* 101: 160-169, 1998.

101. **Shiba T, Inoguchi T, Sportsman JR, Heath WF, Bursell S and King GL**. Correlation of diacylglycerol level and protein kinase C activity in rat retina to retinal circulation. *Am J Physiol* 265: E783-E793, 1993.

102. **Inoguchi T, Battan R, Handler E, Sportsman JR, Heath W and King GL**. Preferential elevation of protein kinase C isoform beta II and diacylglycerol levels in the aorta and heart of diabetic rats: differential reversibility to glycemic control by islet cell transplantation. *Proc Natl Acad Sci U S A* 89: 11059-11063, 1992.

103. **Craven PA, Davidson CM and DeRubertis FR**. Increase in diacylglycerol mass in isolated glomeruli by glucose from de novo synthesis of glycerolipids. *Diabetes* 39: 667-674, 1990.

104. **Koya D and King GL**. Protein kinase C activation and the development of diabetic complications. *Diabetes* 47: 859-866, 1998.

105. **Ishii H, Jirousek MR, Koya D, Takagi C, Xia P, Clermont A, Bursell SE, Kern TS, Ballas LM, Heath WF, Stramm LE, Feener EP and King GL**. Amelioration of vascular dysfunctions in diabetic rats by an oral PKC beta inhibitor. *Science* 272: 728-731, 1996.

106. **Kuboki K, Jiang ZY, Takahara N, Ha SW, Igarashi M, Yamauchi T, Feener EP, Herbert TP, Rhodes CJ and King GL**. Regulation of endothelial constitutive nitric oxide synthase gene expression in endothelial cells and in vivo : a specific vascular action of insulin. *Circulation* 101: 676-681, 2000.

107. **Ido Y, McHowat J, Chang KC, rrigoni-Martelli E, Orfalian Z, Kilo C, Corr PB and Williamson JR**. Neural dysfunction and metabolic imbalances in diabetic rats. Prevention by acetyl-L-carnitine. *Diabetes* 43: 1469-1477, 1994.

108. **Nakamura J, Kato K, Hamada Y, Nakayama M, Chaya S, Nakashima E, Naruse K, Kasuya Y, Mizubayashi R, Miwa K, Yasuda Y, Kamiya H, Ienaga K, Sakakibara F, Koh N and Hotta N**. A protein kinase C-beta-selective inhibitor ameliorates neural dysfunction in streptozotocin-induced diabetic rats. *Diabetes* 48: 2090-2095, 1999.

109. **Diana S.Beattie**. Bioenergetics and Oxidative Metabolism. In: Textbook of Biochemistry with Clinical Correlations, edited by Thomas M Devlin. New York: Wiley-Liss, 2002, p. 538-595.

110. **Vincent AM and Feldman EL**. New insights into the mechanisms of diabetic neuropathy. *Rev Endocr Metab Disord* 5: 227-236, 2004.

111. **Sima AA**. New insights into the metabolic and molecular basis for diabetic neuropathy. *Cell Mol Life Sci* 60: 2445-2464, 2003.

112. **Feldman EL**. Oxidative stress and diabetic neuropathy: a new understanding of an old problem. *J Clin Invest* 111: 431-433, 2003.

113. **Bravenboer B, Kappelle AC, Hamers FP, van BT, Erkelens DW and Gispen WH**. Potential use of glutathione for the prevention and treatment of diabetic neuropathy in the streptozotocin-induced diabetic rat. *Diabetologia* 35: 813-817, 1992.

114. **Greene DA, Stevens MJ, Obrosova I and Feldman EL**. Glucose-induced oxidative stress and programmed cell death in diabetic neuropathy. *Eur J Pharmacol* 375: 217-223, 1999.

115. **Stevens MJ, Obrosova I, Cao X, Van HC and Greene DA**. Effects of DL-alpha-lipoic acid on peripheral nerve conduction, blood flow, energy metabolism, and oxidative stress in experimental diabetic neuropathy. *Diabetes* 49: 1006-1015, 2000.

116. **Ayo SH, Radnik RA, Glass WF, Garoni JA, Rampt ER, Appling DR and Kreisberg JI**. Increased extracellular matrix synthesis and mRNA in mesangial cells grown in high-glucose medium. *Am J Physiol* 260: F185-F191, 1991.

117. **Kunisaki M, Bursell SE, Umeda F, Nawata H and King GL**. Normalization of diacylglycerol-protein kinase C activation by vitamin E in aorta of diabetic rats and cultured rat smooth muscle cells exposed to elevated glucose levels. *Diabetes* 43: 1372-1377, 1994.

118. **Kakkar R, Kalra J, Mantha SV and Prasad K**. Lipid peroxidation and activity of antioxidant enzymes in diabetic rats. *Mol Cell Biochem* 151: 113-119, 1995.

119. **Haffner SM, Agil A, Mykkanen L, Stern MP and Jialal I**. Plasma oxidizability in subjects with normal glucose tolerance, impaired glucose tolerance, and NIDDM. *Diabetes Care* 18: 646-653, 1995.

120. **Nourooz-Zadeh J, Rahimi A, Tajaddini-Sarmadi J, Tritschler H, Rosen P, Halliwell B and Betteridge DJ**. Relationships between plasma measures of oxidative stress and metabolic control in NIDDM. *Diabetologia* 40: 647-653, 1997.

121. **Nourooz-Zadeh J, Tajaddini-Sarmadi J, McCarthy S, Betteridge DJ and Wolff SP**. Elevated levels of authentic plasma hydroperoxides in NIDDM. *Diabetes* 44: 1054-1058, 1995.

122. **Gopaul NK, Anggard EE, Mallet AI, Betteridge DJ, Wolff SP and Nourooz-Zadeh J**. Plasma 8-epi-PGF2 alpha levels are elevated in individuals with non-insulin dependent diabetes mellitus. *FEBS Lett* 368: 225-229, 1995.

123. **Feldman EL, Stevens MJ and Greene DA**. Pathogenesis of diabetic neuropathy. *Clin Neurosci* 4: 365-370, 1997.

124. **Du XL, Edelstein D, Dimmeler S, Ju Q, Sui C and Brownlee M**. Hyperglycemia inhibits endothelial nitric oxide synthase activity by posttranslational modification at the Akt site. *J Clin Invest* 108: 1341-1348, 2001.

125. **Packer L**. Antioxidant properties of lipoic acid and its therapeutic effects in prevention of diabetes complications and cataracts. *Ann N Y Acad Sci* 738: 257-264, 1994.

126. **Packer L, Kraemer K and Rimbach G**. Molecular aspects of lipoic acid in the prevention of diabetes complications. *Nutrition* 17: 888-895, 2001.

127. **Garrett NE, Malcangio M, Dewhurst M and Tomlinson DR**. alpha-Lipoic acid corrects neuropeptide deficits in diabetic rats via induction of trophic support. *Neurosci Lett* 222: 191-194, 1997.

128. **Ziegler D**. Thioctic acid for patients with symptomatic diabetic polyneuropathy: a critical review. *Treat Endocrinol* 3: 173-189, 2004.

129. **Ziegler D**. Treatment of diabetic polyneuropathy: Update 2006. *Ann N Y Acad Sci* 1084: 250-266, 2006.

130. **Foster TS**. Efficacy and safety of alpha-lipoic acid supplementation in the treatment of symptomatic diabetic neuropathy. *Diabetes Educ* 33: 111-117, 2007.

131. **Singh U and Jialal I**. Alpha-lipoic acid supplementation and diabetes. *Nutr Rev* 66: 646-657, 2008.

132. **Pompella A, Visvikis A, Paolicchi A, De T, V and Casini AF**. The changing faces of glutathione, a cellular protagonist. *Biochem Pharmacol* 66: 1499-1503, 2003.

133. **Luberda Z**. The role of glutathione in mammalian gametes. *Reprod Biol* 5: 5-17, 2005.

134. **Mates JM, Perez-Gomez C and Nunez dC, I**. Antioxidant enzymes and human diseases. *Clin Biochem* 32: 595-603, 1999.

135. **Komosinska-Vassev K, Olczyk K, Olczyk P and Winsz-Szczotka K**. Effects of metabolic control and vascular complications on indices of oxidative stress in type 2 diabetic patients. *Diabetes Res Clin Pract* 68: 207-216, 2005.

136. **Dincer Y, Akcay T, Alademir Z and Ilkova H**. Assessment of DNA base oxidation and glutathione level in patients with type 2 diabetes. *Mutat Res* 505: 75-81, 2002.

137. **Tainer JA, Getzoff ED, Richardson JS and Richardson DC**. Structure and mechanism of copper, zinc superoxide dismutase. *Nature* 306: 284-287, 1983.

138. **Zelko IN, Mariani TJ and Folz RJ**. Superoxide dismutase multigene family: a comparison of the CuZn-SOD (SOD1), Mn-SOD (SOD2), and EC-SOD (SOD3) gene structures, evolution, and expression. *Free Radic Biol Med* 33: 337-349, 2002.

139. **Ihnat MA, Thorpe JE, Kamat CD, Szabo C, Green DE, Warnke LA, Lacza Z, Cselenyak A, Ross K, Shakir S, Piconi L, Kaltreider RC and Ceriello A**. Reactive oxygen species mediate a cellular 'memory' of high glucose stress signalling. *Diabetologia* 50: 1523-1531, 2007.

140. **Song F, Jia W, Yao Y, Hu Y, Lei L, Lin J, Sun X and Liu L**. Oxidative stress, antioxidant status and DNA damage in patients with impaired glucose regulation and newly diagnosed Type 2 diabetes. *Clin Sci (Lond)* 112: 599-606, 2007.

141. **Flekac M, Skrha J, Hilgertova J, Lacinova Z and Jarolimkova M**. Gene polymorphisms of superoxide dismutases and catalase in diabetes mellitus. *BMC Med Genet* 9: 30, 2008.

142. **Bhatia S, Shukla R, Venkata MS, Kaur GJ and Madhava PK**. Antioxidant status, lipid peroxidation and nitric oxide end products in patients of type 2 diabetes mellitus with nephropathy. *Clin Biochem* 36: 557-562, 2003.

143. **Godin DV, Wohaieb SA, Garnett ME and Goumeniouk AD**. Antioxidant enzyme alterations in experimental and clinical diabetes. *Mol Cell Biochem* 84: 223-231, 1988.

144. **Aydin A, Orhan H, Sayal A, Ozata M, Sahin G and Isimer A**. Oxidative stress and nitric oxide related parameters in type II diabetes mellitus: effects of glycemic control. *Clin Biochem* 34: 65-70, 2001.

145. **Obrosova IG, Fathallah L and Stevens MJ**. Taurine counteracts oxidative stress and nerve growth factor deficit in early experimental diabetic neuropathy. *Exp Neurol* 172: 211-219, 2001.

146. **Bogdan C**. Nitric oxide and the regulation of gene expression. *Trends Cell Biol* 11: 66-75, 2001.

147. **Dimmeler S, Fleming I, Fisslthaler B, Hermann C, Busse R and Zeiher AM**. Activation of nitric oxide synthase in endothelial cells by Akt-dependent phosphorylation. *Nature* 399: 601-605, 1999.

148. **Gingerich S and Krukoff TL**. Activation of ERbeta increases levels of phosphorylated nNOS and NO production through a Src/PI3K/Akt-dependent pathway in hypothalamic neurons. *Neuropharmacology* 55: 878-885, 2008.

149. **Brown GC**. Mechanisms of inflammatory neurodegeneration: iNOS and NADPH oxidase. *Biochem Soc Trans* 35: 1119-1121, 2007.

150. **Bogdan C**. Nitric oxide and the immune response. *Nat Immunol* 2: 907-916, 2001.

151. **Korhonen R, Lahti A, Kankaanranta H and Moilanen E**. Nitric oxide production and signaling in inflammation. *Curr Drug Targets Inflamm Allergy* 4: 471-479, 2005.

152. **Korhonen R, Lahti A, Kankaanranta H and Moilanen E**. Nitric oxide production and signaling in inflammation. *Curr Drug Targets Inflamm Allergy* 4: 471-479, 2005.

153. **Toda N and Nakanishi-Toda M**. Nitric oxide: ocular blood flow, glaucoma, and diabetic retinopathy. *Prog Retin Eye Res* 26: 205-238, 2007.

154. **Ellis EA, Guberski DL, Hutson B and Grant MB**. Time course of NADH oxidase, inducible nitric oxide synthase and peroxynitrite in diabetic retinopathy in the BBZ/WOR rat. *Nitric Oxide* 6: 295-304, 2002.

155. **Jesmin S, Zaedi S, Maeda S, Yamaguchi I, Goto K and Miyauchi T**. Effects of a selective endothelin a receptor antagonist on the expressions of iNOS and eNOS in the

heart of early streptozotocin-induced diabetic rats. *Exp Biol Med (Maywood)* 231: 925-931, 2006.

156. **Nagareddy PR, Xia Z, McNeill JH and MacLeod KM**. Increased expression of iNOS is associated with endothelial dysfunction and impaired pressor responsiveness in streptozotocin-induced diabetes. *Am J Physiol Heart Circ Physiol* 289: H2144-H2152, 2005.

157. **Ishikawa T, Kohno F, Kawase R, Yamamoto Y and Nakayama K**. Contribution of nitric oxide produced by inducible nitric oxide synthase to vascular responses of mesenteric arterioles in streptozotocin-diabetic rats. *Br J Pharmacol* 141: 269-276, 2004.

158. **Steinle JJ**. Sympathetic neurotransmission modulates expression of inflammatory markers in the rat retina. *Exp Eye Res* 84: 118-125, 2007.

159. **Rajesh M, Mukhopadhyay P, Batkai S, Hasko G, Liaudet L, Drel VR, Obrosova IG and Pacher P**. Cannabidiol attenuates high glucose-induced endothelial cell inflammatory response and barrier disruption. *Am J Physiol Heart Circ Physiol* 293: H610-H619, 2007.

160. **Ramana KV, Friedrich B, Bhatnagar A and Srivastava SK**. Aldose reductase mediates cytotoxic signals of hyperglycemia and TNF-alpha in human lens epithelial cells. *FASEB J* 17: 315-317, 2003.

161. **Powell LA, Warpeha KM, Xu W, Walker B and Trimble ER**. High glucose decreases intracellular glutathione concentrations and upregulates inducible nitric oxide synthase gene expression in intestinal epithelial cells. *J Mol Endocrinol* 33: 797-803, 2004.

162. **Empl M, Renaud S, Erne B, Fuhr P, Straube A, Schaeren-Wiemers N and Steck AJ**. TNF-alpha expression in painful and nonpainful neuropathies. *Neurology* 56: 1371-1377, 2001.

163. **Noh H, Ha H, Yu MR, Kang SW, Choi KH, Han DS and Lee HY**. High glucose increases inducible NO production in cultured rat mesangial cells. Possible role in fibronectin production. *Nephron* 90: 78-85, 2002.

164. **Vareniuk I, Pavlov IA and Obrosova IG**. Inducible nitric oxide synthase gene deficiency counteracts multiple manifestations of peripheral neuropathy in a streptozotocin-induced mouse model of diabetes. *Diabetologia* 51: 2126-2133, 2008.

165. **Forstermann U, Boissel JP and Kleinert H**. Expressional control of the 'constitutive' isoforms of nitric oxide synthase (NOS I and NOS III). *FASEB J* 12: 773-790, 1998.

166. **Park JW, Park SJ, Park SH, Kim KY, Chung JW, Chun MH and Oh SJ**. Up-regulated expression of neuronal nitric oxide synthase in experimental diabetic retina. *Neurobiol Dis* 21: 43-49, 2006.

167. **Takeda M, Mori F, Yoshida A, Takamiya A, Nakagomi S, Sato E and Kiyama H**. Constitutive nitric oxide synthase is associated with retinal vascular permeability in early diabetic rats. *Diabetologia* 44: 1043-1050, 2001.

168. **Adeghate E, al-Ramadi B, Saleh AM, Vijayarasathy C, Ponery AS, Arafat K, Howarth FC and El-Sharkawy T**. Increase in neuronal nitric oxide synthase content of the gastroduodenal tract of diabetic rats. *Cell Mol Life Sci* 60: 1172-1179, 2003.

169. **Yabuki A, Tahara T, Taniguchi K, Matsumoto M and Suzuki S**. Neuronal nitric oxide synthase and cyclooxygenase-2 in diabetic nephropathy of type 2 diabetic OLETF rats. *Exp Anim* 55: 17-25, 2006.

170. **Okada S, Saito M, Kazuyama E, Hanada T, Kawaba Y, Hayashi A, Satoh K and Kanzaki S**. Effects of N-hexacosanol on nitric oxide synthase system in diabetic rat nephropathy. *Mol Cell Biochem* 315: 169-177, 2008.

171. **Ii M, Nishimura H, Kusano KF, Qin G, Yoon YS, Wecker A, Asahara T and Losordo DW**. Neuronal nitric oxide synthase mediates statin-induced restoration of vasa nervorum and reversal of diabetic neuropathy. *Circulation* 112: 93-102, 2005.

172. **Vareniuk I, Pacher P, Pavlov IA, Drel VR and Obrosova IG**. Peripheral neuropathy in mice with neuronal nitric oxide synthase gene deficiency. *Int J Mol Med* 23: 571-580, 2009.

173. **Cosentino F, Hishikawa K, Katusic ZS and Luscher TF**. High glucose increases nitric oxide synthase expression and superoxide anion generation in human aortic endothelial cells. *Circulation* 96: 25-28, 1997.

174. **Srinivasan S, Hatley ME, Bolick DT, Palmer LA, Edelstein D, Brownlee M and Hedrick CC**. Hyperglycaemia-induced superoxide production decreases eNOS expression via AP-1 activation in aortic endothelial cells. *Diabetologia* 47: 1727-1734, 2004.

175. **Chatterjee A, Black SM and Catravas JD**. Endothelial nitric oxide (NO) and its pathophysiologic regulation. *Vascul Pharmacol* 49: 134-140, 2008.

176. **Seckin D, Ilhan N, Ilhan N and Ertugrul S**. Glycaemic control, markers of endothelial cell activation and oxidative stress in children with type 1 diabetes mellitus. *Diabetes Res Clin Pract* 73: 191-197, 2006.

177. **Thomas DD, Ridnour LA, Isenberg JS, Flores-Santana W, Switzer CH, Donzelli S, Hussain P, Vecoli C, Paolocci N, Ambs S, Colton CA, Harris CC, Roberts DD and Wink DA**. The chemical biology of nitric oxide: implications in cellular signaling. *Free Radic Biol Med* 45: 18-31, 2008.

178. **van d, V, Eiserich JP, Shigenaga MK and Cross CE**. Reactive nitrogen species and tyrosine nitration in the respiratory tract: epiphenomena or a pathobiologic mechanism of disease? *Am J Respir Crit Care Med* 160: 1-9, 1999.

179. **Webster RP, Roberts VH and Myatt L**. Protein nitration in placenta - functional significance. *Placenta* 29: 985-994, 2008.

180. **Obrosova IG, Mabley JG, Zsengeller Z, Charniauskaya T, Abatan OI, Groves JT and Szabo C**. Role for nitrosative stress in diabetic neuropathy: evidence from studies with a peroxynitrite decomposition catalyst. *FASEB J* 19: 401-403, 2005.

181. **Gow AJ, Farkouh CR, Munson DA, Posencheg MA and Ischiropoulos H**. Biological significance of nitric oxide-mediated protein modifications. *Am J Physiol Lung Cell Mol Physiol* 287: L262-L268, 2004.

182. **Abello N, Kerstjens HA, Postma DS and Bischoff R**. Protein tyrosine nitration: selectivity, physicochemical and biological consequences, denitration, and proteomics methods for the identification of tyrosine-nitrated proteins. *J Proteome Res* 8: 3222-3238, 2009.

183. **Kaminsky DA, Mitchell J, Carroll N, James A, Soultanakis R and Janssen Y**. Nitrotyrosine formation in the airways and lung parenchyma of patients with asthma. *J Allergy Clin Immunol* 104: 747-754, 1999.

184. **Turko IV and Murad F**. Protein nitration in cardiovascular diseases. *Pharmacol Rev* 54: 619-634, 2002.

185. **Wang XL, Rainwater DL, Leone A and Mahaney MC**. Effects of diabetes on plasma nitrotyrosine levels. *Diabet Med* 21: 577-580, 2004.

186. **Gow AJ, Duran D, Malcolm S and Ischiropoulos H**. Effects of peroxynitrite-induced protein modifications on tyrosine phosphorylation and degradation. *FEBS Lett* 385: 63-66, 1996.

187. **Newman PJ, Hillery CA, Albrecht R, Parise LV, Berndt MC, Mazurov AV, Dunlop LC, Zhang J and Rittenhouse SE**. Activation-dependent changes in human platelet PECAM-1: phosphorylation, cytoskeletal association, and surface membrane redistribution. *J Cell Biol* 119: 239-246, 1992.

188. **Saeki M and Maeda S**. p130cas is a cellular target protein for tyrosine nitration induced by peroxynitrite. *Neurosci Res* 33: 325-328, 1999.

189. **Pacher P, Beckman JS and Liaudet L**. Nitric oxide and peroxynitrite in health and disease. *Physiol Rev* 87: 315-424, 2007.

190. **Liaudet L, Vassalli G and Pacher P**. Role of peroxynitrite in the redox regulation of cell signal transduction pathways. *Front Biosci* 14: 4809-4814, 2009.

191. **Song P, Wu Y, Xu J, Xie Z, Dong Y, Zhang M and Zou MH**. Reactive nitrogen species induced by hyperglycemia suppresses Akt signaling and triggers apoptosis by upregulating phosphatase PTEN (phosphatase and tensin homologue deleted on chromosome 10) in an LKB1-dependent manner. *Circulation* 116: 1585-1595, 2007.

192. **Foster MW, Hess DT and Stamler JS**. Protein S-nitrosylation in health and disease: a current perspective. *Trends Mol Med* 15: 391-404, 2009.

193. **Paige JS, Xu G, Stancevic B and Jaffrey SR**. Nitrosothiol reactivity profiling identifies S-nitrosylated proteins with unexpected stability. *Chem Biol* 15: 1307-1316, 2008.

194. **Foster MW, McMahon TJ and Stamler JS**. S-nitrosylation in health and disease. *Trends Mol Med* 9: 160-168, 2003.

195. **Yasukawa T, Tokunaga E, Ota H, Sugita H, Martyn JA and Kaneki M**. S-nitrosylation-dependent inactivation of Akt/protein kinase B in insulin resistance. *J Biol Chem* 280: 7511-7518, 2005.

196. **Carvalho-Filho MA, Ueno M, Hirabara SM, Seabra AB, Carvalheira JB, de Oliveira MG, Velloso LA, Curi R and Saad MJ**. S-nitrosation of the insulin receptor, insulin receptor substrate 1, and protein kinase B/Akt: a novel mechanism of insulin resistance. *Diabetes* 54: 959-967, 2005.

197. **Sugita H, Fujimoto M, Yasukawa T, Shimizu N, Sugita M, Yasuhara S, Martyn JA and Kaneki M**. Inducible nitric-oxide synthase and NO donor induce insulin receptor substrate-1 degradation in skeletal muscle cells. *J Biol Chem* 280: 14203-14211, 2005.

198. **Woodhouse BC and Dianov GL**. Poly ADP-ribose polymerase-1: an international molecule of mystery. *DNA Repair (Amst)* 7: 1077-1086, 2008.

199. **Pacher P and Szabo C**. Role of poly(ADP-ribose) polymerase 1 (PARP-1) in cardiovascular diseases: the therapeutic potential of PARP inhibitors. *Cardiovasc Drug Rev* 25: 235-260, 2007.

200. **Pacher P and Szabo C**. Role of the peroxynitrite-poly(ADP-ribose) polymerase pathway in human disease. *Am J Pathol* 173: 2-13, 2008.

201. **Feldman EL**. Diabetic neuropathy. *Curr Drug Targets* 9: 1-2, 2008.

202. **Du X, Matsumura T, Edelstein D, Rossetti L, Zsengeller Z, Szabo C and Brownlee M**. Inhibition of GAPDH activity by poly(ADP-ribose) polymerase activates three major pathways of hyperglycemic damage in endothelial cells. *J Clin Invest* 112: 1049-1057, 2003.

203. **Obrosova IG, Li F, Abatan OI, Forsell MA, Komjati K, Pacher P, Szabo C and Stevens MJ**. Role of poly(ADP-ribose) polymerase activation in diabetic neuropathy. *Diabetes* 53: 711-720, 2004.

204. **Obrosova IG, Xu W, Lyzogubov VV, Ilnytska O, Mashtalir N, Vareniuk I, Pavlov IA, Zhang J, Slusher B and Drel VR**. PARP inhibition or gene deficiency counteracts intraepidermal nerve fiber loss and neuropathic pain in advanced diabetic neuropathy. *Free Radic Biol Med* 44: 972-981, 2008.

205. **Obrosova IG, Minchenko AG, Frank RN, Seigel GM, Zsengeller Z, Pacher P, Stevens MJ and Szabo C**. Poly(ADP-ribose) polymerase inhibitors counteract diabetes- and hypoxia-induced retinal vascular endothelial growth factor overexpression. *Int J Mol Med* 14: 55-64, 2004.

206. **Lodish H, Berk A, Zipursky SL, Matsudaira P, Baltimore D and Darnell J**. Cell-to-Cell Signaling Hormones and Receptors. In: Molecular Cell Biology, edited by Lodish H, Berk A, Zipursky SL, Matsudaira P, Baltimore D and Darnell J. New York: W. H. Freeman and Company, 2000, p. 848-909.

207. **Junttila MR, Li SP and Westermarck J**. Phosphatase-mediated crosstalk between MAPK signaling pathways in the regulation of cell survival. *FASEB J* 22: 954-965, 2008.

208. **Purves T, Middlemas A, Agthong S, Jude EB, Boulton AJ, Fernyhough P and Tomlinson DR**. A role for mitogen-activated protein kinases in the etiology of diabetic neuropathy. *FASEB J* 15: 2508-2514, 2001.

209. **Price SA, Agthong S, Middlemas AB and Tomlinson DR**. Mitogen-activated protein kinase p38 mediates reduced nerve conduction velocity in experimental diabetic neuropathy: interactions with aldose reductase. *Diabetes* 53: 1851-1856, 2004.

210. **Almhanna K, Wilkins PL, Bavis JR, Harwalkar S and Berti-Mattera LN**. Hyperglycemia triggers abnormal signaling and proliferative responses in Schwann cells. *Neurochem Res* 27: 1341-1347, 2002.

211. **Daulhac L, Mallet C, Courteix C, Etienne M, Duroux E, Privat AM, Eschalier A and Fialip J**. Diabetes-induced mechanical hyperalgesia involves spinal mitogen-activated protein kinase activation in neurons and microglia via N-methyl-D-aspartate-dependent mechanisms. *Mol Pharmacol* 70: 1246-1254, 2006.

212. **Kultz D, Garcia-Perez A, Ferraris JD and Burg MB**. Distinct regulation of osmoprotective genes in yeast and mammals. Aldose reductase osmotic response element is induced independent of p38 and stress-activated protein kinase/Jun N-terminal kinase in rabbit kidney cells. *J Biol Chem* 272: 13165-13170, 1997.

213. **Kultz D and Burg M**. Evolution of osmotic stress signaling via MAP kinase cascades. *J Exp Biol* 201: 3015-3021, 1998.

214. **Price SA, Hounsom L, Purves-Tyson TD, Fernyhough P and Tomlinson DR**. Activation of JNK in sensory neurons protects against sensory neuron cell death in diabetes and on exposure to glucose/oxidative stress in vitro. *Ann N Y Acad Sci* 1010: 95-99, 2003.

215. **Middlemas AB, Agthong S and Tomlinson DR**. Phosphorylation of c-Jun N-terminal kinase (JNK) in sensory neurones of diabetic rats, with possible effects on nerve conduction and neuropathic pain: prevention with an aldose reductase inhibitor. *Diabetologia* 49: 580-587, 2006.

216. **Purves TD and Tomlinson DR**. Are mitogen-activated protein kinases glucose transducers for diabetic neuropathies? *Int Rev Neurobiol* 50: 83-114, 2002.

217. **Fernyhough P, Gallagher A, Averill SA, Priestley JV, Hounsom L, Patel J and Tomlinson DR**. Aberrant neurofilament phosphorylation in sensory neurons of rats with diabetic neuropathy. *Diabetes* 48: 881-889, 1999.

218. **Ciruela A, Dixon AK, Bramwell S, Gonzalez MI, Pinnock RD and Lee K**. Identification of MEK1 as a novel target for the treatment of neuropathic pain. *Br J Pharmacol* 138: 751-756, 2003.

219. **Yuan Z, Feng W, Hong J, Zheng Q, Shuai J and Ge Y**. p38MAPK and ERK promote nitric oxide production in cultured human retinal pigmented epithelial cells induced by high concentration glucose. *Nitric Oxide* 20: 9-15, 2009.

220. **Ishiki M and Klip A**. Minireview: recent developments in the regulation of glucose transporter-4 traffic: new signals, locations, and partners. *Endocrinology* 146: 5071-5078, 2005.

221. **Kim D and Chung J**. Akt: versatile mediator of cell survival and beyond. *J Biochem Mol Biol* 35: 106-115, 2002.

222. **Zdychova J and Komers R**. Emerging role of Akt kinase/protein kinase B signaling in pathophysiology of diabetes and its complications. *Physiol Res* 54: 1-16, 2005.

223. **Schleicher ED and Weigert C**. Role of the hexosamine biosynthetic pathway in diabetic nephropathy. *Kidney Int Suppl* 77: S13-S18, 2000.

224. **Birdsall TC**. Therapeutic applications of taurine. *Altern Med Rev* 3: 128-136, 1998.

225. **Li F, Obrosova IG, Abatan O, Tian D, Larkin D, Stuenkel EL and Stevens MJ**. Taurine replacement attenuates hyperalgesia and abnormal calcium signaling in sensory neurons of STZ-D rats. *Am J Physiol Endocrinol Metab* 288: E29-E36, 2005.

226. **Takahashi K, Harada H, Schaffer SW and Azuma J**. Effect of taurine on intracellular calcium dynamics of cultured myocardial cells during the calcium paradox. *Adv Exp Med Biol* 315: 153-161, 1992.

227. **Laidlaw SA, Shultz TD, Cecchino JT and Kopple JD**. Plasma and urine taurine levels in vegans. *Am J Clin Nutr* 47: 660-663, 1988.

228. **Tappaz ML**. Taurine biosynthetic enzymes and taurine transporter: molecular identification and regulations. *Neurochem Res* 29: 83-96, 2004.

229. **Warskulat U, Flogel U, Jacoby C, Hartwig HG, Thewissen M, Merx MW, Molojavyi A, Heller-Stilb B, Schrader J and Haussinger D**. Taurine transporter knockout depletes muscle taurine levels and results in severe skeletal muscle impairment but leaves cardiac function uncompromised. *FASEB J* 18: 577-579, 2004.

230. **Sturman JA**. Cysteinesulfinic acid decarboxylase activity in the mammalian nervous system: absence from axons. *J Neurochem* 36: 304-306, 1981.

231. **Brand A, Richter-Landsberg C and Leibfritz D**. Metabolism of acetate in rat brain neurons, astrocytes and cocultures: metabolic interactions between neurons and glia cells, monitored by NMR spectroscopy. *Cell Mol Biol (Noisy -le-grand)* 43: 645-657, 1997.

232. **Warskulat U, Borsch E, Reinehr R, Heller-Stilb B, Monnighoff I, Buchczyk D, Donner M, Flogel U, Kappert G, Soboll S, Beer S, Pfeffer K, Marschall HU, Gabrielsen M, miry-Moghaddam M, Ottersen OP, Dienes HP and Haussinger D**. Chronic liver disease is triggered by taurine transporter knockout in the mouse. *FASEB J* 20: 574-576, 2006.

233. **Gaull GE, Rassin DK, Raiha NC and Heinonen K**. Milk protein quantity and quality in low-birth-weight infants. III. Effects on sulfur amino acids in plasma and urine. *J Pediatr* 90: 348-355, 1977.

234. **Sturman JA, Hepner GW, Hofmann AF and Thomas PJ**. Metabolism of [35S]taurine in man. *J Nutr* 105: 1206-1214, 1975.

235. **De LG, Calpona PR, Caponetti A, Romano G, Di BA, Cucinotta D and Di Giorgio RM**. Taurine and osmoregulation: platelet taurine content, uptake, and release in type 2 diabetic patients. *Metabolism* 50: 60-64, 2001.

236. **Han X, Patters AB, Jones DP, Zelikovic I and Chesney RW**. The taurine transporter: mechanisms of regulation. *Acta Physiol (Oxf)* 187: 61-73, 2006.

237. **Lambert IH**. Regulation of the cellular content of the organic osmolyte taurine in mammalian cells. *Neurochem Res* 29: 27-63, 2004.

238. **Hayes KC**. Nutritional problems in cats: taurine deficiency and vitamin A excess. *Can Vet J* 23: 2-5, 1982.

239. **Warskulat U, Heller-Stilb B, Oermann E, Zilles K, Haas H, Lang F and Haussinger D**. Phenotype of the taurine transporter knockout mouse. *Methods Enzymol* 428: 439-458, 2007.

240. **Heller-Stilb B, van RC, Rascher K, Hartwig HG, Huth A, Seeliger MW, Warskulat U and Haussinger D**. Disruption of the taurine transporter gene (taut) leads to retinal degeneration in mice. *FASEB J* 16: 231-233, 2002.

241. **Kilb W, Hanganu IL, Okabe A, Sava BA, Shimizu-Okabe C, Fukuda A and Luhmann HJ**. Glycine receptors mediate excitation of subplate neurons in neonatal rat cerebral cortex. *J Neurophysiol* 100: 698-707, 2008.

242. **Chepkova AN, Doreulee N, Yanovsky Y, Mukhopadhyay D, Haas HL and Sergeeva OA**. Long-lasting enhancement of corticostriatal neurotransmission by taurine. *Eur J Neurosci* 16: 1523-1530, 2002.

243. **Smith KE, Borden LA, Wang CH, Hartig PR, Branchek TA and Weinshank RL**. Cloning and expression of a high affinity taurine transporter from rat brain. *Mol Pharmacol* 42: 563-569, 1992.

244. **Liu QR, Lopez-Corcuera B, Nelson H, Mandiyan S and Nelson N**. Cloning and expression of a cDNA encoding the transporter of taurine and beta-alanine in mouse brain. *Proc Natl Acad Sci U S A* 89: 12145-12149, 1992.

245. **Uchida S, Kwon HM, Yamauchi A, Preston AS, Marumo F and Handler JS**. Molecular cloning of the cDNA for an MDCK cell Na(+)- and Cl(-)-dependent taurine transporter that is regulated by hypertonicity. *Proc Natl Acad Sci U S A* 90: 7424, 1993.

246. **Jhiang SM, Fithian L, Smanik P, McGill J, Tong Q and Mazzaferri EL**. Cloning of the human taurine transporter and characterization of taurine uptake in thyroid cells. *FEBS Lett* 318: 139-144, 1993.

247. **Ramamoorthy S, Leibach FH, Mahesh VB, Han H, Yang-Feng T, Blakely RD and Ganapathy V**. Functional characterization and chromosomal localization of a cloned taurine transporter from human placenta. *Biochem J* 300 (Pt 3): 893-900, 1994.

248. **Ramamoorthy S, Del Monte MA, Leibach FH and Ganapathy V**. Molecular identity and calmodulin-mediated regulation of the taurine transporter in a human retinal pigment epithelial cell line. *Curr Eye Res* 13: 523-529, 1994.

249. **Vinnakota S, Qian X, Egal H, Sarthy V and Sarkar HK**. Molecular characterization and in situ localization of a mouse retinal taurine transporter. *J Neurochem* 69: 2238-2250, 1997.

250. **Qian X, Vinnakota S, Edwards C and Sarkar HK**. Molecular characterization of taurine transport in bovine aortic endothelial cells. *Biochim Biophys Acta* 1509: 324-334, 2000.

251. **Han X, Budreau AM and Chesney RW**. Identification of promoter elements involved in adaptive regulation of the taurine transporter gene: role of cytosolic Ca2+ signaling. *Adv Exp Med Biol* 483: 535-544, 2000.

252. **Ganapathy V, Ramamoorthy JD, Del Monte MA, Leibach FH and Ramamoorthy S**. Cyclic AMP-dependent up-regulation of the taurine transporter in a human retinal pigment epithelial cell line. *Curr Eye Res* 14: 843-850, 1995.

253. **Miyamoto Y, Marczin N, Catravas JD and Del Monte MA**. Cholera toxin enhances taurine uptake in cultures of human retinal pigment epithelial cells. *Curr Eye Res* 15: 229-236, 1996.

254. **Han X, Budreau AM and Chesney RW**. Cloning and characterization of the promoter region of the rat taurine transporter (TauT) gene. *Adv Exp Med Biol* 483: 97-108, 2000.

255. **Strange K, Emma F and Jackson PS**. Cellular and molecular physiology of volume-sensitive anion channels. *Am J Physiol* 270: C711-C730, 1996.

256. **Pierce SK and Warren JW**. The Taurine Efflux Portal Used to Regulate Cell Volume in Response to Hypoosmotic Stress Seems to Be Similar in Many Cell Types: Lessons to Be Learned from Molluscan Red Blood Cells. *AMER ZOOL* 41: 710-720, 2001.

257. **Franconi F, Bennardini F, Mattana A, Miceli M, Ciuti M, Mian M, Gironi A, Anichini R and Seghieri G**. Plasma and platelet taurine are reduced in subjects with insulin-dependent diabetes mellitus: effects of taurine supplementation. *Am J Clin Nutr* 61: 1115-1119, 1995.

258. **Merheb M, Daher RT, Nasrallah M, Sabra R, Ziyadeh FN and Barada K**. Taurine intestinal absorption and renal excretion test in diabetic patients: a pilot study. *Diabetes Care* 30: 2652-2654, 2007.

259. **Malone JI, Benford SA and Malone J, Jr.** Taurine prevents galactose-induced cataracts. *J Diabetes Complications* 7: 44-48, 1993.

260. **Trachtman H, Futterweit S and Bienkowski RS**. Taurine prevents glucose-induced lipid peroxidation and increased collagen production in cultured rat mesangial cells. *Biochem Biophys Res Commun* 191: 759-765, 1993.

261. **Stevens MJ, Hosaka Y, Masterson JA, Jones SM, Thomas TP and Larkin DD**. Downregulation of the human taurine transporter by glucose in cultured retinal pigment epithelial cells. *Am J Physiol* 277: E760-E771, 1999.

262. **Li F, Abatan OI, Kim H, Burnett D, Larkin D, Obrosova IG and Stevens MJ**. Taurine reverses neurological and neurovascular deficits in Zucker diabetic fatty rats. *Neurobiol Dis* 22: 669-676, 2006.

263. **Lee EA, Seo JY, Jiang Z, Yu MR, Kwon MK, Ha H and Lee HB**. Reactive oxygen species mediate high glucose-induced plasminogen activator inhibitor-1 up-regulation in mesangial cells and in diabetic kidney. *Kidney Int* 67: 1762-1771, 2005.

264. **Tas S, Sarandol E, Ayvalik SZ, Serdar Z and Dirican M**. Vanadyl sulfate, taurine, and combined vanadyl sulfate and taurine treatments in diabetic rats: effects on the oxidative and antioxidative systems. *Arch Med Res* 38: 276-283, 2007.

265. **Tang C, Han P, Oprescu AI, Lee SC, Gyulkhandanyan AV, Chan GN, Wheeler MB and Giacca A**. Evidence for a role of superoxide generation in glucose-induced beta-cell dysfunction in vivo. *Diabetes* 56: 2722-2731, 2007.

266. **Aruoma OI, Halliwell B, Hoey BM and Butler J**. The antioxidant action of taurine, hypotaurine and their metabolic precursors. *Biochem J* 256: 251-255, 1988.

267. **Vesce S, Kirk L and Nicholls DG**. Relationships between superoxide levels and delayed calcium deregulation in cultured cerebellar granule cells exposed continuously to glutamate. *J Neurochem* 90: 683-693, 2004.

268. **Chen WQ, Jin H, Nguyen M, Carr J, Lee YJ, Hsu CC, Faiman MD, Schloss JV and Wu JY**. Role of taurine in regulation of intracellular calcium level and neuroprotective function in cultured neurons. *J Neurosci Res* 66: 612-619, 2001.

269. **El IA and Trenkner E**. Growth factors and taurine protect against excitotoxicity by stabilizing calcium homeostasis and energy metabolism. *J Neurosci* 19: 9459-9468, 1999.

270. **Schuller-Levis GB and Park E**. Taurine and its chloramine: modulators of immunity. *Neurochem Res* 29: 117-126, 2004.

271. **Park E, Schuller-Levis G and Quinn MR**. Taurine chloramine inhibits production of nitric oxide and TNF-alpha in activated RAW 264.7 cells by mechanisms that involve transcriptional and translational events. *J Immunol* 154: 4778-4784, 1995.

272. **Liu Y, Tonna-DeMasi M, Park E, Schuller-Levis G and Quinn MR**. Taurine chloramine inhibits production of nitric oxide and prostaglandin E2 in activated C6 glioma cells by suppressing inducible nitric oxide synthase and cyclooxygenase-2 expression. *Brain Res Mol Brain Res* 59: 189-195, 1998.

273. **Barua M, Liu Y and Quinn MR**. Taurine chloramine inhibits inducible nitric oxide synthase and TNF-alpha gene expression in activated alveolar macrophages: decreased NF-kappaB activation and IkappaB kinase activity. *J Immunol* 167: 2275-2281, 2001.

274. **Ramana KV, Tammali R, Reddy AB, Bhatnagar A and Srivastava SK**. Aldose reductase-regulated tumor necrosis factor-alpha production is essential for high glucose-induced vascular smooth muscle cell growth. *Endocrinology* 148: 4371-4384, 2007.

275. **Ogasawara M, Nakamura T, Koyama I, Nemoto M and Yoshida T**. Reactivity of taurine with aldehydes and its physiological role. *Adv Exp Med Biol* 359: 71-78, 1994.

276. **Nandhini TA and Anuradha CV**. Inhibition of lipid peroxidation, protein glycation and elevation of membrane ion pump activity by taurine in RBC exposed to high glucose. *Clin Chim Acta* 336: 129-135, 2003.

277. **Selvaraj N, Bobby Z and Sathiyapriya V**. Effect of lipid peroxides and antioxidants on glycation of hemoglobin: an in vitro study on human erythrocytes. *Clin Chim Acta* 366: 190-195, 2006.

278. **Nandhini AT, Thirunavukkarasu V and Anuradha CV**. Stimulation of glucose utilization and inhibition of protein glycation and AGE products by taurine. *Acta Physiol Scand* 181: 297-303, 2004.

279. **Devamanoharan PS, Ali AH and Varma SD**. Prevention of lens protein glycation by taurine. *Mol Cell Biochem* 177: 245-250, 1997.

280. **Carneiro EM, Latorraca MQ, Araujo E, Beltra M, Oliveras MJ, Navarro M, Berna G, Bedoya FJ, Velloso LA, Soria B and Martin F**. Taurine supplementation modulates glucose homeostasis and islet function. *J Nutr Biochem* 20: 503-511, 2009.

281. **Hall KE, Sima AA and Wiley JW**. Opiate-mediated inhibition of calcium signaling is decreased in dorsal root ganglion neurons from the diabetic BB/W rat. *J Clin Invest* 97: 1165-1172, 1996.

282. **Verkhratsky A and Fernyhough P**. Mitochondrial malfunction and Ca2+ dyshomeostasis drive neuronal pathology in diabetes. *Cell Calcium* 44: 112-122, 2008.

283. **Foos TM and Wu JY**. The role of taurine in the central nervous system and the modulation of intracellular calcium homeostasis. *Neurochem Res* 27: 21-26, 2002.

284. **Takahashi K, Hashimoto H, Baba A, Schaffer SW and Azuma J**. Effect of taurine on angiotensin II-induced expression of immediate early response genes in primary cultured neonatal rat heart cells. *Adv Exp Med Biol* 403: 297-304, 1996.

285. **Vague P, Coste TC, Jannot MF, Raccah D and Tsimaratos M**. C-peptide, Na+,K(+)-ATPase, and diabetes. *Exp Diabesity Res* 5: 37-50, 2004.

286. **Di Leo MA, Santini SA, Cercone S, Lepore D, Gentiloni SN, Caputo S, Greco AV, Giardina B, Franconi F and Ghirlanda G**. Chronic taurine supplementation ameliorates oxidative stress and Na+ K+ ATPase impairment in the retina of diabetic rats. *Amino Acids* 23: 401-406, 2002.

287. **Kocak-Toker N, Giris M, Tulubas F, Uysal M and ykac-Toker G**. Peroxynitrite induced decrease in Na+, K+-ATPase activity is restored by taurine. *World J Gastroenterol* 11: 3554-3557, 2005.

288. **Nakaya Y, Minami A, Harada N, Sakamoto S, Niwa Y and Ohnaka M**. Taurine improves insulin sensitivity in the Otsuka Long-Evans Tokushima Fatty rat, a model of spontaneous type 2 diabetes. *Am J Clin Nutr* 71: 54-58, 2000.

289. **Zhang M, Bi LF, Fang JH, Su XL, Da GL, Kuwamori T and Kagamimori S**. Beneficial effects of taurine on serum lipids in overweight or obese non-diabetic subjects. *Amino Acids* 26: 267-271, 2004.

290. **Spohr C, Brons C, Winther K, Dyerberg J and Vaag A**. No effect of taurine on platelet aggregation in men with a predisposition to type 2 diabetes mellitus. *Platelets* 16: 301-305, 2005.

291. **Nittynen L, Nurminen ML, Korpela R and Vapaatalo H**. Role of arginine, taurine and homocysteine in cardiovascular diseases. *Ann Med* 31: 318-326, 1999.

292. **Militante JD and Lombardini JB**. Treatment of hypertension with oral taurine: experimental and clinical studies. *Amino Acids* 23: 381-393, 2002.

293. **Fukunaga M, Miyata S, Higo S, Hamada Y, Ueyama S and Kasuga M**. Methylglyoxal induces apoptosis through oxidative stress-mediated activation of p38 mitogen-activated protein kinase in rat Schwann cells. *Ann N Y Acad Sci* 1043: 151-157, 2005.

294. **Li F, Drel VR, Szabo C, Stevens MJ and Obrosova IG**. Low-dose poly(ADP-ribose) polymerase inhibitor-containing combination therapies reverse early peripheral diabetic neuropathy. *Diabetes* 54: 1514-1522, 2005.

295. **Li F, Drel VR, Szabo C, Stevens MJ and Obrosova IG**. Low-dose poly(ADP-ribose) polymerase inhibitor-containing combination therapies reverse early peripheral diabetic neuropathy. *Diabetes* 54: 1514-1522, 2005.

296. **Arima Y, Hayashi H, Kamata K, Goto TM, Sasaki M, Kuramochi A and Saya H**. Decreased expression of neurofibromin contributes to epithelial-mesenchymal transition in neurofibromatosis type 1. *Exp Dermatol* 19: e136-e141, 2010.

297. **Lei L, Han D, Gong S, Zheng J and Xu J**. Mpz gene suppression by shRNA increases Schwann cell apoptosis in vitro. *Neurol Sci* 31: 603-608, 2010.

298. **Meyer Zu HG, Heidenreich H, Lehmann HC, Ferrone S, Hartung HP, Wiendl H and Kieseier BC**. Expression of antigen processing and presenting molecules by Schwann cells in inflammatory neuropathies. *Glia* 58: 80-92, 2010.

299. **Laemmli UK**. Cleavage of structural proteins during the assembly of the head of bacteriophage T4. *Nature* 227: 680-685, 1970.

300. **Saiki RK, Gelfand DH, Stoffel S, Scharf SJ, Higuchi R, Horn GT, Mullis KB and Erlich HA**. Primer-directed enzymatic amplification of DNA with a thermostable DNA polymerase. *Science* 239: 487-491, 1988.

301. **Livak KJ and Schmittgen TD**. Analysis of relative gene expression data using real-time quantitative PCR and the 2(-Delta Delta C(T)) Method. *Methods* 25: 402-408, 2001.

302. **Thomas TP, Feldman EL, Nakamura J, Kato K, Lien M, Stevens MJ and Greene DA**. Ambient glucose and aldose reductase-induced myo-inositol depletion modulate basal and carbachol-stimulated inositol phospholipid metabolism and diacylglycerol accumulation in human retinal pigment epithelial cells in culture. *Proc Natl Acad Sci U S A* 90: 9712-9716, 1993.

303. **Stevens MJ, Lattimer SA, Kamijo M, Van HC, Sima AA and Greene DA**. Osmotically-induced nerve taurine depletion and the compatible osmolyte hypothesis in experimental diabetic neuropathy in the rat. *Diabetologia* 36: 608-614, 1993.

304. **Obrosova IG, Drel VR, Oltman CL, Mashtalir N, Tibrewala J, Groves JT and Yorek MA**. Role of nitrosative stress in early neuropathy and vascular dysfunction in streptozotocin-diabetic rats. *Am J Physiol Endocrinol Metab* 293: E1645-E1655, 2007.

305. **Xu YX, Wagenfeld A, Yeung CH, Lehnert W and Cooper TG**. Expression and location of taurine transporters and channels in the epididymis of infertile c-ros receptor tyrosine kinase-deficient and fertile heterozygous mice. *Mol Reprod Dev* 64: 144-151, 2003.

306. **Roos S, Powell TL and Jansson T**. Human placental taurine transporter in uncomplicated and IUGR pregnancies: cellular localization, protein expression, and regulation. *Am J Physiol Regul Integr Comp Physiol* 287: R886-R893, 2004.

307. **Satsu H, Terasawa E, Hosokawa Y and Shimizu M**. Functional characterization and regulation of the taurine transporter and cysteine dioxygenase in human hepatoblastoma HepG2 cells. *Biochem J* 375: 441-447, 2003.

308. **El-Sherbeny A, Naggar H, Miyauchi S, Ola MS, Maddox DM, Martin PM, Ganapathy V and Smith SB**. Osmoregulation of taurine transporter function and expression in retinal pigment epithelial, ganglion, and muller cells. *Invest Ophthalmol Vis Sci* 45: 694-701, 2004.

309. **Friling RS, Bensimon A, Tichauer Y and Daniel V**. Xenobiotic-inducible expression of murine glutathione S-transferase Ya subunit gene is controlled by an electrophile-responsive element. *Proc Natl Acad Sci U S A* 87: 6258-6262, 1990.

310. **Moinova HR and Mulcahy RT**. An electrophile responsive element (EpRE) regulates beta-naphthoflavone induction of the human gamma-glutamylcysteine synthetase regulatory subunit gene. Constitutive expression is mediated by an adjacent AP-1 site. *J Biol Chem* 273: 14683-14689, 1998.

311. **Kunisaki M, Bursell SE, Umeda F, Nawata H and King GL**. Normalization of diacylglycerol-protein kinase C activation by vitamin E in aorta of diabetic rats and cultured rat smooth muscle cells exposed to elevated glucose levels. *Diabetes* 43: 1372-1377, 1994.

312. **Ayo SH, Radnik RA, Glass WF, Garoni JA, Rampt ER, Appling DR and Kreisberg JI**. Increased extracellular matrix synthesis and mRNA in mesangial cells grown in high-glucose medium. *Am J Physiol* 260: F185-F191, 1991.

313. **Kunisaki M, Bursell SE, Umeda F, Nawata H and King GL**. Normalization of diacylglycerol-protein kinase C activation by vitamin E in aorta of diabetic rats and cultured rat smooth muscle cells exposed to elevated glucose levels. *Diabetes* 43: 1372-1377, 1994.

314. **Kakkar R, Kalra J, Mantha SV and Prasad K**. Lipid peroxidation and activity of antioxidant enzymes in diabetic rats. *Mol Cell Biochem* 151: 113-119, 1995.

315. **Obrosova IG, Drel VR, Pacher P, Ilnytska O, Wang ZQ, Stevens MJ and Yorek MA**. Oxidative-nitrosative stress and poly(ADP-ribose) polymerase (PARP) activation in experimental diabetic neuropathy: the relation is revisited. *Diabetes* 54: 3435-3441, 2005.

316. **Obrosova IG, Xu W, Lyzogubov VV, Ilnytska O, Mashtalir N, Vareniuk I, Pavlov IA, Zhang J, Slusher B and Drel VR**. PARP inhibition or gene deficiency counteracts intraepidermal nerve fiber loss and neuropathic pain in advanced diabetic neuropathy. *Free Radic Biol Med* 44: 972-981, 2008.

317. **Obrosova IG, Li F, Abatan OI, Forsell MA, Komjati K, Pacher P, Szabo C and Stevens MJ**. Role of poly(ADP-ribose) polymerase activation in diabetic neuropathy. *Diabetes* 53: 711-720, 2004.

318. **Li F, Drel VR, Szabo C, Stevens MJ and Obrosova IG**. Low-dose poly(ADP-ribose) polymerase inhibitor-containing combination therapies reverse early peripheral diabetic neuropathy. *Diabetes* 54: 1514-1522, 2005.

319. **Soriano FG, Virag L and Szabo C**. Diabetic endothelial dysfunction: role of reactive oxygen and nitrogen species production and poly(ADP-ribose) polymerase activation. *J Mol Med* 79: 437-448, 2001.

320. **Garcia SF, Virag L, Jagtap P, Szabo E, Mabley JG, Liaudet L, Marton A, Hoyt DG, Murthy KG, Salzman AL, Southan GJ and Szabo C**. Diabetic endothelial dysfunction: the role of poly(ADP-ribose) polymerase activation. *Nat Med* 7: 108-113, 2001.

321. **Stevens MJ, Lattimer SA, Kamijo M, Van HC, Sima AA and Greene DA**. Osmotically-induced nerve taurine depletion and the compatible osmolyte hypothesis in experimental diabetic neuropathy in the rat. *Diabetologia* 36: 608-614, 1993.

322. **Malone JI, Benford SA and Malone J, Jr.** Taurine prevents galactose-induced cataracts. *J Diabetes Complications* 7: 44-48, 1993.

323. **Trachtman H, Futterweit S and Bienkowski RS**. Taurine prevents glucose-induced lipid peroxidation and increased collagen production in cultured rat mesangial cells. *Biochem Biophys Res Commun* 191: 759-765, 1993.

324. **Almolki A, Taille C, Martin GF, Jose PJ, Zedda C, Conti M, Megret J, Henin D, Aubier M and Boczkowski J**. Heme oxygenase attenuates allergen-induced airway inflammation and hyperreactivity in guinea pigs. *Am J Physiol Lung Cell Mol Physiol* 287: L26-L34, 2004.

325. **Bruckner SR, Perry G and Estus S**. 4-hydroxynonenal contributes to NGF withdrawal-induced neuronal apoptosis. *J Neurochem* 85: 999-1005, 2003.

326. **Cipriani G, Rapizzi E, Vannacci A, Rizzuto R, Moroni F and Chiarugi A**. Nuclear poly(ADP-ribose) polymerase-1 rapidly triggers mitochondrial dysfunction. *J Biol Chem* 280: 17227-17234, 2005.

327. **Liaudet L, Soriano FG, Szabo E, Virag L, Mabley JG, Salzman AL and Szabo C**. Protection against hemorrhagic shock in mice genetically deficient in poly(ADP-ribose)polymerase. *Proc Natl Acad Sci U S A* 97: 10203-10208, 2000.

328. **Los M, Mozoluk M, Ferrari D, Stepczynska A, Stroh C, Renz A, Herceg Z, Wang ZQ and Schulze-Osthoff K**. Activation and caspase-mediated inhibition of PARP: a molecular switch between fibroblast necrosis and apoptosis in death receptor signaling. *Mol Biol Cell* 13: 978-988, 2002.

329. **Cheng C and Zochodne DW**. Sensory neurons with activated caspase-3 survive long-term experimental diabetes. *Diabetes* 52: 2363-2371, 2003.

330. **Russell JW, Golovoy D, Vincent AM, Mahendru P, Olzmann JA, Mentzer A and Feldman EL**. High glucose-induced oxidative stress and mitochondrial dysfunction in neurons. *FASEB J* 16: 1738-1748, 2002.

331. **Catherwood MA, Powell LA, Anderson P, McMaster D, Sharpe PC and Trimble ER**. Glucose-induced oxidative stress in mesangial cells. *Kidney Int* 61: 599-608, 2002.

332. **Sadi G, Yilmaz O and Guray T**. Effect of vitamin C and lipoic acid on streptozotocin-induced diabetes gene expression: mRNA and protein expressions of Cu-Zn SOD and catalase. *Mol Cell Biochem* 309: 109-116, 2008.

333. **Aruoma OI, Halliwell B, Hoey BM and Butler J**. The antioxidant action of taurine, hypotaurine and their metabolic precursors. *Biochem J* 256: 251-255, 1988.

334. **Penttila KE**. Role of cysteine and taurine in regulating glutathione synthesis by periportal and perivenous hepatocytes. *Biochem J* 269: 659-664, 1990.

335. **Suzuki T, Suzuki T, Wada T, Saigo K and Watanabe K**. Novel taurine-containing uridine derivatives and mitochondrial human diseases. *Nucleic Acids Res Suppl* 257-258, 2001.

336. **Suzuki T, Suzuki T, Wada T, Saigo K and Watanabe K**. Taurine as a constituent of mitochondrial tRNAs: new insights into the functions of taurine and human mitochondrial diseases. *EMBO J* 21: 6581-6589, 2002.

337. **Kirino Y, Goto Y, Campos Y, Arenas J and Suzuki T**. Specific correlation between the wobble modification deficiency in mutant tRNAs and the clinical features of a human mitochondrial disease. *Proc Natl Acad Sci U S A* 102: 7127-7132, 2005.

338. **Jeng BH, Shadrach KG, Meisler DM, Hollyfield JG, Connor JT, Koeck T, Aulak KS and Stuehr DJ**. Immunohistochemical detection and Western blot analysis of nitrated protein in stored human corneal epithelium. *Exp Eye Res* 80: 509-514, 2005.

339. **Ayata C, Ayata G, Hara H, Matthews RT, Beal MF, Ferrante RJ, Endres M, Kim A, Christie RH, Waeber C, Huang PL, Hyman BT and Moskowitz MA**. Mechanisms of reduced striatal NMDA excitotoxicity in type I nitric oxide synthase knock-out mice. *J Neurosci* 17: 6908-6917, 1997.

340. **Fischer PA, Dominguez GN, Cuniberti LA, Martinez V, Werba JP, Ramirez AJ and Masnatta LD**. Hyperhomocysteinemia induces renal hemodynamic dysfunction: is nitric oxide involved? *J Am Soc Nephrol* 14: 653-660, 2003.

341. **Hinson JA, Michael SL, Ault SG and Pumford NR**. Western blot analysis for nitrotyrosine protein adducts in livers of saline-treated and acetaminophen-treated mice. *Toxicol Sci* 53: 467-473, 2000.

342. **Vincent AM, McLean LL, Backus C and Feldman EL**. Short-term hyperglycemia produces oxidative damage and apoptosis in neurons. *FASEB J* 19: 638-640, 2005.

343. **Erdamar H, Turkozkan N, Balabanli B, Ozan G and Bircan FS**. The relationship between taurine and 3-nitrotyrosine level of hepatocytes in experimental endotoxemia. *Neurochem Res* 32: 1965-1968, 2007.

344. **Schuller-Levis GB and Park E**. Taurine: new implications for an old amino acid. *FEMS Microbiol Lett* 226: 195-202, 2003.

345. **Thomas TP, Porcellati F, Kato K, Stevens MJ, Sherman WR and Greene DA**. Effects of glucose on sorbitol pathway activation, cellular redox, and metabolism of myo-inositol, phosphoinositide, and diacylglycerol in cultured human retinal pigment epithelial cells. *J Clin Invest* 93: 2718-2724, 1994.

346. **Wittmack EK, Rush AM, Hudmon A, Waxman SG and Dib-Hajj SD**. Voltage-gated sodium channel Nav1.6 is modulated by p38 mitogen-activated protein kinase. *J Neurosci* 25: 6621-6630, 2005.

347. **Lornejad-Schafer MR, Schafer C, Schoffl H and Frank J**. Cytoprotective role of mitogen-activated protein kinase phosphatase-1 in light-damaged human retinal pigment epithelial cells. *Photochem Photobiol* 85: 834-842, 2009.

348. **Yoshimura H, Nariai Y, Terashima M, Mitani T and Tanigawa Y**. Taurine suppresses platelet-derived growth factor (PDGF) BB-induced PDGF-beta receptor phosphorylation by protein tyrosine phosphatase-mediated dephosphorylation in vascular smooth muscle cells. *Biochim Biophys Acta* 1745: 350-360, 2005.

349. **Stevens MJ, Henry DN, Thomas TP, Killen PD and Greene DA**. Aldose reductase gene expression and osmotic dysregulation in cultured human retinal pigment epithelial cells. *Am J Physiol* 265: E428-E438, 1993.

350. **Gaston BM, Carver J, Doctor A and Palmer LA**. S-nitrosylation signaling in cell biology. *Mol Interv* 3: 253-263, 2003.

351. **Forrester MT, Foster MW, Benhar M and Stamler JS**. Detection of protein S-nitrosylation with the biotin-switch technique. *Free Radic Biol Med* 46: 119-126, 2009.

352. **Hess DT, Foster MW and Stamler JS**. Assays for S-nitrosothiols and S-nitrosylated proteins and mechanistic insights into cardioprotection. *Circulation* 120: 190-193, 2009.

353. **Kuncewicz T, Sheta EA, Goldknopf IL and Kone BC**. Proteomic analysis of S-nitrosylated proteins in mesangial cells. *Mol Cell Proteomics* 2: 156-163, 2003.

354. **Jaffrey SR, Erdjument-Bromage H, Ferris CD, Tempst P and Snyder SH**. Protein S-nitrosylation: a physiological signal for neuronal nitric oxide. *Nat Cell Biol* 3: 193-197, 2001.

355. **Ji RR and Suter MR**. p38 MAPK, microglial signaling, and neuropathic pain. *Mol Pain* 3: 33, 2007.

356. **Agthong S and Tomlinson DR**. Inhibition of p38 MAP kinase corrects biochemical and neurological deficits in experimental diabetic neuropathy. *Ann N Y Acad Sci* 973: 359-362, 2002.

357. **Romio L, Zegarra M, Varesio L and Galietta LJV**. Regulation of taurine transport in murine macrophages. *Amino Acids* 21: 151-160, 2001.

358. **Oermann E, Warskulat U, Heller-Stilb B, Haussinger D and Zilles K**. Taurine-transporter gene knockout-induced changes in GABA(A), kainate and AMPA but not NMDA receptor binding in mouse brain. *Anat Embryol (Berl)* 210: 363-372, 2005.